RMI 5477
Adams

STIC-ILL

From: Schnizer, Richard
Sent: Tuesday, July 17, 2001 7:02 AM
To: STIC-ILL
Subject: 09/330,903

Please ~~send me copies of:~~

TI Oligonucleotides as modulators of cancer gene ***expression*** .
AU Curcio L D; Bouffard D Y; Scanlon K J
SO PHARMACOLOGY AND THERAPEUTICS, (1997) 74 (3) 317-32. Ref: 156

TI Therapeutic potential and mechanism of action of oligonucleotides and ***ribozymes*** .
AU Lavrovsky Y; Chen S; Roy A K
SO BIOCHEMICAL AND MOLECULAR MEDICINE, (1997 Oct) 62 (1) 11-22. Ref: 173

TI ***Ribozymes*** as therapeutic ***tools*** for genetic disease.
AU Phylactou L A; Kilpatrick M W; Wood M J
SO HUMAN MOLECULAR GENETICS, (1998) 7 (10) 1649-53. Ref: 54

TI ***Ribozymes*** : the characteristics and properties of catalytic RNAs.
AU Tanner N K
SO FEMS MICROBIOLOGY REVIEWS, (1999 Jun) 23 (3) 257-75. Ref: 105

TI ***Ribozymes*** and the anti-gene therapy: how a catalytic RNA can be used to inhibit gene function.
AU Muotri A R; da Veiga Pereira L; dos Reis Vasques L; Menck C F
SO GENE, (1999 Sep 17) 237 (2) 303-10. Ref: 93

Thank you-

Richard Schnizer, Ph.D.
Patent Examiner
Art Unit 1632
CM1 12E17
703-306-5441

Pharmacol. Ther. Vol. 74, No. 3, pp. 317–332, 1997

ISSN 0163-7258/97 $32.00
PII S0163-7258(97)00005-3

Oligonucleotides as Modulators of Cancer Gene Expression

Lisa D. Curcio,‡ David Y. Bouffard† and Kevin J. Scanlon†§*

*DEPARTMENT OF GENERAL AND ONCOLOGIC SURGERY, CITY OF HOPE NATIONAL MEDICAL CENTER, 1500 EAST DUARTE ROAD, DUARTE, CA 91010, USA

†BERLEX BIOSCIENCES, DEPARTMENT OF CANCER RESEARCH, 15049 SAN PABLO AVENUE, P.O. BOX 4099, RICHMOND, CA 94804-0099, USA

ABSTRACT. The delineation of gene function has always been an intensive subject of investigations. Recent advances in the synthesis and chemistry of oligonucleotides have now made these molecules important tools to study and identify gene function and regulation. Modulation of gene expression using oligonucleotides has been targeted at different levels of the cellular machinery. Triplex forming oligonucleotides, as well as peptide nucleic acids, have been used to inhibit gene expression at the level of transcription; after binding of these specific oligonucleotides, conformational change of the DNA's helical structure prevents any further DNA/protein interactions necessary for efficient transcription. Gene regulation can also be achieved by targeting the translation of mRNAs. Antisense oligonucleotides have been used to down-regulate mRNA expression by annealing to specific and determined region of an mRNA, thus inhibiting its translation by the cellular machinery. The exact mechanism of this type of inhibition is still under intense investigation and is thought to be related to the activation of RNase H, a ribonuclease that is widely available that can cleave the RNA/DNA duplex, thus making it inactive. Another well-characterized means of interfering with the translation of mRNAs is the use of ribozymes. Ribozymes are small catalytic RNAs that possess both site specificity and cleavage capability for an mRNA substrate, inhibiting any further protein formation. This review describes how these different oligonucleotides can be used to define gene function and discusses in detail their chemical structure, mechanism of action, advantages and disadvantages, and their applications. PHARMACOL. THER. 74(3): 317–332, 1997. © 1997 Elsevier Science Inc.

KEY WORDS. Review, oligonucleotide, antisense, ribozyme, triplex, cancer.

CONTENTS

ABBREVIATIONS. ALL, acute lymphocytic leukemia; ASO, antisense oligonucleotide; CML, chronic myelogenous leukemia; FGF, fibroblast growth factor; HDV, hepatitis delta virus; HIV, human immunodeficiency virus; HPV, human papillomavirus; MDR, multidrug resistance; ODN, oligodeoxynucleotide; PDGF, platelet-derived growth factor; PKC, protein kinase C; PNA, peptide nucleic acid; PTN, pleiotrophin; TFO, triplex forming oligonucleotide.

1. INTRODUCTION

Research over the last several decades has made tremendous strides in the identification of the human genome. Basic to this understanding is that cellular DNA serves as a template for the multitude of cellular functions. Genetic information is manifested by DNA translation into functional proteins through the intermediate RNA. This has led to new concepts in the pathogenesis of disease. Many disease processes have been identified as having a genetic basis, either inherited or acquired. This information has and will lead to new and innovative therapies to treat these processes, based on the identified genetic 'flaw' or omission. Recent studies have defined the molecular basis for cell growth and differentiation (for reviews, see Cantley *et al.*, 1991; Hunter, 1991; Roberts, 1992; Egan and Weinberg, 1993). Cellular growth and proliferation are initiated by a cascade of signal transduction events and are tightly regulated by proto-oncogenes and tumor suppressor genes. The etiology of carcinogenesis is increasingly being understood to be the abnormal expression of proto-oncogenes and tumor suppressor genes. Oncogenes are normally present within the cell as proto-oncogenes. The first proto-oncogene was described over 19 years ago by Stehelin *et al.*

‡Corresponding author.
§Requests for reprints.

(1976). Oncogenes function as modulators of critical cellular functions, including signal transduction and transcription, through their expressed proteins. A single mutant allele is all that is required for malignant transformation. This mutation may be the sequelae of a point mutation, amplification, translocation or rearrangement (Table 1). Tumor suppressor genes, in contrast, require the loss of function of both alleles either by mutation, deletion or a combination of both to convert to the malignant phenotype. Identification of these genes opens the door for innovative therapies to target these genetic errors either at the level of the DNA, RNA or expressed proteins.

Other exciting targets for oligonucleotides include the human immunodeficiency virus (HIV)-1, the virus causing acquired immunodeficiency syndrome. If replication of this virus can be interrupted, the subsequent cytopathologic effects can be down-regulated and the fate of the disease process may be altered (Agris *et al.*, 1986; Lemaitre *et al.*, 1987; Zamecnik *et al.*, 1986). Other viral disease processes potentially treatable with gene therapy include influenza, hepatitis, and the lymphocytic choriomeningitis virus. Metabolic diseases, such as Alzheimer's disease and diabetes, have the potential to be modulated by oligonucleotides. As the pathogenesis of many more disease processes are delineated, the boundaries of what may be treated with gene therapy surely will increase dramatically.

TABLE 1. Potential Proto-oncogene Targets for Cancer Gene Therapy

Proto-oncogene	Type of anomaly	Cancer phenotype
gip	Point mutation	Ovarian and adrenal carcinomas
gsp	Point mutation	Pituitary adenoma and thyroid carcinoma
H-*ras*	Point mutation	Lung, pancreas and colon carcinomas, and melanoma
K-*ras*	Point mutation	Leukemia (AML, ALL), thyroid carcinoma, and lung cancer
N-*ras*	Point mutation	Genitourinary and thyroid carcinomas, and melanoma
Erb-B1	Amplification	Squamous cell carcinoma, and astrocytoma
Erb-B2	Amplification	Breast, prostate, ovarian, and gastric carcinomas
L-*myc*	Amplification	Lung carcinoma
N-*myc*	Amplification	Small cell lung cancer
K-*sam*	Amplification	Gastric carcinoma
c-*myc*	Amplification and translocation	Breast, lung and cervical carcinomas, and Burkitt's lymphoma
bcr-abl	Translocation	Leukemia (CML)
ret	Rearrangement	Thyroid carcinoma
ros	Unknown	Astrocytoma
sis	Unknown	Astrocytoma
src	Unknown	Colon carcinoma

Still early in its evolution, gene therapy possesses several means to effect these changes: oligonucleotides, each with their own set of advantages and limitations. Only the future will tell which one of these, or combination of these, oligonucleotides will become the best tool for gene therapy. This review will focus on the different types of oligonucleotides now available: triplex, antisense, and ribozymes. It will provide insight into their structure, function and biology, as well as their limitations, and what present applications hold in store for the future in this exciting new field.

2. TRIPLEX DNA

The history of triplex DNA starts with the pioneering work of Felsenfeld *et al.* in the 1950s, who described double-stranded polynucleotides containing purines in one strand and pyrimidines in the other (Felsenfeld *et al.*, 1957; Felsenfeld and Rich, 1957). These strands were able to undergo stoichiometric transitions forming triple-stranded structures containing one polypurine and two polypyrimidine strands (Riley *et al.*, 1966; Morgan and Wells, 1968; Lee *et al.*, 1979). These DNA, RNA and RNA/DNA hybrids were widely studied in the 1960s. The first evidence of their ability to inhibit transcription was made by Morgan and Wells (1968) using RNA as a third strand in an *in vitro Escherichia coli* system. Since then, triplex had escaped wide attention until the 1980s, when interest arose secondary to two major developments: (1) homopurine-homopyrimidine stretches in supercoiled plasmids were found to adopt an unusual DNA structure called H-DNA [these include a triplex as the major structural element (Lyamichev *et al.*, 1986; Mirkin *et al.*, 1987)], and (2) when several groups demonstrated that homopyrimidine and some purine-rich oligonucleotides can form stable and sequence-specific complexes with corresponding homopurine-homopyrimidine sites of duplex DNA (Le Doan *et al.*, 1987; Moser and Dervan, 1987; Lyamichev *et al.*, 1988). These complexes were found to be triplex structures rather than D-loops, where the oligonucleotide invades the double helix and displaces one strand. A characteristic feature of all these triplexes is that the two chemically homologous strands (both pyrimidine and purine) are antiparallel. These findings led to an increased interest in triplex studies.

Triplex forming oligonucleotides (TFOs) may be universal drugs that demonstrate sequence-specific recognition of duplex DNA based on the simple recognition principle of Hoogsten pairing rules between a purine strand of the DNA duplex and the TFO bases. This method of recognition is limited, however, because the homopurine-homopyrimidine sites are preferentially recognized. It soon became clear that for triplex DNA to be effective drugs for future studies in gene therapy, two criteria must be satisfied: (1) they must demonstrate a strong affinity for their targets and bind with reasonable stability and (2) they should be specific for their target. However, TFOs that bind avidly to their target tend to demonstrate less selectivity. Selectivity experiments

of modified TFOs are incomplete at present and may actually demonstrate less selectivity than the original TFOs.

2.1. *Chemical Structure and Biology*

Many studies have shown that triplex structures vary greatly. A triplex may consist of two pyrimidine and one purine strand, YR*Y, or two purine and one pyrimidine strand, YR*R (where Y = pyrimidine and R = purine). The strand may be composed of RNA or DNA chains or their combination. The collinear association of three oligodeoxynucleotide (ODN) strands may occur when a third strand binds to the major groove of a DNA double helix, forming Hoogsten pairs with purines of the Watson-Crick base pairs. Intramolecular triplexes may form when a part of the DNA double helix folds back upon itself in homopurine-homopyrimidine regions of supercoiled DNA (Johnston, 1988; Letai *et al.*, 1988).

To form (YR*Y) triplexes, the CG*C and TA*T triad are necessary. Essential to these triads is the positioning of the third strand within the major groove of the double helix that is forming Hoogsten hydrogen bonds with the purine strand. Formation of the CG*C triad requires N_3 protonation of cytosine in the third strand, making it more stable in an acidic environment. The YR*R and YR*Y are alike in two ways: (1) the duplex involved in triplex formation must have a homopurine sequence in one strand, and (2) the orientation of the two chemically homologous strands is antiparallel (for a review, see Frank-Kamentskii and Mirkin, 1995).

Hybrid triplexes consisting of both DNA and RNA are less understood and consist only of YR*Y triplexes. Studies do show that triplexes are more stable when DNA represents the central homopurine strand. Affinity cleavage data shows that the orientation of homologous chains in hybrid triplexes is also antiparallel. Intermolecular triplexes are the most frequently studied due to their potential therapeutic utility, use in gene mapping, and their ease of synthesis. The use of TFOs as gene modulators is based on their affinity to bind to a target gene and potentially interfere with RNA transcription, with resultant down-regulation in the targeted gene expression. Triplex holds several advantages over other strategies used to inhibit gene expression. TFOs are capable of targeting the desired gene directly rather than inhibiting at the level of the mRNA (i.e., they act at the transcriptional level rather than the translational level). Because of its specificity and DNA-directed mechanism of action, only a few molecules of TFO are needed (in theory) compared with the excess antisense or ribozyme molecules needed to bind and cleave at the mRNA level. The stability of DNA triplexes is of paramount importance to realize their biological application. The YR*Y triplexes are most favorable under acidic conditions, while YR*R triplexes require bivalent cations for their stability, and this may limit their use in biological systems. Numerous studies have been aimed at the stabilization of DNA triplexes at physiological conditions. YR*R triplex studies have concentrated on mechanisms to overcome pH dependency. A few studies have shown that polyamines can enhance inter- and intramolecular YR*R triplex stability at physiological pH (Moser and Dervan, 1987; Hampel *et al.*, 1991, 1993). This effect most likely is due to reduced repulsion between the phosphate backbones after the binding polyamines. Overcoming the need for cytosine protonation is necessary to produce pH-independent triplexes (Jetter and Hobbs, 1993; Koh and Dervan, 1992; Krawczyk *et al.*, 1992; Lee *et al.*, 1984; Maher *et al.*, 1989; Ono *et al.*, 1991; Plum *et al.*, 1990). Further stability can be seen when triplexes are bound to a third strand, which is represented by an oligonucleotide-intercalator conjugate. This was first demonstrated in acridine derivatives (Le Doan *et al.*, 1987) and later was shown for other oligonucleotides and intercalators (Mouscadet *et al.*, 1994; Orson *et al.*, 1994; Sun *et al.*, 1991). The interposition of the ligand into the DNA at the duplex-triplex junction confers additional stability, and for uncertain reasons, the most stable complex is formed when the intercalator is positioned at the 5′-end of the TFO.

2.2. *Mechanism of Action*

The basic premise of action for triplex DNA is that binding of the TFO to a particular gene should prevent its normal function and expression (Fig. 1). The TFO binds to the purine-rich strand of DNA via Hoogsten hydrogen bonds between the third-strand nucleotide and its complement in the purine-rich strand. The third strand may contain either polypurines or polypyrimidines. Thermal studies have identified that the most stable combinations for polypurine third strands are A-A:T and G-G:C (Letai *et al.*, 1988). However, to form the G-G:C bond, multivalent cations such as Mg^{2+} must be present. The optimal triplet combinations in a polypyrimidine third strand are T-A:T and C+-G:C. As mentioned in the previous section, the formation of C+-G:C bonds requires an acidic pH for optimal stability.

The specificity of triplex formation is the direct result of the formation of complementary sequences between the purine-rich strand of the target DNA and the TFO. DNase I protection and electrophoresis mobility shift assays have shown that TFOs have the ability to discriminate to one base triplet (Mergny *et al.*, 1991). After TFO binding, the physical presence of a third strand, as well as the conformational change of the helical structure, prevents the DNA/protein interactions necessary for efficient transcription (Maher *et al.*, 1989, 1992).

2.3. *Limitations*

The limitations that triplex displays should not be fatal. Even if TFOs do not demonstrate themselves to be the ultimate tool in gene therapy, there are presently many synthetic analogs that also exhibit triplex-type behavior. These are oligonucleotides with non-natural bases that are able to bind the duplex more strongly than can the natural TFOs. Other modifications have replaced the sugar-phosphate backbone of ordinary TFOs with another backbone

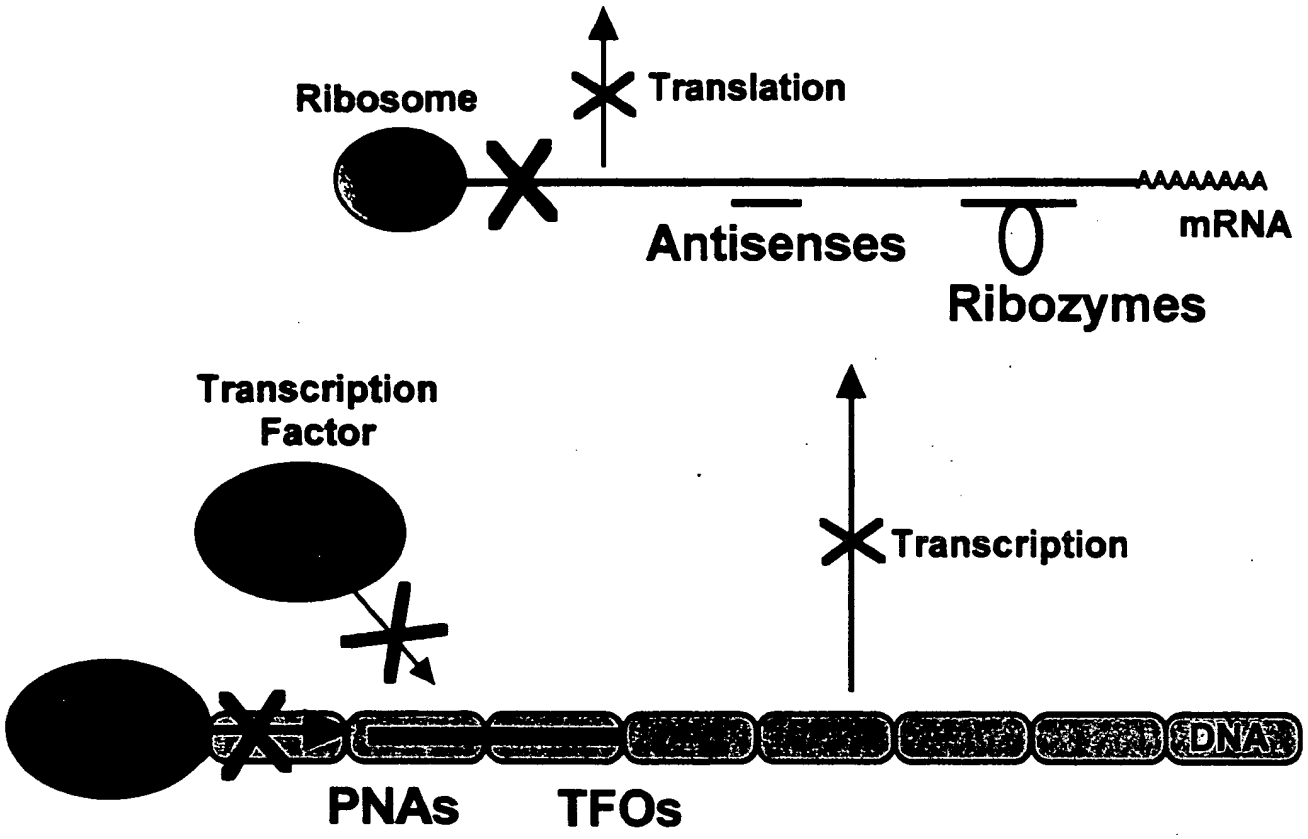

FIGURE 1. Targets for oligonucleotide modulation of gene expression. Oligonucleotides can be targeted to alter gene expression at different levels. Antisenses and ribozymes bind specifically to a region in their target mRNA and inhibit their translation by ribosomes resulting in the blocking of protein formation. TFOs and PNAs are perturbing gene expression by associating to a specific region of a promoter to alter the transcription of the regulated gene.

consisting of uncharged peptide-like structures; this has been called peptide nucleic acid (PNA). PNAs have been found to form remarkably strong and sequence-specific complexes with the target DNA by displacing one of the DNA strands and forming a triplex with two PNA molecules (Cherny *et al.*, 1993; Demidov *et al.*, 1993).

The binding and stability of the TFO is of concern; a single interruption in the oligopurine/oligopyrimidine strands or a single mismatch in the third strand is enough to destabilize the triplex structure (Mergny *et al.*, 1991). Triplexes display short half-lives secondary to intracellular nucleases. The binding of the TFO to target sites is transient, resulting in only temporary inhibition of the target gene. Others have reported a nonspecific inhibitory effect on the *in vitro* transcription when a large excess of ODN is present (Ebbinghaus *et al.*, 1993).

2.4. *Modifications*

Some of the basic problems of TFO and their innate stability have been circumvented by modifications of the TFO structure. PNA is a synthetic form of TFOs in which the phosphated backbone is replaced by a protein-like backbone. PNAs have the ability to form P-loops during interaction with the duplex DNA. Also, PNAs may form a stable triplex with one of the strands of DNA and subsequently displace the other strand. Kessler *et al.* (1993) and Jayasena and Johnston (1992) have shown that interruptions in the homopurine/homopyrimidine target sites can be bridged by using a linker molecule incorporated into the TFO. This intercalator molecule can serve as a bridge and can bind to the homopurine regions on alternate strands. This can also provide additional binding energy to further stabilize the triple helix structure, enabling the target strand to be irreversibly displaced and to stabilize cross-linkage with the two duplex strands (Hélène, 1991). McShan *et al.* (1992) have demonstrated improved stability of the TFO intracellularly by attaching a free amine group to the 3′-end of the oligonucleotide. This confers increased resistance to enzymatic degradation by intracellular nucleases.

2.5. In vitro *Studies*

The well-known oncogene c-*myc* has been the focus of the majority of these studies. C-*myc* overexpression has been identified in several tumors and is seen consistently with cervical and ovarian carcinoma. The gene for *c-myc* expression is a ready target for triplex DNA. The triplex may bind strongly to the purine-rich sequence 125 bp upstream of its P1 promoter region. This exposure has been shown to lead to reduced transcription levels of the *c-myc* gene (Cooney

et al., 1988) and to lead to growth suppression of ovarian and cervical carcinomas (Helm *et al.*, 1993).

Postel *et al.* (1991) have shown that the same effect could be achieved at physiologic pH and temperature in cell culture models. Cleavage analysis studies have shown that the oligonucleotide acts in a site-specific fashion to form a triplex with the c-*myc* target and subsequently reduce mRNA levels of the target gene when introduced into the HeLa cell line. A control oligonucleotide that did not possess the ability to bind to the c-*myc* target site did not result in decreased mRNA levels. This confirms that the reduction in transcription was caused by site-specific triplex formation.

Further studies implicate that this TFO target site may function as a binding site for a protein that may function as an activator for transcriptional initiation. Other studies using lymphocytes have shown a synthetic TFO targeted to the promoter region of the interleukin-2-α receptor gene can reduce its mRNA levels (Orson *et al.*, 1991). The reduction in mRNA may be the direct result of blocked transcriptional activity due to the triplex formation.

Other target genes have been studied in a limited fashion. A TFO termed HR21ap has been used to target the promoter region of the H-*ras* gene. This promoter region contains two of the three Sp1 binding sites needed for transcription. Confirmation that the TFO formed a triple helix with the target site was determined by DNase I footprinting and gel mobility shift analysis (Mayfield *et al.*, 1994). Consequently, transcription was found to be inhibited in nuclear extracts. It was also shown that HR21ap did not bind to a similar nontarget distal sequence that contains a consensus Sp1 site, affirming the specificity of the TFO. Another study has also demonstrated the ability of TFOs to inhibit the binding of Sp1 at the level of the dihydrofolate reductase promoter and prevent its transcription (Gee *et al.*, 1992).

HER-2/*neu* oncogene is overexpressed in about 25% of human breast cancers and is correlated to its poor prognosis. Triplex formation has also been shown to down-regulate *in vitro* transcription by binding to a purine-rich motif in its promoter region (Ebbinghaus *et al.*, 1993). Binding and triplex formation was found to interfere with nuclear protein binding and to inhibit the subsequent transcription of the HER-2/*neu* oncogene.

Other studies have demonstrated TFOs capable of inhibiting the expression of the HIV genome (McShan *et al.*, 1992). Synthetic oligonucleotides were constructed and targeted to the transcription initiation and SP1 binding sites. The TFOs were readily taken up by infected MT4 and U937 mammalian cells in a culture medium and resulted in the inhibition of viral-induced cytotoxicity, including cellular aggregation, synthesis of viral products and expression of intact mRNA. Control oligonucleotides did not have the same effects in either cell line.

Moser and Dervan (1987) have developed TFOs with EDTA-Fe at the 5′-end, which can lead to sequence-specific double-strand breaks. Other modified TFOs, such as ellipticine (Perroualt *et al.*, 1990), phenanthroline-copper chelate (Francois *et al.*, 1989), and staphylococcal nuclease (Pie *et al.*, 1990), were investigated and have been shown to exert effects similar to an artificial restriction enzyme. However, the efficiency and specificity of cleavage was found to be less than that of restriction enzymes. Strobel and Dervan (1991) used an Achilles' heel cleavage (Koob *et al.*, 1988) technique to improve these limitations, and were able to demonstrate that the newly modified TFO had the ability to target the double-strand with an efficiency of 95%, with greater site specificity. Povsic and co-workers (1992) devised a new strategy to cleave the double-strand site using a pair of *N*-bromoacetyloligo-deoxyribonucleotides. These modifications improved the efficiency and site specificity from previous reports. Thus, the modified TFO moiety may hold promise as a useful tool for gene mapping and gene therapy because of its site specificity, as well as cleavage capacity.

3. ANTISENSE THERAPY

The theoretical basis of antisense is not new and was first proposed in 1967. The realization of its potential in the treatment of various disease processes did not occur until 1978 when *in vitro* experiments were able to demonstrate sequence-specific inhibition of the expression of Rous sarcoma virus (Zamecnik and Stephenson, 1978). Subsequently, antisense RNA, artificially synthesized, was demonstrated to alter gene expression upon injection into frog oocytes (Izant and Weintraub, 1984; Melton, 1985).

Antisense oligonucleotides (ASOs) refer to any single-stranded DNA or RNA that possess the ability to block the transfer of information from the genetic template to the expressed protein by interfering with the expression of mRNA (Crooke, 1992). This is a naturally occurring process that allows the regulation and balance of various genes by the complementary pairing of sense and antisense nucleic acid strands.

ASO RNA demonstrates sensitivity within biological fluids and requires delivery vehicles in order to demonstrate sustained production. ASO levels have been shown to slowly decrease in prolonged cell cultures (this is proposed to be due to the inherent redundancy seen in many cellular growth control pathways). ASO RNA are large molecules and may bind to more than one site, producing nonsequence-specific effects. ASO DNAs are more stable in biological fluids, but necessitate repeated applications due to their transient expression that may adversely affect the intracellular nucleotide pool and lead to cellular toxicity and/or mutagenesis (Crooke, 1991; Neckers *et al.*, 1992; Stein and Cheng, 1993).

The underlying mechanism of action of ASOs lies in the interaction of single-stranded DNA or RNA within the cellular milieu through complementary base-pairing with a targeted mRNA. This leads to changes in the intermediary metabolism of mRNA and interferes with information transfer from the gene to the protein. ASOs specifically di-

rected to a particular cellular mRNA can target this one mRNA without adversely affecting the expression of others. This intrinsic specificity offers advantages over other forms of treatment and allows the specific designing of antisense molecules against an identified overexpressed mRNA involved in a pathologic process. Additionally, the effects of ASOs are localized and contained (either they are taken up cellularly and trapped or they are rapidly degraded by extracellular nucleases). ASOs are being actively investigated as potential tools in the treatment of various disease processes.

3.1. *Chemical Structure and Biology*

Naturally occurring ASOs are composed of phosphodiester oligomers that are sensitive to extracellular fluid nucleases. ASO half-life in serum is 15–60 min. Phosphodiesters undergo bulk internalization predominantly from pinocytosis (fluid-phase endocytosis) and are transported intracellularly. Various studies in HL-60 cells have demonstrated that the net cellular accumulation of oligonucleotides may rely on the activity of protein kinase C (PKC), a calcium- and phospholipid-dependent protein kinase. Intracellular substrates are phosphorylated at the serine and threonine residues by PKC, which is the major intracellular signal transduction protein (Stein *et al.*, 1993). These studies have also shown that phosphodiester oligonucleotides are of appropriate chain length to alter the kinase activity of PKC *in vitro*, and this correlates with the rates of intracellular internalization of some fluid phase markers.

3.2. *Mechanism of Action*

There are several proposed theories concerning the mechanism of action of ASOs (Fig. 2). The first theory involves direct binding of the ASO to its mRNA target through standard Watson-Crick base-pairing, thereby physically inhibiting the translation by ribosomes (Crooke, 1992; Leonetti *et al.*, 1993; Neckers *et al.*, 1992). Other theories implicate the 5′-capping site attachment to mRNA that inhibits the binding of translational factors (Boiziau *et al.*, 1991; Leonetti *et al.*, 1993). The binding of the ASO to the targeted RNA may lead to its degradation via RNase (a ribonuclease that is widely available and cleaves mRNA in hybrid RNA/DNA duplex, thus making it inactive). The latter theory is felt to be the most prevalent and effective mechanism in decreasing specific gene expression. In the case of DNA-RNA hybrids, the RNA involved in base-pairing becomes the target of intracellular RNase H (Crooke, 1993; Walder and Walder, 1988). The RNase H enzyme is located within the nucleus and is involved in DNA replication. The RNA-RNA duplexes may be substrates to another cellular enzyme, adenosine deaminase, which covalently modifies both the antisense and target RNA by converting adenines to inosines that functionally inactivate both RNA molecules (Bass and Weintraub, 1988).

3.3. *Limitations*

There are several disadvantages to antisense therapy. The most concerning of these disadvantages is the nonantisense mechanisms of action that cause confusion in the interpretation of results. Antisenses are also incapable of multiple turnovers, and thus, large quantities are needed to inhibit a particular gene, which may lead to toxicity problems. Stability is also problematic for ASOs. Cellular incorporation of both modified and unmodified ASOs is inefficient. Chemical modifications offer advantages, but carry with them a host of their own disadvantages (the need for spe-

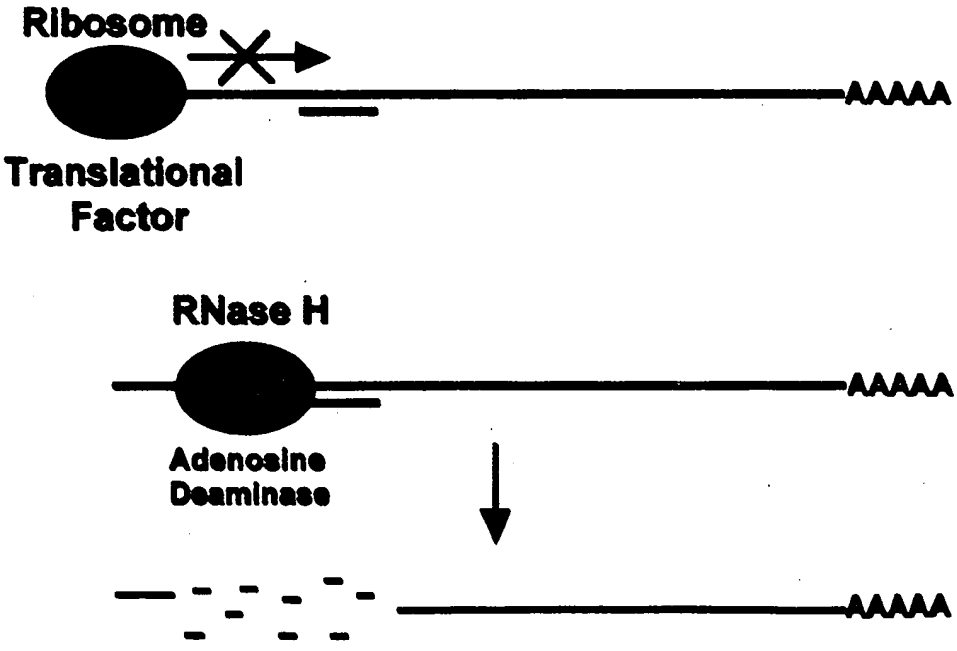

FIGURE 2. ASO mechanism of action. Once the antisense binds to the targeted region of an mRNA, activation of RNase H leads to the degradation of the duplex antisense-mRNA. Since the mRNA is eliminated, no protein can be formed, leading to a phenotypic change. Adenosine deaminase is also suspected to be involved in the degradation of the antisense/mRNA duplex.

cialized delivery systems and the escape from RNase activity). The phosphothioates have a tendency to bind to heparin-binding proteins (b-fibroblast growth factor [FGF], aFGF, FGF-4, platelet-derived growth factor [PDGF] and vascular endothelial growth factor), and this may lead to behavior changes in the oligonucleotides. Certain phosphothioate ODNs may be immunomodulating. Studies have shown that those possessing the Cp-G motif stimulate mouse spleen cells after intraperitoneal administration into mice. This can lead to marked increases in immunoglobulin secretion within hours of administration and to increase in the expression of activation markers such as Major Histocompatibility Class II.

Delivery mechanisms have been problematic in antisense therapy. In order to maximize intracellular accumulation of ASOs, the concentrations needed may be cytotoxic to various cell lines. New mechanisms are being investigated to develop more selective delivery systems to the targeted cells. One method utilizes a noncovalent salt bridge between a polylysine carrier and a plasmid vector (Wny and Wu, 1987). Other investigators have shown the potential of using a transferrin receptor antibody-oligonucleotide conjugate to improve the cellular delivery of antisense molecules (Walker *et al.*, 1995). A different study has utilized an asialoglycoprotein moiety as a ligand to target the asialoglycoprotein receptor found on hepatocytes, and encoded proteins were found to be effectively expressed both *in vitro* and *in vivo* (Lu, X.-M. *et al.*, 1994). Others have used liposome-mediated delivery to obtain high intracellular concentrations of ASOs. Further modifications of the liposome can allow more specific delivery of these molecules to targeted cells. This has been found to be successful *in vitro*, but *in vivo* studies are still lacking (Leonetti *et al.*, 1990).

3.4. *Modifications*

Pendant groups are used to chemically modify the ASOs and may make them more resistant. Various modalities can be used, such as fluorochrome attachments, tagging with cross-linking agents or the use of intercalating agents to modify the biological activity (Neckers *et al.*, 1992). The most commonly used oligonucleotides are the methylphosphonates and the phosphothioates. Phosphothioates involve a substitution of a sulfur at each of the original phosphorus groups from the phosphodiesters. They retain. the net charge of these natural oligonucleotides and are soluble in aqueous solutions. It is thought that they gain entrance to the cell through receptor-mediated endocytosis and can be slowly digested by S1 and P1 nucleases, producing inactive mononucleotides that may later accumulate and cause toxicity to the innate cellular DNA (Stein and Cheng, 1993).

At low concentrations, phosphothioates are sequence-specific and elicit RNase activity, but at high concentrations, they may inhibit RNase production. Methylphosphonates involve the substitution of a methyl group rather than a sulfur atom at the nonbridging O_2; this produces nuclease-resistant oligonucleotides without a charge, enabling them to enter the cell via passive diffusion (Crooke, 1992). Methylphosphonates must rely on ribosomal inhibition because they are not recognized by RNase H. They demonstrate minimal toxicity and high stability in their action by inhibiting ribosomal translation.

3.5. *Disadvantages*

There are several disadvantages to the chemically modified ASOs. They are less permeable to the cell and often require delivery vehicles, which, in turn, can be cytotoxic to the cells. Further investigation will be needed to maximize their ability as therapeutic agents. Studies have tried to elucidate the exact mechanism of cellular transport, but this still remains unclear (Crooke, 1992; Neckers *et al.*, 1992). To be effective antisense agents, the following criteria should be met: (1) they must be resilient to cellular degradation and nucleases; (2) they should possess suitable pharmacokinetics, which would allow specific delivery to the targeted tissue in nontoxic and cost-effective doses; (3) they should be efficiently transported through cellular membranes; (4) they should demonstrate high affinity and specific binding to the mRNA target; and finally, (5) they should effectively down-regulate the translation of the abnormal protein.

3.6. *Applications*

There are many potential applications of antisense therapy, but more recently, efforts have concentrated predominantly on cancer biology (Table 1). Inhibition of an abnormally expressed protein from an activated oncogene at the level of the mRNA provides an attractive and promising tool in gene therapy. The design of ASOs allows for a target-specific interaction mitigating the adverse sequelae that are commonly seen with nonspecific therapies.

The proto-oncogene c-*myb* has been studied widely, and is felt to be implicated in the proliferation and differentiation of hematopoietic cells. Several studies have shown the *in vitro* inhibition of leukemic cells and human bone marrow mononuclear cells using an ASO targeted against c-*myb* (Citro *et al.*, 1992; Gewirtz and Calabretta, 1988). The inhibition was shown to demonstrate a dose-response, with increasing amounts of the antisense increasing the degree of inhibition of the colonies. Similar studies using melanoma cells have shown that the injection of ASO against c-*myb* can produce a 50% reduction in overall tumor size (Hijiya *et al.*, 1994). However, these results were transient, and withdrawal of the ASO led to tumor regrowth. Presently, a clinical trial is underway using a c-*myb* antisense to eliminate CML cells from bone marrow samples of patients to be further used for autologous bone marrow transplantation.

Other studies have shown that the use of antisense directed against N-*myc* can be efficacious *in vitro* and *in vivo* (Whitesell *et al.*, 1991; Wickstrom *et al.*, 1992). ASOs directed against N-*myc* administered locally to athymic mice with subcutaneous xenografts of N-*myc* expressing human neuroectodermal cells demonstrated a substantial reduction

in tumor size. Antisense was also shown to decrease N-*myc* protein expression, as well as to decrease the neuroendocrine differentiation marker protein secretogranin I when compared with the sense controls (Whitesell *et al.*, 1991).

The *ras* genes have been implicated in 10–20% of all human tumors. A mutation in one of the three *ras* genes (Ha-*ras*, Ki-*ras*, N-*ras*) has been identified. This leads to the production of p21 ras oncoproteins, which are thought to be responsible for the malignant phenotype (Bos, 1989). H460a human lung cancer cell line has been found to have a K-*ras* mutation. *In vitro* studies have demonstrated a 3-fold suppression in cell growth by using a full-length K-*ras* ASO (Mukhopadhyay *et al.*, 1991). Also, the mutated K-Ras p21 protein synthesis was down-regulated by 95% after antisense treatment. Overall, Ras protein levels were only slightly decreased in this study. Another *in vivo* study using a retroviral vector driven by a cytomegalovirus promoter and harboring K-*ras* antisense was able to demonstrate that 87% of the ASO-treated mice remained tumor free vs. 90% of the control mice treated with K-*ras* sense, DNA vector or medium alone (Georges *et al.*, 1993). These studies seem to implicate that suppression of the mutated K-*ras* expression may down-regulate malignant cellular proliferation *in vivo*.

The *bcr-abl* gene is a hybrid derived from the proto-oncogene c-*abl* on chromosome 9 translocated to the breakpoint cluster region (c-*bcr*) on chromosome 22 (Rowley, 1973). This is seen in 98% of all chronic myelogenous leukemia (CML) patients and 50% of all acute lymphocytic leukemia (ALL) patients. Cells treated with an ASO against this hybrid gene were found to form fewer colonies with a lower ratio of blast cells/colony when compared with control and mismatched ASO-treated cells. BCR-ABL ASO can eliminate *bcr-abl* mRNA from all blast cells; 25% of the blast cells can survive (Szczylik *et al.*, 1991). Leukemic mice cells exposed to the BCR-ABL ASO lived for 18–23 weeks vs. 8–13 weeks in the untreated and sense-treated mice, suggesting a positive effect of the antisense molecule (Skorski *et al.*, 1994).

The down-regulation of abnormally expressed c-*myc* has been investigated both at the level of translation and transcription. One study used an ASO RNA generated by a vector directed against a single-stranded fragment in the c-*myc* leader sequence of a human promyelocytic cell line HL-60, which has been shown to overexpress the c-*myc* oncogene. The subsequent reduction in c-*myc* transcription allowed increased monocytic differentiation in the HL-60 cells and led to the decrease of cellular proliferation (Wickstrom *et al.*, 1988; Yokoyama and Imamoto, 1987). In a similar fashion, the translocation of the c-*myc* gene in Burkitt's lymphoma causes the expression of an abnormal RNA molecule that retains normally spliced intron sequences. ASOs targeting this abnormal intron sequence were able to inhibit the proliferation of the Burkitt's cell lines without any adverse effects on the normal cells (McManaway *et al.*, 1990).

Also, ASOs are being studied as antiviral agents. In theory, HIV makes an attractive potential target site. If the activity of the reverse transcriptase in HIV RNA can be interrupted, the further infection of normal cells could be prevented. Several studies have shown that ASOs are capable of inhibiting HIV replication in both the acutely and chronically infected cell lines (Goodchild *et al.*, 1988; Wicz *et al.*, 1992). The mismatched and random inactive oligonucleotides caused delays, but did not inhibit viral replication, and only demonstrated effectiveness in the acutely infected cells. Another study showed that ASOs targeted against the *gag* and *rev* sequences were able to inhibit viral replication for more than 80 days, with a 10-fold reduction in ASO concentration after the initial pretreatment, with higher doses still maintaining viral inhibition (Lisziewicz *et al.*, 1993).

4. RIBOZYMES

Ribozymes are small RNA molecules capable of catalytic activity. They were discovered originally within the Group I intervening sequence of the pre-rRNA of *Tetrahymena thermophila*. This sequence catalyzes its own excision, and has been termed self-splicing (Cech *et al.*, 1981; Kruger *et al.*, 1982). The RNA portion of a RNase enzyme purified from *E. coli* was the first reported truly catalytic ribozyme (Guerrier-Takada *et al.*, 1983). Other studies have shown that the plus strand of the tobacco ring spot virus possesses a hammerhead shape and the minus strand exhibits a hairpin shape. Initially, ribozymes were thought to act only in *cis* conformation for cleavage reactions, but the hammerhead ribozyme has been found to act in *trans* (Uhlenbeck, 1987; Fig. 3), as well as the hairpin ribozyme (Hampel *et al.*, 1990).

4.1. *Mechanism of Action*

There are two postulated mechanisms for the activity of ribozymes: (1) sterile blocking, where the binding of a substrate to the mRNA prevents any further translation or metabolism of the RNA molecule, or (2) cleavage and inactivation of the targeted mRNA: ribozymes offer these theoretical advantages over antisense since they are capable of cleaving and permanently inactivating the substrate, as well as demonstrating the capacity for multiple turnovers; one ribozyme molecule may inactivate multiple RNA molecules (Fig. 4). Up to now, there have been six types of RNA motifs identified: Group I introns, RNase P, hammerhead ribozymes, hairpin ribozymes, axehead ribozymes of the hepatitis delta virus (HDV), and RNA transcripts of the mitochondrial DNA plasmid of *Neurospora* (Kijima *et al.*, 1995; Symons, 1994).

4.2. *Structure and Biology*

The rearrangement of phosphodiester bonds is the mechanism by which ribozymes are capable of catalysis (Kumar and Ellington, 1995; van Tol *et al.*, 1990). The hammer-

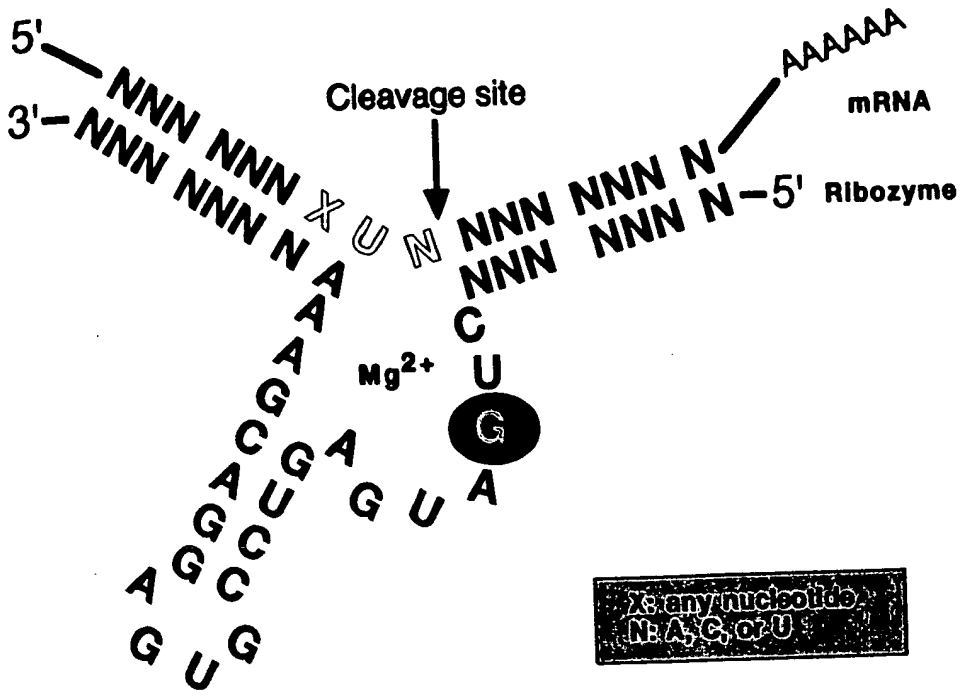

FIGURE 3. Structure of a hammerhead ribozyme. The flanking sequences of the ribozyme confer specificity for its target mRNA. The ribozyme does not require any energy source for cleaving the mRNA, but only needs a source of divalent cation such as Mg^{2+}. A single mutation in the stem of the ribozyme (indicated by a filled circle) is enough for blocking the cleaving activity of the ribozyme. The ribozyme can cleave any XUN site, where X can be any nucleotide and N is A, C, or U.

head, hairpin and HDV ribozymes catalyze the activation of the adjacent 2′-hydroxyl to form a cyclic 2′,3′-phosphate with concurrent elimination of the 5′-terminus. The hammerhead ribozyme works in *trans* through the nonhydrolytic transesterification of its substrate with its required divalent cation cofactors (Buzayan *et al.*, 1988; Ohkawa *et al.*, 1995). The three-dimensional structure of the ribozymes allows them to perform the catalytic reactions (Tuschl *et al.*, 1994). The secondary structure of the ribozyme-substrate complex consists of three helical areas, a catalytic core, and a loop sequence. The ribozyme proceeds to bind its substrate through two helices (Helix I and Helix III).

The hammerhead ribozyme has the ability to discern target RNA molecules that differ by only 1 bp mutation (Koizumi *et al.*, 1989). The ribozyme efficiently cleaves substrates with GUC, GUA, GUU, UUC, and CUC triplet sequences. The enzymatic kinetics of ribozymes favor short substrates (25 bases), and demonstrate lower efficiency with longer substrates (200–1000 bases). The length and base composition of the flanking sequences (in Helix I and Helix III) will also play a role in enzyme kinetics. Dissociation of the ribozyme from the substrate is prolonged when the flanking sequences are increased (Herschlag, 1991). Twelve base pairs have been found to be the optimal flanking sequence length in a ribozyme (Bertrand *et al.*, 1994).

The hairpin ribozyme is derived from the minus strand of the tobacco ring spot virus (Feldstein *et al.*, 1989; Hampel and Tritz, 1989). It works in *trans* to selectively cleave its RNA substrate. Like the hammerhead ribozyme, it uses the nonhydrolytic transesterification of substrates with the requirement for divalent cations (Kumar and Ellington, 1995; van Tol *et al.*, 1990). The primary difference between the hammerhead and the hairpin ribozyme is that a phosphothioate modification strongly inhibits self-cleavage of the hammerhead, but not of the hairpin (Buzayan *et al.*, 1988). HDV is a satellite virus of the hepatitis B virus, and consists of a minus single-stranded RNA of 1700 bp (Symons, 1994; Wang *et al.*, 1986). Replication of the HDV proceeds by a rolling circle mechanism, and RNA cleavage has also been shown

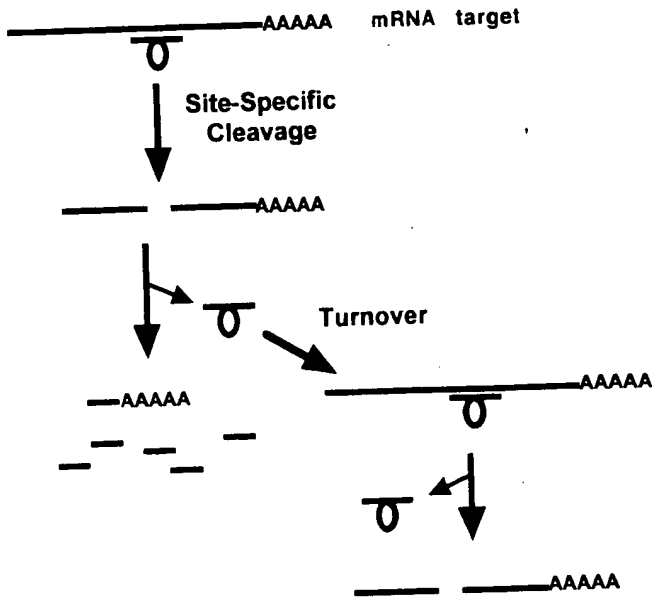

FIGURE 4. Mechanism of action of ribozyme. Ribozymes are capable of multiple turnovers. Once the ribozyme cuts its target mRNA, it is able to dissociate from the target and cleave a second mRNA. The cleaved mRNA is thought to be inactivated and then degraded by unspecific nucleases, leading to suppression of mRNA translation and protein production.

to occur in *trans* (Koizumi *et al.*, 1992; Kumar *et al.*, 1994; Thill *et al.*, 1993).

4.3. *Applications*

Anti-*ras* ribozymes have been tested in several settings. An anti-*ras* ribozyme was designed to discriminate the mutated GUC sequence (from GGC) of the H-*ras* oncogene in codon 12 (Kashani-Sabet *et al.*, 1992; Tone *et al.*, 1993). A human anti-activated-*ras* ribozyme was tested and shown to be effective in an EJ human bladder cell line (Funato *et al.*, 1994; Tone *et al.*, 1993). It was demonstrated that this ribozyme selectively cleaved the mutated gene while preserving the normal H-*ras* proto-oncogene by changes in the morphology, as well as growth characteristics (Funato *et al.*, 1994). Both H-*ras* and its corresponding protein product (p21) was shown to be down-regulated. *In vivo* studies in athymic mice confirmed the suppressed tumorigenicity of EJ transfected cells with the anti-H-*ras* ribozyme (Feng *et al.*, 1995). This ribozyme was found to be more effective than a mutant ribozyme that lacked cleavage activity. In another *in vivo* model, EJ cells alone and those transfected with the anti-*ras* ribozyme were injected orthotopically through a transurethral injection into the bladder of athymic mice (Perotta and Been, 1992). Those mice inoculated with the ribozyme-transfected cells demonstrated less malignant characteristics with less invasion of the tumor and a prolonged overall survival in the mice. More recent studies have shown the anti-*ras*-ribozyme delivered by an adenoviral vector to be efficacious both *in vitro* and *in vivo* without any adverse sequelae (Feng *et al.*, 1995).

The FEM human melanoma cell line was used to test a ribozyme targeted against the GUC heterozygous mutation in the H-*ras* mRNA. This mutation of H-*ras* is felt to be involved in aberrant cell growth. Down-regulation of H-*ras* mRNA expression and tumor growth was demonstrated in cells transfected with the ribozyme (Ohta et al., 1994, 1996a,b). Transfected cells demonstrated a more differentiated melanocytic phenotype. They also demonstrated increased melanin synthesis and a more dendritic phenotype, as well as increased responsivity to 12-O-tetradecanoylphorbol-13-acetate. Another study demonstrated that NIH3T3 cells transfected with the DNA of human melanoma cells FEMX-1, which contain a mutated H-*ras* codon 12 mutation, produced aggressive tumors when injected into nude mice (Kashani-Sabet *et al.*, 1994). Furthermore, the tumorigenicity was shown to be suppressed by treatment with an anti-ras ribozyme. On the other hand, cell lines that did not contain the mutated GUC cleavage site were not affected by this ribozyme treatment (Funato *et al.*, 1994; Koizumi *et al.*, 1992).

The K-*ras* mutation in human pancreatic carcinoma has also been a target for ribozyme therapy. K-*ras* mutations are found in more than 90% of human pancreatic cancers, and 95% of these are located at codon 12 (Almoguera *et al.*, 1988; Grunewald *et al.*, 1989). A ribozyme has been developed against the mutated K-ras codon (GUU) in the human pancreatic cell line, Capan-1 (Kijima *et al.*, 1996). Using various delivery systems, anti-K-*ras* ribozymes were transfected into these cells. The results showed that cell growth and the malignant phenotype were able to be down-regulated by use of the anti-K-*ras* ribozyme (the effectiveness of the ribozyme was shown to be dependent on the particular vector system used in the assay). The adenoviral vector system in these experiments was found to be the most efficacious in reducing the growth of Capan-1 cells.

The *bcr-abl* gene has also been studied for ribozyme-mediated therapy. This hybrid gene is formed when the proto-oncogene (*abl*) from chromosome 9 translocates to the breakpoint cluster region (*bcr*) of chromosome 22 (Rowley, 1973). This produces a new fusion gene, which contains portions of the *bcr* and *abl* genes and codes for a new 8.5 kb mRNA, which translates into a 210 kDa protein (p210) with enhanced tyrosine kinase activity. This translocation has been termed the Philadelphia chromosome, and can be seen in up to 95% of cases of CML and 50% of cases of ALL (Kurzock *et al.*, 1988). An anti-*bcr-abl* ribozyme has been constructed against the GUU triplet found adjacent to the junction of the c-*bcr* and c-*abl* fused genes (Shore *et al.*, 1993; Snyder *et al.*, 1993). The efficacy of this ribozyme has been demonstrated *in vitro* with diminished cell growth and transient reductions in the activity of p210. Under these circumstances, however, the ribozyme was also found to cleave the normal *bcr* gene (Wright *et al.*, 1993). The *bcr-abl* fusion region has been demonstrated to possess an inauspicious secondary structure that may make ribozymal access difficult (Pachuk *et al.*, 1993). More recently, multi-unit ribozymes have been found to have improved efficacy, especially when compared with single or double ribozymes (Leopold *et al.*, 1995). Delivery has been difficult with this ribozyme. Liposomal transfection has resulted in only transient expression of the ribozyme and intermittent down-regulation of the protein product p210.

Similarly, the fusion gene *AML1/MTG8* has been involved in the pathogenesis of AML. This gene is formed when the *AML1* gene translocates to *MTG8* (ETO) gene on 8q22. Two hammerhead ribozymes have been designed against two separate target sites: (1) the CUC sequence located 3 bases upstream from the fusion site and (2) the AUC located 3 bases in a downstream direction from the fusion site. Both of these ribozymes were shown to inhibit growth when transfected into Kasumi-1 cells (Matsushita *et al.*, 1995).

Cervical carcinoma has been shown to have a 90% incidence of human papillomavirus (HPV) infection (Lowy *et al.*, 1994). Oral cancers have a 75% association with HPV and less frequently, ano-genital cancers have been associated with HPV. The subtypes HPV-16 and HPV-18 have been strongly associated with malignancy. HPV exerts its effect through other cellular proteins. HPV infection causes disruption of E6 and E7 gene expression secondary to deregulation of E2, a major cellular regulatory gene. The E6 protein then becomes bound to the tumor suppressor gene p53 and prevents its normal function (Inouye, 1988; Lechner *et*

al., 1992; Werness *et al.*, 1990). The HPV E7 protein can also cooperate with an activated *ras* oncogene or transactivate the E2 adenovirus promoter and use transforming factor-β to prevent repression of c-*myc*. One group has shown a hammerhead ribozyme to be efficacious *in vitro* by cleaving the HPV-16 E6 and E7 open reading frames, which play a major role in viral DNA regulation, as well as cellular gene regulation (He *et al.*, 1993). An adeno-associated virus vector has been specifically constructed and encodes the ribozyme designed specifically to cleave the HPV-15 E6 and E7 mRNA. *In vitro*, this ribozyme has been shown to cleave RNA in HPV-infected cells (Lu, C.D. *et al.*, 1994). Further studies need to be carried out to delineate the role of ribozymes in the therapy of HPV-related malignancies.

PDGF-β, as well as its receptors, have been identified to be overexpressed in malignant mesothelioma. It is postulated that the mesothelioma cells may be stimulated by the PDGF in an autocrine mechanism (Versnel *et al.*, 1988, 1991). With the help of a constitutive vector, a specific hammerhead ribozyme was able to decrease levels of PDGF-β mRNA. The clones expressing the ribozyme demonstrated diminished cellular growth (Dorai *et al.*, 1994). This ribozyme was found to be more active than the mutant ribozyme lacking cleavage ability.

Pleiotrophin (PTN) is a polypeptide growth factor that has been found to be expressed in many types of tumors. A ribozyme directed against PTN was used to target PTN expression in a melanoma cell line known to overexpress PTN. Co-transfection of the ribozyme was shown to inhibit PTN-mediated colony formation, and was more active than the ribozyme lacking cleavage capability (Czubayko *et al.*, 1994). This demonstrates that growth factors can be down-regulated when they are found to be overexpressed, and may prove to be useful tools in gene therapy.

Ribozymal reversal of acquired drug resistance has been studied extensively. The development of acquired or intrinsic drug resistance can become a major obstacle in the effective treatment of any cancer. By definition, multidrug resistance (MDR) is associated with the resistance to a variety of different lipophilic compounds that is difficult to overcome (Endicott and Ling, 1989; Gottesman and Pastan, 1993; Roninson, 1991). It has been found that many multi-resistant cells overexpress a certain membrane P-glycoprotein (Juliano and Ling, 1976; Kartner *et al.*, 1983, 1985). This P-glycoprotein is encoded by the MDR gene, *MDR-1* (Fojo *et al.*, 1987; Gros *et al.*, 1986; Roninson *et al.*, 1986). The P-glycoprotein has been studied at length, and although there have been found several drugs that inhibit its function, their toxicity profiles have prevented their use in the clinical arena (Ford and Hait, 1993).

The use of ribozymes targeted against the MDR phenotype has been the goal of several investigators (for a review, see Bouffard *et al.*, 1996). One group described the *in vitro* cleavage efficacy of two ribozymes, as well as the ability of one of these ribozymes to lower the resistance of an acute leukemic cell line to vincristine by 35-fold (Kobayashi *et al.*, 1994). Another group designed a unique ribozyme targeted to the *MDR-1* mRNA. This ribozyme was able to cleave the 3′-end of the GUC triplet in exon 21 (Holm *et al.*, 1994). This target site was positioned between two ATP-binding sites (Teeter *et al.*, 1991). Kinetic studies have demonstrated efficient catalytic activity of the anti-*MDR-1* ribozyme (Holm *et al.*, 1996). This ribozyme was cloned into the pHβApr-1-neo plasmid (Gunning *et al.*, 1987) and transfected into a daunorubicin-resistant pancreatic cell line. P-glycoprotein levels and *MDR-1* mRNA levels were not detectable. Those clones found to express the ribozyme demonstrated a 300-fold reduction in daunorubicin resistance (Holm *et al.*, 1994). Other ribozymes have been designed against the *MDR-1* GUC sequence at triplet 880, as well as an anti-*fos* ribozyme that has been shown to decrease the actinomycin D resistance in a human ovarian carcinoma cell line (Scanlon *et al.*, 1994). Also, the expression of c-*fos*, *MDR-1* and topoisomerase II mRNA were shown to be down-regulated. It is thought that since the *MDR-1* gene has an AP-1 binding site, it may be responsive to alterations in the c-*fos* gene. Others have used liposome-mediated transfer to affect the reversal of the MDR phenotype (Kiehntopf *et al.*, 1994). In this series, 98% of the cells incorporated labeled ribozyme and 93% showed down-regulated P-glycoprotein expression. Liposome-mediated delivery of the anti-*MDR-1* ribozyme nearly reversed the MDR.

5. CONCLUSION

Modulation of cancer gene expression has been demonstrated using specific oligonucleotides directed to different pathways of gene expression. Antisenses and ribozymes are able to specifically alter a gene function by disabling the translation of mRNAs. The problem arising from this technology is that these oligonucleotides must be present in excess numbers when compared with the target in order to completely ablate the gene function. *A priori*, ribozymes should have an edge over antisenses due to their capacity for multiple turnover reactions with their targets, as demonstrated *in vitro*. At the moment, no clinical trial data is available from ribozyme therapeutics to demonstrate this potential *in vivo*. Other oligonucleotides, such as PNAs and TFOs, are also being used *in vitro* to demonstrate that a cancer phenotype can be reversed at the level of gene transcription. The refinement of these technologies surely will have an impact for future treatment of diseases. Since the human genome is anticipated to be completely sequenced over the next decade, it becomes clearer that techniques involving oligonucleotides surely will play a primary role in delineating the function of new genes at the cellular level.

The potential and realm of gene therapy have been demonstrated in different laboratories at the cellular level. The real challenge for the years to come will be to demonstrate the feasibility of this approach in cancer or in diseased patients. To this end, the development of more efficient delivery systems will be required in order to target and express genes or oligonucleotides more efficiently in cancer cells.

Acknowledgements–We would like to thank Ms. Carol Polchow and Ms. Alverto Harty for their kind help in the preparation of this manuscript. Dr. Lisa D. Curcio is the recipient of a City of Hope Fellowship Award in the Department of General and Oncologic Surgery. David Y. Bouffard is the recipient of a Terry Fox Research Fellow Award from the National Cancer Institute of Canada provided by the Terry Fox Run (Award #6597).

References

Agris, C. H., Blake, K. R., Miller, P. S., Reddy, M. P. and Ts'o, P. O. P. (1986) Inhibition of vesicular stomatitis virus protein synthesis and infection by sequence-specific oligodeoxyribonucleoside methylphosphonates. Biochemistry 25: 6268–6275.

Almoguera, C., Shibata, D., Forrester, K., Martin, J., Arnheim, N. and Perucho, M. (1988) Most human carcinomas of the exocrine pancreas contain mutant c-K-*ras* genes. Cell 53: 549–554.

Bass, B. L. and Weintraub, H. (1988) An unwinding activity that covalently modifies its double-stranded RNA substrate. Cell 31: 1089–1098.

Bertrand, E., Pictet, R. and Grange, T. (1994) Can hammerhead ribozymes be efficient tools to inactivate gene function? Nucl. Acids Res. 22: 293–300.

Boiziau, C., Kufurst, R., Cazenave, C., Roig, V., Thuong, N. T. and Toulme, J.-J. (1991) Inhibition of translation by antisense oligonucleotides via an RNase-H independent mechanism. Nucl. Acids Res. 19: 1113–1119.

Bos, J. L. (1989) *ras* Oncogene in human cancer: a review. Cancer Res. 49: 4682–4689.

Bouffard, D. Y., Ohkawa, T., Kijima, H., Irie, A., Suzuki, T., Curcio, L. D., Holm, P. S., Sassani, A. and Scanlon, K. J. (1996) Oligonucleotide modulation of MDR resistance. Eur. J. Cancer: 32A: 1010–1018.

Buzayan, J. M., Feldstein, P. A., Bruening, G. and Eckstein, F. (1988) RNA mediated formation of a phosphorothioate diester bond. Biochem. Biophys. Res. Commun. 156: 340–347.

Cantley, L. C., Auger, K. R., Carpenter, C., Duckworth, B., Graziani, A., Kapeller, R. and Soltoff, S. (1991) Oncogenes and signal transduction. Cell 64: 281–302.

Cech, T. R., Zaug, A. J. and Grabowski, P. J. (1981) *In vitro* splicing of the ribosomal RNA precursor of Tetrahymena: involvement of a guanosine nucleotide in the excision of the intervening sequence. Cell 27: 487–496.

Cherny, D. Y., Belotserkovskii, B. P., Frank-Kamenetskii, M. D., Egholm, M., Buchardt, O., Berg, R. H. and Nielsen, P. E. (1993) DNA unwinding upon strand-displacement binding of a thymine substituted polyamide to double-stranded DNA. Proc. Natl. Acad. Sci. USA 90: 1667–1670.

Citro, G., Perotti, D., Cuci, C., D'Agnano, I., Sacchi, A., Zupi, G. and Calabretta, B. (1992) Inhibition of leukemic cell proliferation by receptor-mediated uptake of c-myb antisense oligonucleotides. Proc. Natl. Acad. Sci. USA 89: 7031–7035.

Cooney, M., Czernuszewicz, G., Postel, E. H., Flint, S. J. and Hogan, M. E. (1988) Site-specific oligonucleotide binding represses transcription of the human *c-myc* gene *in vitro*. Science 241: 456–459.

Crooke, R. M. (1991) *In vitro* toxicology and pharmacokinetics of antisense oligonucleotides. Anticancer Drug Des. 6: 609–646.

Crooke, S. T. (1992) Therapeutic applications of oligonucleotides. Annu. Rev. Pharmacol. Toxicol. 32: 329–376.

Crooke, S. T. (1993) Progress toward oligonucleotide therapeutics: pharmacodynamic properties. FASEB J. 7: 533–539.

Czubayko, F., Riegel, A. T. and Wellstein, A. (1994) Ribozyme-targeting elucidates a direct role of pleiotropin in tumor growth. J. Biol. Chem. 269: 21358–21363.

Demidov, V., Frank-Kamentskii, M. D., Egholm, M., Buchardt, O. and Nielson, P. E. (1993) Sequence selective double strand DNA cleavage by peptide nucleic acid (PNA) targeting using nuclease S1. Nucl. Acids Res. 21: 2103–2107.

Dorai, T., Kobayashi, H., Holland, J. F. and Ohnuma, T. (1994) Modulation of platelet-derived growth factor-beta mRNA expression and cell growth in a human mesothelioma cell line by a hammerhead ribozyme. Mol. Pharmacol. 46: 437–444.

Ebbinghaus, S. W., Gee, J. E., Rodu, B., Mayfield, C. A., Sanders, G. and Miller, D. M. (1993) Triplex formation inhibits HER-2/*neu* transcription *in vitro*. J. Clin. Invest. 92: 2433–2439.

Egan, S. E. and Weinberg, R. A. (1993) The pathway to signal achievement. Nature 365: 781–783.

Endicott, J. A. and Ling, V. (1989) The biochemistry of P-glycoprotein mediated multidrug resistance. Annu. Rev. Biochem. 58: 131–171.

Feldstein, P. A., Buzayan, J. M. and Bruening, G. (1989) Two sequences participating in the autolytic processing of satellite tobacco ringspot virus complementary RNA. Gene 82: 53–61.

Felsenfeld, G. and Rich, A. (1957) Studies on the formation of two- and three-stranded polyribonucleotides. Biochem. Biophys. Acta 26: 457–468.

Felsenfeld, G., Davies, D. R. and Rich, A. (1957) Formation of a three-stranded polynucleotide molecule. J. Am. Chem. Soc. 79: 2023–2024.

Feng, M., Cabrera, G., Deshane, J., Scanlon, K. J. and Curiel, D. T. (1995) Neoplastic reversion accomplished by high efficiency adenoviral mediated delivery of anti-*ras* ribozymes. Cancer Res. 55: 2024–2028.

Fojo, A. T., Ueda, K., Slamon, D. J., Poplack, D. G., Gottesman, M. M. and Pastan, I. (1987) Expression of multidrug-resistance gene in human tumors and tissues. Proc. Natl. Acad. Sci. USA 84: 265–269.

Ford, J. M. and Hait, W. N. (1993) Pharmacologic circumvention of multidrug resistance. Cytotechnology 12: 171–212.

Francois, J.-C., Saison-Behmoaras, T., Barbier, C., Chassignal, M., Thuong, N. T. and Hélène, C. (1989) Sequence-specific recognition of duplex DNA via triple-helix formation for oligonucleotides covalently linked to a phenanthroline-copper chelate. Proc. Natl. Acad. Sci. USA 87: 9858–9862.

Frank-Kamentskii, M. D. and Mirkin, S. M. (1995) Triplex DNA structures. Annu. Rev. Biochem. 64: 65–95.

Funato, T., Shitara, T., Tone, T., Jiao, L., Kashani-Sabet, M. and Scanlon, K. J. (1994) Suppression of H-*ras*-mediated transformation in NIH3T3 cells by a *ras* ribozyme. Biochem. Pharmacol. 48: 1471–1475.

Gee, J. E., Blume, S., Snyder, R. C., Ray, R. and Miller, D. M. (1992) Triplex formation prevents Sp1 binding to the dihydrofolate reductase promoter. J. Biol. Chem. 267: 11163–11167.

Georges, R. N., Mukhopadhyay, T., Zhang, Y., Yen, N. and Roth, J. A. (1993) Prevention of orthotopic human lung cancer growth by intratracheal instillation of a retroviral antisense K-*ras* construct. Cancer Res. 53: 1743–1746.

Gewirtz, A. M. and Calabretta, B. (1988) A c-myb antisense oligonucleotide inhibits normal human hematopoiesis *in vitro*. Science 242: 1303–1306.

Goodchild, J., Agrawal, S., Civeira, M. P., Sarin, P. S., Sun, D. and Zamecnik, P. C. (1988) Inhibition of human immunodeficiency virus replication by anti-sense oligodeoxynucleotides. Proc. Natl. Acad. Sci. USA 85: 5507–5511.

Gottesman, M. M. and Pastan, I. (1993) Biochemistry of multidrug resistance mediated by the multidrug transporter. Annu. Rev. Biochem. 62: 385–427.

Gros, P., Croop, J., Roninson, I., Varshavsky, A. and Housman, D. E. (1986) Isolation and characterization of DNA sequences amplified in multidrug resistant hamster cells. Proc. Natl. Acad. Sci. USA 83: 337–341.

Grunewald, K., Lyons, J., Frohlich, A., Feichtinger, H., Weger, R. A., Schwab, G., Janssen, J. W. and Bartram, C. R. (1989) High frequency of Ki-*ras* codon 12 mutations in pancreatic adenocarcinomas. Int. J. Cancer 43: 1037–1041.

Guerrier-Takada, C., Gardiner, K., Marsh, T., Pace, N. and Altman, S. (1983) The RNA moiety of ribonuclease P is the catalytic subunit of the enzyme. Cell 35: 849–857.

Gunning, P., Leavitt, J., Muscat, G., Ng, S. and Kedes, L. (1987) A human beta-actin expression vector system directs high-level accumulation of antisense transcripts. Proc. Natl. Acad. Sci. USA 84: 4831–4835.

Hampel, A. and Tritz, R. (1989) RNA catalytic properties of the minimum (-)sTRSV sequence. Biochemistry 28: 4929–4933.

Hampel, A., Tritz, R., Hicks, M. and Cruz, P. (1990) "Hairpin" catalytic RNA model: evidence for helices and sequence requirement for substrate RNA. Nucl. Acids Res. 18: 299–304.

Hampel, K. J., Crosson, P. and Lee, J. S. (1991) Polyamines favor DNA triplex formation at neutral pH. Biochemistry 30: 4455–4459.

Hampel, K. J., Burkholder, G. D. and Lee, J. S. (1993) Plasmid dimerization mediated by triplex formation between polypyrimidine-polypurine repeats. Biochemistry 32: 1072–1077.

He, Y.-K., Lu, C. D. and Qi, G. (1993) *In vitro* cleavage of HPV16 E6 and E7 RNA fragments by synthetic ribozymes and transcribed ribozymes from RNA-trimming plasmids. FEBS Lett. 322: 21–24.

Hélène, C. (1991) Rational design of sequence-specific oncogene inhibitors based on antisense and antigene oligonucleotides. Eur. J. Cancer 27: 1466–1471.

Helm, C. W., Shrestha, K., Thomas, S., Shingleton, H. M. and Miller, D. M. (1993) A unique *c-myc*-targeted triplex-forming oligonucleotide inhibits the growth of ovarian and cervical carcinomas *in vitro*. Gynecol. Oncol. 49: 339–343.

Herschlag, D. (1991) Implications of ribozyme kinetics for targeting the cleavage of specific RNA molecules *in vivo*: more isn't always better. Proc. Natl. Acad. Sci. USA 88: 6921–6925.

Hijiya, N., Zhang, J., Ratajczak, M. Z., Kant, J. A., DeRiel, K., Herlyn, M., Zon, G. and Gewirtz, A. (1994) Biological and therapeutic significance of MYB expression in human melanoma. Proc. Natl. Acad. Sci. USA 91: 4499–4503.

Holm, P. S., Scanlon, K. J. and Dietel, M. (1994) Reversion of multidrug resistance in the P-glycoprotein-positive human pancreatic cell line (EPP85-181RDB) by introduction of a hammerhead ribozyme. Br. J. Cancer 70: 239–243.

Holm, P. S., Dietel, M. and Krupp, G. (1996) Similar cleavage efficiencies of an oligoribonucleotide substrate and an *mdr1* mRNA segment by a hammerhead ribozyme. Gene 167: 221–225.

Hunter, T. (1991) Cooperation between oncogenes. Cell 64: 249–270.

Inouye, M. (1988) Antisense RNA: its functions and applications in gene regulation–a review. Gene 72: 25–34.

Izant, J. G. and Weintraub, H. (1984) Inhibition of thymidine kinase gene expression by antisense RNA: a molecular approach to genetic analysis. Cell 36: 1007–1010.

Jayasena, S. D. and Johnston, B. H. (1992) Oligonucleotide-directed triple helix formation at adjacent oligopurine and oligopyrimidine DNA tracts by alternate strand recognition. Nucl. Acids Res. 20: 5279–5288.

Jetter, M. C. and Hobbs, F. W. (1993) 7,8-Dihydro-8-oxoadenine as a replacement for cytosine in the third strand of triple helices. Triplex formation without hypochromicity. Biochemistry 32: 3249–3254.

Johnston, B. H. (1988) The S1-sensitive form of $d(C\text{-}T)_n$-$d(A\text{-}G)_n$: chemical evidence for a three-stranded structure in plasmids. Science 241: 1800–1804.

Juliano, R. L. and Ling, V. (1976) A surface glycoprotein modulating drug permeability in Chinese hamster ovary cell mutants. Biochem. Biophys. Acta 455: 152–162.

Kartner, N., Riordan, J. R. and Ling, V. (1983) Cell surface P-glycoprotein associated with multidrug resistance in mammalian cell lines. Science 221: 1285–1288.

Kartner, N., Evernden-Porelle, D., Bradley, G. and Ling, V. (1985) Detection of P-glycoprotein in multidrug resistant cell lines by monoclonal antibodies. Nature (London) 316: 820–823.

Kashani-Sabet, M., Funato, T., Tone, T., Jiao, L., Wang, W., Yoshida, E., Kashfian, B. I., Shitara, T., Wu, A. M., Moreno, J. G., Traweek, S. T., Ahlering, T. E. and Scanlon, K. J. (1992) Reversal of the malignant phenotype by an anti-*ras* ribozyme. Antisense Res. Dev. 2: 3–15.

Kashani-Sabet, M., Funato, T., Florenes, V. A., Fodstad, O. and Scanlon, K. J. (1994) Suppression of the neoplastic phenotype *in vivo* by an anti-*ras* ribozyme. Cancer Res. 54: 900–902.

Kessler, D. J., Pettit, B. M., Cheng, Y.-K., Smith, S. R., Jayaraman, K., Vu, H. M. and Hogan, M. E. (1993) Triple helix formation at distant sites: hybrid oligonucleotides containing a polymeric linker. Nucl. Acids Res. 21: 4810–4815.

Kiehntopf, M., Brach, M. A., Licht, T., Petschauer, S., Karawajew, L., Kirschning, C. and Hermann, F. (1994) Ribozyme-mediated cleavage of the MDR-1 transcript restores chemosensitivity in previously resistant cancer cells. EMBO J. 13: 4645–4652.

Kijima, H., Ishida, H., Ohkawa, T., Kashani-Sabet, M. and Scanlon, K. J. (1995) Therapeutic application of ribozymes. Pharmacol. Ther. 68: 247–267.

Kijima, H., Bouffard, D. Y. and Scanlon, K. J. (1996) Ribozyme-mediated reversal of human pancreatic carcinoma phenotype. In: Bone Marrow Transplantation-Basic and Clinical Studies, pp. 153–163, Ikehara, S., Takaku, F. and Good, R. A. (eds.) Springer-Verlag, Tokyo.

Kobayashi, H., Dorai, T., Holland, J. F. and Ohnuma, T. (1994) Reversal of drug sensitivity in multidrug-resistant tumor cells by MDR-1 (PGY-1) ribozyme. Cancer Res. 54: 1271–1275.

Koh, J. S. and Dervan, P. B. (1992) Design of a non natural deoxyribonucleoside for recognition of GC base pairs by oligonucleotide-directed triple helix formation. J. Am. Chem. Soc. 114: 1470–1478.

Koizumi, M., Hayase, Y., Iwai, S., Kamiya, H., Inoue, H. and Ohtsuka, E. (1989) Design of RNA enzymes distinguishing a single base mutation in RNA. Nucl. Acids Res. 17: 7059–7071.

Koizumi, M., Kamiya, H. and Ohtsuka, E. (1992) Ribozymes designed to inhibit transformation of NIH3T3 cells by the activated c-Ha-*ras* gene. Gene 117: 179–184.

Koob, M., Grimes, E. and Szybalski, W. (1988) Conferring operator specificity on restriction endonucleases. Science 241: 1084–1086.

Krawczyk, S. H., Milligan, J. F., Wadwani, S., Moulds, C., Froehler, B. C. and Matteucci, M. D. (1992) Oligonucleotide-mediated triple helix formation using an N^3-protonated deoxycytidine analog exhibiting pH-independent binding within the physiological range. Proc. Natl. Acad. Sci. USA 89: 3761–3764.

Kruger, K., Grabowski, P. J., Zaug, A. J., Sands, J., Gottschling, D. E. and Cech, T. R. (1982) Self-splicing RNA: autoexcision and autocyclization of the ribosomal RNA intervening sequence of Tetrahymena. Cell 31: 147–157.

Kumar, P. K. R. and Ellington, A. D. (1995) Artificial evolution and natural ribozymes. FASEB J. 9: 1183–1195.

Kumar, P. K. R., Taira, K. and Nishikawa, S. (1994) Chemical probing studies of variants of the genomic hepatitis delta virus ribozyme by primer extension analysis. Biochemistry 33: 583–592.

Kurzock, R., Gutterman, J. U. and Talpaz, M. (1988) The molecular genetics of Philadelphia chromosome-positive leukemias. N. Engl. J. Med. 319: 990–998.

Lechner, M. S., Mack, D. H., Finicle, A. B., Crook, T., Vousden, K. H. and Laimins, L. A. (1992) Human papillomavirus E6 proteins bind *p53 in vivo* and abrogate *p53*-mediated repression of transcription. EMBO J. 11: 3045–3052.

Le Doan, T., Perrouault, L., Praseuth, D., Habhoub, N., Decout, J. L., Thoung, T., Lhomme, J. and Hélène, C. (1987) Sequence-specific recognition photo crosslinking and cleavage of the DNA double helix by an oligo-[alpha]- thymidylate covalently linked to an azidoproflavine derivatives. Nucl. Acids Res. 15: 7749–7760.

Lee, J. S., Johnson, D. A. and Morgan, A. R. (1979) Complexes formed by (pyrimidine)n . (purine)n DNAs on lowering the pH are three stranded. Nucl. Acids Res. 6: 3073–3091.

Lee, J. S., Woodsworth, M. L., Latimer, L. J. and Moran, J. R. (1984) Poly(pyrimidine)·· poly(purine) synthetic DNAs containing 5-methylcytosine form stable triplexes at neutral pH. Nucl. Acids Res. 12: 6603–6614.

Lemaitre, M., Bayard, B. and Lebleu, B. (1987) Specific antiviral activity of a poly(L-lysine)-conjugated oligodeoxyribonucleotide sequence complementary to vesicular stomatitis virus N protein mRNA initiation site. Proc. Natl. Acad. Sci. USA 84: 648–652.

Leonetti, J. P., Machy, P., Degols, G., Lebleu, B. and Leserman, L. (1990) Antibody-targeted liposomes containing oligodeoxynucleotides complementary to viral RNA selectively inhibits viral replication. Proc. Natl. Acad. Sci. USA 87: 2448–2451.

Leonetti, J. P., Degols, C., Clarenc, J. P., Mechti, N. and Lebleu, B. (1993) Cell delivery and mechanism of action of anti-sense oligonucleotides. Prog. Nucl. Acid Res. Mol. Biol. 44: 143–166.

Leopold, L. H., Shore, S. K., Newkirk, T. A., Reddy, R. M. V. and Reddy, E. P. (1995) Multi-unit ribozyme mediated cleavage of *bcr-abl* mRNA in myeloid leukemias. Blood 85: 2162–2170.

Letai, A. G., Palladino, M. A., Fromm, E., Rizzo, V. and Fresco, J. R. (1988) Specificity in formation triple-stranded nucleic acid helical complexes: studies with agarose-linked poly-ribonucleotide affinity columns. Biochemistry 28: 9108–9112.

Lisziewicz, J., Sun, D., Metelev, V., Zamecnik, P., Gallo, R. C. and Agrawal, S. (1993) Long-term treatment of human immunodeficiency virus-infected cells with anti-sense oligonucleotide phosphorothioates. Proc. Natl. Acad. Sci. USA 90: 3860–3864.

Lowy, D. R., Kirnbauer, R. and Schiller, J. T. (1994) Genital human papillomavirus infection. Proc. Natl. Acad. Sci. USA 91: 2436–2440.

Lu, C. D., Chatterjee, S., Brar, D. and Wong, K. K., Jr. (1994) Ribozyme-mediated *in vitro* cleavage of transcripts arising from the major transforming genes of human papillomavirus type 16. Cancer Gene Ther. 1: 267–277.

Lu, X.-M., Fischman, A. J., Jyawook, S. L., Hendricks, K., Tompkins, R. G. and Yarmusch, M. L. (1994) Antisense DNA delivery *in vivo*: liver targeting by receptor-mediated uptake. J. Nucl. Med. 35: 269–275.

Lyamichev, V. I., Mirkin, S. M. and Frank-Kamenetskii, M. D. (1986) Structure of homopurine-homopyrimidine trait in superhelical DNA. J. Biomol. Struct. Dyn. 3: 667–669.

Lyamichev, V. I., Mirkin, S. M., Frank-Kamenetskii, M. D. and Cantor, C. R. (1988) A stable complex between homopyrimidine oligomers and the homologous regions of duplex DNAs. Nucl. Acids Res. 16: 2165–2178.

Maher, L. J., Wold, B. and Dervan, P. B. (1989) Inhibition of DNA binding proteins by oligonucleotide-directed triple helix formation. Science 245: 725–730.

Maher, L. J., Dervan, P. B. and Wold, B. (1992) Analysis of promoter-specific repression by triple-helical DNA complexes in a eukaryotic cell-free transcription system. Biochemistry 31: 70–81.

Matsushita, H., Kobayashi, H., Mori, S., Kizaki, M. and Ikeda, Y. (1995) Ribozymes cleave the AML1/MTG8 fusion transcript and inhibit proliferation of leukemic cells with t(8;21). Biochem. Biophys. Res. Commun. 215: 431–437.

Mayfield, C., Ebbinghaus, S., Gee, J., Jones, D., Rodu, B., Squibb, M. and Miller, D. (1994) Triplex formation by the human Ha-*ras* promoter inhibits Sp1 binding and *in vitro* transcription. J. Biol. Chem. 269: 18232–18238.

McManaway, M. E., Neckers, L. M., Loke, S. L., Al-Nasser, A. A., Redner, R. L., Shiramizu, B. T., Goldschmidts, W. L., Huber, B. E., Bhatia, K. and Magrath, I. T. (1990) Tumor-specific inhibition of lymphoma growth by an anti-sense oligodeoxynucleotide. Lancet 335: 808–811.

McShan, W. M., Rossen, R. D., Laughter, A. H., Trial, J., Kessler, D. J., Zendegui, J. G., Hogan, M. E. and Orson, F. M. (1992) Inhibition of transcription of HIV-1 in infected human cells by oligonucleotides designed to form DNA triple helices. J. Biol. Chem. 267: 5712–5721.

Melton, D. A. (1985) Injected antisense RNAs specifically block messenger RNA translation *in vivo*. Proc. Natl. Acad. Sci. USA 82: 144–148.

Mergny, J.-L., Sun, J.-S., Rougee, M., Montenay-Garestier, T., Barcelo, F., Chomilier, J. and Hélène, C. (1991) Sequence specificity on triple-helix formation: experimental and theoretical studies of the effect of mismatches on triplex stability. Biochemistry 30: 9791–9798.

Mirkin, S. M., Lyamichev, V. I., Drushlyak, K. N., Dobrynin, V. N., Filippov, S. A. and Frank-Kamenetskii, M. D. (1987) DNA H form requires a homopurine-homopyrimidine mirror repeat. Nature 330: 495–497.

Morgan, A. R. and Wells, R. D. (1968) Specificity of the three-stranded complex formation between double-stranded DNA and single-stranded RNA containing repeating nucleotide sequences. J. Mol. Biol. 37: 63–80.

Moser, H. E. and Dervan, P. B. (1987) Sequence-specific cleavage of double helical DNA by triple helix formation. Science 238: 645–650.

Mouscadet, J. F., Ketterlé, C., Goulaouic, H., Carteau, S., Subra, F., Le Bret, M. and Auclair, C. (1994) Triple helix formation with short oligonucleotide-intercalator conjugates matching the HIV-1 U3 LTR end sequence. Biochemistry 33: 4187–4196.

Mukhopadhyay, T., Tansky, M., Cavender, A. and Roth, J. A. (1991) Specific inhibition of K-*ras* expression and tumorigenicity of lung cancer cells by antisense RNA. Cancer Res. 51: 1744–1748.

Neckers, L., Whitsell, L., Rosolen, A. and Geselwitz, D. A. (1992) Antisense inhibition of oncogene expression. Crit. Rev. Oncog. 3: 175–231.

Ohkawa, J., Koguma, T., Okhda, T. and Taira, K. (1995) Ribozyme: from mechanistic studies to applications *in vivo*. J. Biochem. 118: 251–258.

Ohta, Y., Tone, T., Shitara, T., Funato, T., Jiao, L., Kashfian, B. I., Yoshida, E., Horng, M., Tsai, P., Lauterbach, K., Kashani-Sabet, M., Florenes, V. A., Fodstad, O. and Scanlon, K. J. (1994) H-*ras* ribozyme mediated alteration of the human melanoma phenotype. Annu. Rev. NY Acad. Sci. 716: 242–253.

Ohta, Y., Kijima, H., Kashani-Sabet, M. and Scanlon, K. J. (1996a) Tissue-specific expression of an anti-*ras* ribozyme inhibits proliferation of human malignant melanoma cells. Nucl. Acids Res. 24: 938–942.

Ohta, Y., Kijima, H., Kashani-Sabet, M. and Scanlon, K. J. (1996b) Suppression of the malignant phenotype of melanoma cells by anti-oncogene ribozymes. J. Invest. Dermatol. 106: 275–280.

Ono, A., Ts'o, P. O. P. and Kan, L.-S. (1991) Triplex formation of oligonucleotides containing 2'-O-methylpseudoisocytidine in substitution for 2'-deoxycytidine. Am. Chem. Soc. 113: 4032–4033.

Orson, F. M., Thomas, D. W., McShan, W. M., Kessler, D. J. and Hogan, M. E. (1991) Oligonucleotide inhibition of IL2R alpha mRNA transcription by promoter region colinear triplex formation in lymphocytes. Nucl. Acids Res. 19: 3435–3441.

Orson, F. M., Kinsey, B. M. and McShan, W. M. (1994) Linkage structures strongly influence the binding cooperativity of DNA intercalators conjugated to triplex forming oligonucleotides. Nucl. Acids Res. 22: 479–484.

Pachuk, C. J., Yoon, K., Moelling, K. and Coney, L. R. (1993) Selective cleavage of bcr-abl chimeric RNAs by a ribozyme targeted to noncontinuous sequences. Nucl. Acids Res. 22: 301–307.

Perotta, A. T. and Been, M. D. (1992) Cleavage of oligoribonucleotides by a ribozyme derived from the hepatitis virus RNA sequence. Biochemistry 31: 16–21.

Perroualt, L., Asseline, U., Rivalle, C., Thuong, N. T., Bisagni, E., Giovannangeli, G., Le Doan, T. and Hélène, C. (1990) Sequence-specific artificial photo-induced endonucleases based on triple helix forming oligonucleotides. Nature 344: 450–460.

Pie, D., Corey, D. R. and Schultz, P. C. (1990) Site-specific cleavage of duplex DNA by a semi-synthetic nuclease via triple-helix formation. Proc. Natl. Acad. Sci. USA 86: 9702–9706.

Plum, G. E., Park, Y.-W., Singleton, S. F., Dervan, P. B. and Breslauer, K. J. (1990) Thermodynamic characterization of the stability and the melting behavior of a DNA triplex: a spectroscopic and calorimetric study. Proc. Natl. Acad. Sci. USA 87: 9436–9440.

Postel, E. H., Flint, S. J., Kessler, D. J. and Hogan, M. E. (1991) Evidence that a triplex-forming oligodeoxyribonucleotide binds to the *c-myc* promoter in HeLa cells, thereby reducing *c-myc* mRNA levels. Proc. Natl. Acad. Sci. USA 88: 8227–8231.

Povsic, T. J., Strobel, S. J. and Dervan, P. B. (1992) Sequence-specific double strand alkylation and cleavage of DNA mediated by triple-helix formation. J. Am. Chem. Soc. 114: 5934–5941.

Riley, M., Maling, B. and Chamberlin, M. J. (1966) Physical and chemical characterization of two- and three-stranded adenine-thymine and adenine-uracil homopolymer complexes. J. Mol. Biol. 20: 359–389.

Roberts, T. M. (1992) A signal chain of events. Nature 360: 534–535.

Roninson, I. B. (1991) Molecular and Cellular Biology of Multidrug Resistance in Tumor Cells. Plenum Press, New York.

Roninson, I. B., Chin, J. E., Choi, K., Gros, P., Housman, D. E., Fojo, A., Gottesman, M. M. and Pastan, I. (1986) Isolation of human mdr DNA sequences amplified in multidrug resistant KB carcinoma cells. Proc. Natl. Acad. Sci. USA 83: 4538–4542.

Rowley, J. D. (1973) A new consistent chromosomal abnormality in chronic myelogenous leukaemia identified by quinacrine flourescence and giemsa staining. Nature (Lond.) 243: 290–293.

Scanlon, K. J., Ishida, H. and Kashani-Sabet, M. (1994) Ribozyme-mediated reversal of the multidrug-resistant phenotype. Proc. Natl. Acad. Sci. USA 91: 11123–11127.

Shore, S. K., Nabriss, P. M. and Reddy, E. P. (1993) Ribozyme-mediated cleavage of the *BCR/ABL* oncogene transcript; *in vitro* cleavage of RNA and *in vivo* loss of P210 protein kinase activity. Oncogene 8: 3183–3188.

Skorski, T., Nieborowska-Skorska, M., Nicolaides, N. C., Szczylik, C., Iverson, P., Iozza, R. V., Zon, G. and Calabretta, B. (1994) Suppression of Philadelphia leukemia cell growth in mice by BCR-ABL antisense oligonucleotide. Proc. Natl. Acad. Sci. USA 91: 4504–4508.

Snyder, D. S., Wu, Y., Wang, J. L., Rossi, J. J., Swiderski, P., Kaplan, B. E. and Forman, S. J. (1993) Ribozyme-mediated inhibition of *bcr-abl* gene expression in a Philadelphia chromosome-positive cell line. Blood 82: 600–605.

Stehelin, D., Varmus, H. E., Bishop, J. M. and Vogt, P. K. (1976) DNA related to the transforming gene(s) of avian sarcoma viruses is present in normal avian DNA. Nature 260: 170–173.

Stein, C. A. and Cheng, Y.-C. (1993) Antisense oligonucleotides as therapeutic agents - is the bullet really magical? Science 261: 1004–1012.

Stein, C. A., Tonkinson, J. L., Zhang, L.-M., Yakubov, L., Gervasoni, J., Taub, R. and Rotenberg, S. A. (1993) Dynamics of internalization of phosphodiester oligodeoxynucleotides in HL60 cells. Biochemistry 32: 4855–4861.

Strobel, S. A. and Dervan, P. B. (1991) Single-site enzymatic cleavage of yeast genomic DNA mediated by triple-helix formation. Nature 350: 172–174.

Sun, J. S., Giovannangeli, C., Francois, J. C., Kurfurst, R., Montenay-Garestier, T., Asseline, U., Saison-Behmoaras, T., Thuong, N. T. and Hélène, C. (1991) Triple-helix formation by oligodeoxynucleotides and oligodeoxynucleotide-intercalator conjugates. Proc. Natl. Acad. Sci. USA 88: 6023–6027.

Symons, R. H. (1994) Ribozymes. Curr. Opin. Struct. Biol. 4: 322–330.

Szczylik, T., Skorski, T., Nicolaides, N. C., Manzella, L., Malaguarnera, L., Venturelli, D., Gewirtz, A. M. and Calabretta, B. (1991) Selective inhibition of leukemia cell growth in mice by BCR-ABL antisense oligodeoxynucleotides. Science 253: 562–565.

Teeter, L. D., Eckersberg, T., Tsai, Y. and Kuo, M. T. (1991) Analysis of the Chinese hamster P-glycoprotein/multidrug resistance gene *pgp1* reveals that the AP-1 site is essential for full promoter activity. Cell Growth Differ. 2: 429–437.

Thill, G., Vasseur, M. and Tanner, N. K. (1993) Structural and sequence elements required for the self-cleaving activity of the hepatitis delta virus ribozyme. Biochemistry 32: 4254–4262.

Tone, T., Kashani-Sabet, M., Funato, T., Shitara, T., Yoshida, E., Kashfian, B. I., Horng, M., Fodstad, O. and Scanlon, K. J. (1993) Suppression of EJ cells tumorigenicity. In Vivo 7: 471–476.

Tuschl, T., Gohlke, C., Jovin, T. M., Westhof, E. and Eckstein, F.

(1994) A three-dimensional model for the hammerhead ribozyme based on fluorescence measurements. Science 266: 785–788.

Uhlenbeck, O. C. (1987) A small catalytic oligoribonucleotide. Nature (Lond.) 328: 596–600.

van Tol, H., Buzayan, J. M., Feldstein, P. A., Eckstein, F. and Bruening, G. (1990) Two autolytic processing reactions of a satellite RNA proceed with inversion of configuration. Nucl. Acids Res. 18: 1971–1975.

Versnel, M. A., Hagemeijer, A., Bouts, M. J., van der Kwast, T. H. and Hoogesteden, H. C. (1988) Expression of c-sis (PDGF-B chain) and PDGF-A chain genes in ten human malignant mesothelioma cell lines derived from primary and metastatic tumors. Oncogene 2: 601–605.

Versnel, M. A., Claesson-Welsh, L., Hammacher, A., Bouts, M. J., van der Kwast, T. H., Eriksson, A., Willemsen, R., Weima, S. M., Hoogesteden, H. C., Hagemeijer, A. and Heldin, C.-H. (1991) Human malignant mesothelioma cell lines express PDGF-beta receptors whereas cultured normal mesothelioma cells express predominately PDGF-alpha receptors. Oncogene 6: 2005–2011.

Walder, R. W. and Walder, J. A. (1988) Role of RNase H in hybrid arrested translation by antisense oligonucleotides. Proc. Natl. Acad. Sci. USA 85: 5011–5015.

Walker, I., Irwin, W. J. and Akhtar, S. (1995) Improved cellular delivery of antisense oligonucleotides using transferrin receptor antibody-oligonucleotide conjugates. Pharm. Res. 12: 1548–1553.

Wang, K.-S., Choo, Q.-L., Weiner, A. J., Ou, J.-H., Najarian, R. C., Thayer, R. M., Mullenbach, G. T., Denninston, K. J., Gerin, J. L. and Houghton, M. (1986) Structure, sequence and expression of the hepatitis delta (d) viral genome. Nature (Lond.) 323: 508–514. Corrigendum: Nature (Lond.) 328: 456.

Werness, B. A., Levine, A. J. and Howley, P. M. (1990) Association of human papillomavirus type 16 and 18 E6 protein with p53. Science 248: 76–79.

Whitesell, L., Rosolen, A. and Neckers, L. M. (1991) *In vivo* modulation of N-*myc* expression by continuous perfusion with an antisense oligonucleotide. Antisense Res. Dev. 1: 343–350.

Wickstrom, E. L., Bacon, T. A., Gonzalez, A., Freeman, D. L., Lyman, G. H. and Wickstrom, E. (1988) Human promyelocytic leukemia HL-60 cell proliferation and c-*myc* protein expression are inhibited by an antisense pentadecadeoxynucleotide targeted against c-*myc* mRNA. Proc. Natl. Acad. Sci. USA 85: 1028–1032.

Wickstrom, E., Bacon, T. A. and Wickstrom, E. L. (1992) Down-regulation of c-MYC antigen expression in lymphocytes of Eμ-c-myc transgenic mice treated with anti-c-*myc* DNA methylphosphonates. Cancer Res. 52: 6741–6745.

Wicz, J., Sun, D., Klotman, M., Agrawal, S., Zamecnik, P. and Gallo, R. (1992) Specific inhibition of human immunodeficiency virus type 1 replication by anti-sense oligonucleotides: an *in vitro* model for treatment. Proc. Natl. Acad. Sci. USA 89: 11209–11213.

Wny, G. Y. and Wu, C. H. (1987) Receptor-mediated *in vitro* gene transformation by a soluble DNA carrier system. J. Biol. Chem. 262: 4429–4432.

Wright, L., Wilson, S. B., Milliken, S., Biggs, J. and Kearney, P. (1993) Ribozyme mediated cleavage of the bcr/abl transcription expressed in chronic myeloid leukemia. Exp. Hematol. 21: 1714–1718.

Yokoyama, K. and Imamoto, F. (1987) Transcriptional control of endogenous MYC proto-oncogenes by antisense RNA. Proc. Natl. Acad. Sci. USA 84: 7363–7367.

Zamecnik, P. C. and Stephenson, M. L. (1978) Inhibition of Rous sarcoma virus replication and cell transformation by a specific oligodeoxynucleotide. Proc. Natl. Acad. Sci. USA 75: 280–284.

Zamecnik, P. C., Goodchild, J., Taguchi, Y. and Sarin, P. S. (1986) Inhibition of replication and expression of human T-cell lymphotropic virus type III in cultured cells by exogenous synthetic oligonucleotides complementary to viral RNA. Proc. Natl. Acad. Sci. USA 83: 4143–4146.

STIC-ILL

From: Schnizer, Richard
Sent: Tuesday, July 17, 2001 6:31 AM
To: STIC-ILL
Subject: 09/330,903

Please send me copies of:

TI Simulated lung ***transfection*** by nebulization of liposome cDNA complexes using a cascade impactor seeded with 2-CFSME0-cells.
AU Schreier H; Gagne L; Conary J T; Laurian G
SO JOURNAL OF AEROSOL MEDICINE, (1998 Spring) 11 (1) 1-13.

TI Delivery of DNA-cationic liposome complexes by small-particle ***aerosol*** .
AU Schwarz L A; Johnson J L; Black M; Cheng S H; Hogan M E; Waldrep J C
SO HUMAN GENE THERAPY, (1996 Apr 10) 7 (6) 731-41.

TI Optimization of formulations and conditions for the ***aerosol*** delivery of functional cationic lipid:DNA complexes.
AU Eastman S J; Tousignant J D; Lukason M J; Murray H; Siegel C S; Constantino P; Harris D J; Cheng S H; Scheule R K
SO HUMAN GENE THERAPY, (1997 Feb 10) 8 (3) 313-22.

Thank you-

Richard Schnizer, Ph.D.
Patent Examiner
Art Unit 1632
CM1 12E17
703-306-5441

HUMAN GENE THERAPY 8:313–322 (February 10, 1997)
Mary Ann Liebert, Inc.

Optimization of Formulations and Conditions for the Aerosol Delivery of Functional Cationic Lipid:DNA Complexes

SIMON J. EASTMAN, JENNIFER D. TOUSIGNANT, MICHAEL J. LUKASON, HEATHER MURRAY, CRAIG S. SIEGEL, PAUL CONSTANTINO, DAVID J. HARRIS, SENG H. CHENG, and RONALD K. SCHEULE

ABSTRACT

We have examined several variables inherent in aerosolizing cationic lipid:DNA complexes using a jet nebulizer and thereby have optimized the delivery of functional complexes. Maximal aerosol transfer efficiency of cationic lipid:pDNA complexes was quantitated and shown to require the presence of at least 25 m*M* NaCl as an excipient. This is possibly related to effects on the measured zeta potentials of the complex, which indicate that the complexes are more highly charged in solutions of physiological ionic strength than in solutions of low ionic strength. Inclusion of saline also resulted in retention of the starting lipid to plasmid DNA (pDNA) ratio following nebulization. These data were used to design *in vitro* aerosolization experiments with tissue culture cells that resulted in the identification of a cationic lipid:pDNA ratio of 0.75:1 (mol:mol) as being optimal for aerosolization. This formulation largely protected pDNA from shear degradation during nebulization and produced a respirable aerosol droplet size (1–3 μm). It was tested further in a mouse model and shown to result in the dose-dependent transfection of mouse lungs, generating the equivalent of several picograms of reporter gene activity per mouse lung. The results of these experiments have provided a set of optimal conditions for nebulizing cationic lipid:pDNA complexes that can be used as a starting point for the further evaluation of aerosol delivery of these nonviral gene delivery vectors *in vivo*.

OVERVIEW SUMMARY

Conditions for nebulizing cationic lipid:DNA complexes were evaluated and optimized for efficient transfer of DNA, maintenance of the lipid:DNA ratio, and protection of pDNA from degradation during nebulization. These studies indicated that the suspending medium must have an ionic component to obtain maximal transfer of the DNA and to maintain the lipid:DNA ratio in the aerosolized material. Maximal DNA transfer was found to occur at cationic lipid:DNA ratios where some of the DNA remained uncomplexed. However, free plasmid DNA (pDNA) was also shown to be rapidly degraded during aerosolization, whereas complexed pDNA was largely protected. *In vitro* transfection results from cells exposed to cationic lipid:pDNA aerosols indicated that complexes prepared at a cationic lipid (GL-53):pDNA ratio of 0.75:1 were optimal for transfection. Exposure of BALB/c mice to an aerosol of GL-67:pCF1-CAT prepared at this ratio resulted in the dose-dependent expression of chloramphenicol acetyltransferase (CAT) in the mouse lungs.

INTRODUCTION

GENE THERAPY EMPLOYING NONVIRAL VECTORS is being explored as a potential approach for treating many human afflictions. A major obstacle to the use of this approach is the ability to deliver the therapeutic agent to the target tissues effectively. For diseases of the lung, it is most likely that nonviral vectors such as cationic lipid:plasmid DNA (pDNA) complexes will be administered as aerosols. However, cationic lipid:pDNA complexes have characteristics that present challenges for aerosol delivery. Because they are relatively inefficient as gene transfer agents compared to viruses on a mass or per mole of DNA basis, it will be necessary to deliver relatively large volumes of highly concentrated, active cationic lipid:pDNA complexes to achieve therapeutic efficacy. Because

Genzyme Corporation, Framingham, MA 0701-9322.

lipid:pDNA complexes are colloidal and tend to precipitate at relatively low concentrations, delivering a high dose by an aerosol route could become therapeutically limiting. In addition to this dosing problem, plasmid DNA is known to be degraded by shear stresses such as those present in a jet nebulizer, so that a method of protecting the pDNA from this potential delivery-related degradation is required.

Complexes formed by combining plasmid DNA with cationic lipid vesicles have demonstrated efficacy both *in vitro* (Felgner *et al.*, 1987; Fasbender *et al.*, 1995) and *in vivo* (Stribling *et al.*, 1992; Yoshimura *et al.*, 1992; Alton *et al.*, 1993; Canonico *et al.*, 1994; Conary *et al.*, 1994; Liu *et al.*, 1995; Logan *et al.*, 1995; McLachlan *et al.*, 1995; Solodin *et al.*, 1995). Of particular relevance to the treatment of lung indications by cationic lipid-based gene therapy are recent results demonstrating our ability to achieve high levels of transgene expression in mammalian lung following intranasal instillation of the cationic lipid:pDNA complex (Lee *et al.*, 1996). Practical application of these results to genetic diseases of the lung such as cystic fibrosis requires that we develop the ability to deliver functional transgenes by an aerosol route.

Several studies have demonstrated that cationic lipid-based vectors are capable of mediating gene transfer to the lung following aerosolization (Stribling *et al.*, 1992; Alton *et al.*, 1993; Conary *et al.*, 1994; McLachlan *et al.*, 1995). The aerosolization studies reported thus far have used either DOTMA (Stribling *et al.*, 1992; Alton *et al.*, 1993; Canonico *et al.*, 1994; Canonico *et al.*, 1994; Conary *et al.*, 1994) or DOTAP (Alton *et al.*, 1993; McLachlan *et al.*, 1995), both of which are univalent cationic lipids. Furthermore, these studies focused primarily on the localization of gene expression, and did not report optimization of the delivery of functional cationic lipid:pDNA complexes. Thus, studies that examine the conditions for more efficient aerosolization of functional transgenes are lacking.

Recently, we have shown that aerosol delivery of lipid:pDNA complexes can be enhanced by selection of an appropriate nebulizer (Schwartz *et al.*, 1996). In the present study, we have extended these optimization studies. Using an *in vitro* assay in which the end point was expression of a reporter transgene following aerosolization onto tissue culture cells, several parameters were evaluated, including cationic lipid:pDNA ratio and excipient. The results indicated that an optimal balance could be found between protecting the pDNA from shearing during nebulization and the transfer efficiency of the complex that preserves the cationic lipid:pDNA ratio and provides for maximal potency of the aerosolized complex. Under conditions shown to be optimal by this *in vitro* assay system, it was found that nebulization produced aerosol droplets in the respirable size range that resulted in dose-dependent transfection of mouse lung.

MATERIALS AND METHODS

Cationic lipids GL-53 and GL-67 were synthesized by Genzyme (Cambridge, MA) as described by Lee *et al.* (1996). All experiments used these cationic lipids formulated with the neutral co-lipid dioleoylphosphatidylethanolamine (DOPE; Avanti Polar Lipids, Alabaster, AL) at a either a 1:1 molar ratio (cationic lipid:DOPE) for lipid GL-53 or a 1:2 molar ratio for lipid GL-67. For formulation, the cationic lipids were dissolved in chloroform ($CHCl_3$) and mixed with $CHCl_3$ solution of DOPE. For fluorescently labeled preparations, *N*-lissamine rhodamine B phosphatidylethanolamine (Rh-PE; Avanti Polar Lipids, Alabaster, AL) was added to the $CHCl_3$ solution. The lipid solution was dried down to a thin film under a stream of nitrogen; residual $CHCl_3$ was removed under high vacuum for 1 hr. Lipid films were stored at −80°C.

Two commercially available nebulizers, the Puritan Bennett Raindrop (Puritan Bennett, Lenexa Medical Division, Lenexa, KA) and the Pari LC Jet Plus (Pari Respiratory Equipment, Inc., Richmond, VA) were employed in these studies.

The fluorescent DNA probe benzothiazolium-4-quinolinium dimer (TOTO-1) was purchased from Molecular Probes (Eugene, OR). Opti-MEM was purchased from GIBCO-BRL (Grand Island, NY). Chloramphenicol acetyltransferase (CAT) was purchased from Boehringer Mannheim (Indianapolis, IN). Silica gel thin-layer chromatography (TLC) plates were from EM Separations Technology (Gibbstown, NJ). [^{14}C]Chloramphenicol was obtained from Dupont NEN (Boston, MA). β-Galactosidase (β-Gal) activity was measured employing chlorophenolred-β-D-galactopyranoside (CPRG; Calbiochem, La Jolla, CA) as a substrate. Protein levels were determined with the Coomassie Plus protein assay reagent (Pierce, Rockland, IL). Acetyl-CoA, β-Gal, and all other chemicals were purchased from Sigma Chemical Co. (St. Louis, MO).

Plasmid DNA

pCMV-βGal (Clontech, Palo Alto, CA) was grown in *Escherichia coli* and purified employing Mega-prep columns (Qiagen, Chatsworth, CA) according to the manufacturer's instructions or by a proprietary column chromatographic procedure (Genzyme). Plasmid concentrations were determined by A_{260} measurements. Plasmid purity was assessed using agarose gel electrophoresis and A_{260}/A_{280} ratios. All plasmid preparations showed a major band of closed circular DNA of the expected size on gels and a minor amount (<25%) of nicked plasmid. Only plasmid preparations with A_{260}/A_{280} ratios ≥1.8 were utilized. Endotoxin levels were quantitated with a Limulus Amebocyte Lysate test (BioWhittaker, Inc., Walkersville, MD). DNA preparations with endotoxin levels >100 E.U./mg of plasmid DNA were extracted with Triton X-114 (Aida and Pabst, 1990) to reduce the endotoxin load below 100 E.U./mg. DNA concentrations given are based on an average nucleotide molecular mass of 330.

Aerosol transfer efficiency of cationic lipid:DNA complexes

Dry lipid films were hydrated in sterile pyrogen-free water (Baxter Diagnostics Inc., McGaw Park, IL) to form liposomes. DNA solutions (pDNA or sheared salmon sperm DNA, [sssDNA; 5 Prime R 3 Prime Inc., Boulder, CO]) were prepared in water. Liposomes were labeled with 2.5 mol % Rh-PE, and DNA was labeled with TOTO-1 (1 TOTO-1/1,000 nucleotides). Cationic lipid:pDNA complexes were prepared in water at cationic lipid:DNA ratios (mole:mole) ranging from 0.25:1 to 1.25:1 by adding cationic lipid vesicles to the DNA and incubating for 15 min at room temperature. The complexes were then diluted with concentrated NaCl to give a final DNA concentration of 0.5 m*M*

and the desired NaCl concentration. The samples were added to the nebulizer and the weight difference between the empty and full nebulizer was used to quantitate the exact amount added. Samples were aerosolized into an all glass impinger (AGI; Ace Glass Inc., Vineland, NJ) containing 4 ml of phosphate-buffered saline (PBS). To prevent the formation of negative pressure over the nebulizer, a Y-shaped tube that was open to the atmosphere was placed between the nebulizer and the impinger. This allowed for the influx of diluting air to compensate for the difference in air flow through the nebulizer and AGI. Using this arrangement, no aerosol was seen to escape from the AGI, although a small amount of aerosol did accumulate on the tubing. The nebulizer was weighed after the aerosolization process to determine the amount of material aerosolized. The AGI was rinsed sequentially with 4 ml of octylglucoside buffer (100 m*M* octylglucoside in distilled H_2O), 4 ml of PBS, and finally with another 4 ml of the octylglucoside buffer. The nebulizer was then weighed to determine the total volume of liquid it contained (~16 ml). The amount of material in the impinger was determined by comparing the fluorescence of the impinger solution to standard curves generated with starting material diluted in a 1:1 (vol:vol) solution of PBS and 100 m*M* octylglucoside. Fluorescence was measured with a constant wavelength analysis program on a Spex Fluoromax spectrofluorometer. The lipid:pDNA molar ratio of the aerosolized material was determined by quantitating the lipid (Rh-PE) and DNA (TOTO-1) fluorescence.

Determination of aerosol particle size

Cationic lipid:DNA complexes were prepared from lipid GL-53:DOPE:Rh-PE (1:1:0.025) and sheared salmon sperm DNA (sssDNA) at molar ratios of cationic lipid:DNA ranging from 0.25:1 to 1.25:1. After a 10-min incubation at room temperature, concentrated NaCl was added to give a final NaCl concentration of 150 m*M*. Samples were then aerosolized for 4–5 min and the aerosol stream sampled with an Anderson cascade impactor. Two aerosolization runs were performed at each lipid:DNA ratio.

Zeta potentials

Zeta potentials of the samples were measured (five measurements per sample) employing a Malvern Zetasizer 4 (Malvern Instruments, Southborough, MA.) in a zeta cell (AZ-104 cell, Malvern Instruments Co.). Dried lipid films containing the cationic lipid and DOPE were hydrated in water. Typically DNA was diluted to a concentration of 300 μM in water. The DNA solution was added to an equal volume of cationic lipid vesicles and incubated at room temperature for 10 min. After complex formation, low- and high-ionic-strength samples were prepared by adding NaCl to a final concentration of 1 m*M* and 150 m*M* NaCl, respectively. Photomultiplier signals were maintained below 4,000 counts per second for optimal signal to noise by diluting samples with the appropriate NaCl solution.

In vitro *transfection activity of aerosolized cationic lipid:pDNA complexes*

The ability of aerosolized cationic lipid:pDNA complexes to transfect cells in culture was assessed using the immortalized cystic fibrosis (CF) airway epithelial cell line CFT1 (Yankaskas *et al.*, 1993). CFT1 cells were plated in 96-well microtiter plates at 7.5×10^3 cells/well and grown to confluency. Cationic lipid:pDNA complexes (GL-53:DOPE:Rh-PE [1:1:0.005]) were prepared at different cationic lipid:pDNA ratios by adding 4 ml of cationic lipid vesicles in water to 4 ml of pDNA in a sterile 15-ml conical tube, mixing by inversion, and then incubating at room temperature for 10 min. Concentrated NaCl (2 ml) was then added, giving final pDNA and NaCl concentrations of 0.5 m*M* and 150 m*M*, respectively, and the sample mixed by inversion. To prevent exposure of half of the cells on the 96-well microtiter plate to the aerosol, one-half of the wells were covered with an adhesive plastic film (SealPlate, Rainin Instruments Co. Inc., Woburn, MA). The medium in the remaining wells were aspirated and replaced with 50 μl of Opti-MEM. The plate was placed in an acrylic box connected to the nebulizer and exposed to one reservoir of aerosol prepared at the desired cationic lipid:pDNA ratio. The box was vented through a Pall BB-50T Breathing Circuit Filter (Pall Biomedical Inc., Fajardo PR 00648). After aerosolization, an additional 50 μl of Opti-MEM was added to each of the wells that had been exposed to the aerosol. After a 4-hr incubation at 37°C, 50 μl of Opti-MEM containing 30% fetal bovine serum (FBS) was added to each well. The cells were fed the next day with 100 μl of Opti-MEM containing 10% FBS. β-Gal activity in the cells was assayed 2 days post-treatment using methods previously described (Felgner *et al.*, 1994).

To quantitate the amount of lipid transferred onto the CFT1 cells following aerosolization, a 96-well microtiter plate containing 100 μl of 1% SDS/well was placed in the acrylic box next to the plate containing the cells. After aerosolizing the complex into the box, the Rh-PE fluorescence in each well of the microtiter plate was measured with a fluorescence plate reader (Cytofluor 2350, Millipore) and quantitated using a standard curve prepared from the starting material. The aerosol was found to distribute evenly over the 96-well plate for all lipid:pDNA ratios tested.

The concentration of the cationic lipid:pDNA complex in the nebulizer reservoir after aerosolization was calculated by comparing the Rh-PE fluorescence of an aliquot to a standard curve of Rh-PE fluorescence prepared from the starting material. The concentration of pDNA was then estimated assuming that the molar ratio of cationic lipid:pDNA remained essentially the same throughout the nebulization procedure (see Fig. 1B).

Aliquots of the starting material (nonaerosolized complex) and material remaining in the nebulizer at the end of the nebulization were removed to compare their *in vitro* transfection efficiencies with that of the aerosolized material. Both the starting and ending material were diluted with Opti-MEM to a DNA concentration of approximately 100 μM. Aliquots (250 μl) of the diluted complexes were added to each of three wells of a 96-well microtiter plate and serially diluted with Opti-MEM to give a range of DNA concentrations (100 μM to 0.78 μM). After aspirating the medium from the CFT1 cells that had been protected from exposure to the aerosol, 100 μl of these serially diluted complexes were added to the corresponding wells of the plate containing the CFT1 cells. After a 4-hr incubation at 37°C, 50 μl of Opti-MEM containing 30% FBS was added to each

well. The cells were fed the next day with 100 μl of Opti-MEM containing 10% FBS. β-Gal activity was assayed 2 days after exposure to the complexes employing methods previously described (Felgner *et al.*, 1994).

Agarose gel electrophoresis

Aliquots of the cationic lipid:pDNA complexes were removed from the nebulizer reservoir after 0, 5, 10, 15, 20, 25, and 30 min of aerosolization at the end of the experiment for agarose gel electrophoresis. Because the cationic lipid:pDNA complexes became concentrated during the aerosolization procedure, the rhodamine fluorescence of each sample, within each group (*i.e.*, each cationic lipid:pDNA ratio), was adjusted to the same level as the non-aerosolized sample. Because the pDNA ratio was maintained during aerosolization, this correction insured that the same amount of pDNA was loaded into each well. Aliquots of each sample were added to two 0.5-ml microcentrifuge tubes and diluted with either water or 1% SDS (0.33% final concentration); 10 μl of loading buffer (25% sucrose, Orange G to color) was added to each sample. Samples were vortexed briefly and 30 μl loaded on a 0.75% (wt/vol) agarose gel (~1.3 μg pDNA/well). Gels were electrophoresed in 1× Tris-borate-EDTA (TBE) at 100 V for 1–1.5 hr, stained overnight with SYBR Green nucleic acid stain (Molecular Probes Inc., Eugene, OR), and photographed employing a SYBR Green photographic filter.

In vivo *transfection by aerosolized cationic lipid:pDNA complexes*

The ability of an aerosolized cationic lipid:pDNA formulation to transfect mouse lungs was assessed employing a pCF1-CAT, a plasmid encoding the CAT gene (Lee *et al.*, 1996). Sixteen female BALB/c mice were placed in an Intox nose-only exposure chamber and exposed to between one and four 10-ml reservoirs of aerosolized cationic lipid GL-67:DOPE (1:2):pDNA complex prepared at a cationic lipid GL-67:pDNA molar ratio of 0.75:1 and a DNA concentration of 2 m*M* in 25 m*M* NaCl. Four mice were removed after aerosol delivery of each reservoir of complex. All mice were sacrificed 2 days after exposure to the aerosol, their lungs excised, perfused with PBS, homogenized, and assayed for CAT activity following reported procedures (see Lee *et al.*, 1996). Mice naive to treatment were used to establish background levels of chloramphenicol acetylation.

RESULTS

Previously, we have identified several cationic lipid:pDNA formulations capable of mediating efficient gene transfer into lungs following intranasal instillation into mice (Lee *et al.*, 1996). Initially, the most potent cationic lipid identified was that designated GL-53. The complexes that produced the highest levels of activity were those prepared at cationic lipid:pDNA molar ratios of approximately 0.25:1. Agarose gel electrophoresis of these complexes indicated the presence of a large excess of unbound DNA. Because the most likely route of administration of gene therapy vectors to the lungs of CF patients is through an aerosol, and because we had observed (unpublished observations) that uncomplexed, or "free" pDNA was rapidly degraded during aerosolization, we sought to optimize aerosol delivery of cationic lipid GL-53:pDNA formulations using a commercially available nebulizer.

Effect of ionic strength of the suspending medium on the transfer efficiency of cationic lipid:DNA complexes

Initial experiments were designed to optimize the amount of lipid:DNA complex delivered by aerosol. Cationic lipid GL-53:DNA complexes were prepared at molar ratios of cationic lipid:DNA ranging from 0.25:1 to 1.25:1. Following preparation the complexes were diluted with water or NaCl and then nebulized. The effects of excipient and cationic lipid:DNA ratio on transfer efficiency were examined using fluorescently labeled lipid and DNA. Figure 1A shows that the transfer efficiency of complexes suspended in water decreased as the cationic lipid:DNA ratio increased. This decrease was much less apparent when complexes were nebulized from a saline-containing solution. For all cationic lipid:DNA ratios above 0.25:1, complexes were transferred by aerosol twice as efficiently from saline as from water. Nebulization from water was also found to result in precipitation of the cationic lipid:DNA complex that adsorbed to the sides of the nebulizer. The amount of this precipitated complex increased as the ratio of lipid to DNA increased; the greatest amount of precipitation by far occurred at the 1.25:1 ratio.

Figure 1B shows that the initial ratio of cationic lipid:DNA was maintained poorly in the aerosol when the complexes were aerosolized from water. For complexes prepared in water at cationic lipid:DNA ratios of ≤0.75:1, DNA was more readily transferred than lipid, resulting in cationic lipid:DNA ratios in the aerosolized material that were 50–70% those of the starting material. This was most likely a result of the loss of complex due to precipitation from water and adsorption to the nebulizer, with subsequent preferential transfer of the remaining uncomplexed DNA. This hypothesis is consistent with the observation that the ratio of cationic lipid:DNA in the aerosolized material was closer to that of the starting ratio for samples produced at higher lipid:DNA ratios (Fig. 1B), where less free DNA was present. For the complex nebulized from water at a 1.25:1 cationic lipid:DNA ratio, cationic lipid was preferentially transferred through the aerosol. This can also be explained by precipitation of the complex, because the relative concentration of DNA would be decreased when precipitated as part of the complex, and excess, uncomplexed cationic lipid would remain in suspension and be transferred.

In contrast to the results using water suspensions, Fig. 1B shows that the initial ratio of cationic lipid:DNA was well maintained when 150 m*M* NaCl was used as the excipient. For complexes prepared with an excess of cationic lipid (molar ratio 1.25:1), the cationic lipid was preferentially aerosolized, resulting in a cationic lipid:DNA molar ratio in the aerosolized material that was ~130% that of the starting ratio. This is significantly better than observed with water, where the ratio of lipid:DNA in the aerosolized material was ~150% that of the starting material. A titration of the NaCl concentration in these experiments indicated that identical transfer efficiencies and maintenance of molar ratios could be obtained by NaCl concentrations as low as 25 m*M* (data not shown).

Effect of ionic strength of the suspending solution on the zeta potential of cationic lipid:DNA complexes

To determine if the differences in transfer efficiencies observed in water and saline were related to the surface charge characteristics of the complexes, zeta potentials of the cationic lipid:pDNA complexes were determined in buffers of low (1 m*M* NaCl) and physiological (150 m*M* NaCl) ionic strength. Figure 1C shows that there were significant differences between the zeta potentials of the complexes in buffers of different ionic strength, the complexes being significantly more negative in a solution of physiological ionic strength than in one of low ionic strength, at any given molar ratio. Thus, for example, at a molar ratio of 1.25, a complex in 1 m*M* NaCl had a positive zeta potential of approximately +20 mV, whereas at the identical molar ratio, a complex in 150 m*M* NaCl exhibited a negative zeta potential of approximately −50 *m*V. As the zeta potential of a colloid determines how it will interact with other surfaces (in terms of ionic interactions), this large difference in zeta potentials may be partially responsible for the differences in stability (resistance to precipitation) of complexes prepared at different ionic strengths.

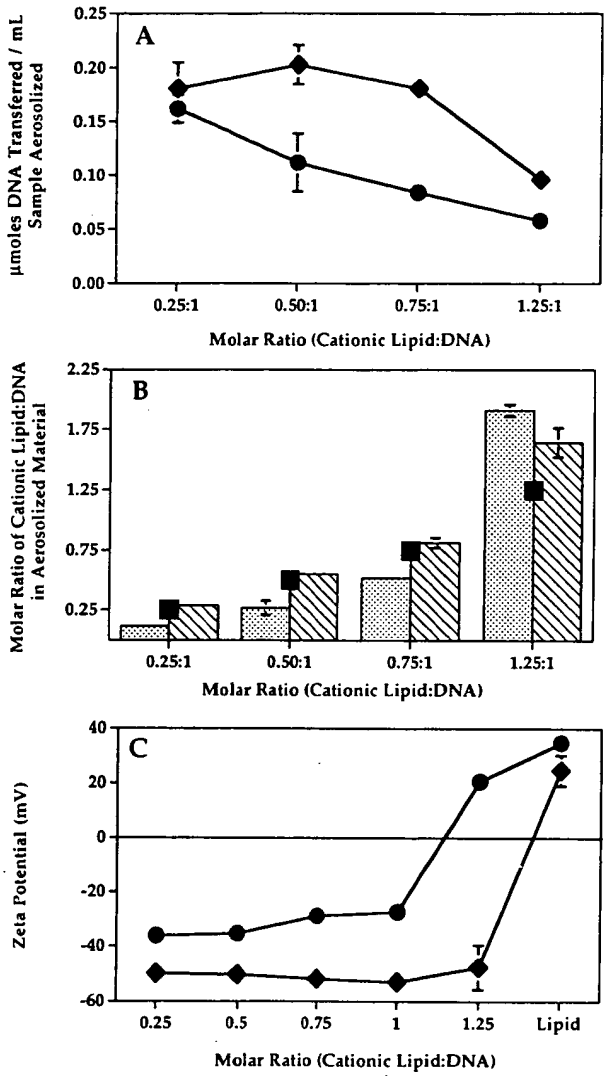

FIG. 1. Effects of salt and molar ratio on aerosolization of cationic lipid:pDNA complexes. Lipid GL-53:DOPE:DNA complexes were prepared at cationic lipid:DNA molar ratios of 0.25:1 to 1.25:1 and aerosolized (Puritan Bennett Raindrop Nebulizer, 50 psi, 8.4 liters/min) into an AGI. Aliquots were quantitated for lipid and pDNA as described in the Methods. A. Transfer efficiency (μmoles of DNA transferred/ml of material aerosolized) of cationic lipid:pDNA complexes in water (●) and 150 m*M* NaCl (◆). B. Maintenance of cationic lipid:pDNA molar ratio in water (shaded bars) and 150 m*M* NaCl (hatched bars); starting ratio (■). C. Zeta potentials of cationic lipid GL-53:DOPE/DNA complexes prepared either in 1 m*M* NaCl (●) or 150 m*M* NaCl (◆). Values shown depict means of three determinations; error bars reflect standard deviation.

Effect of nebulizer shear forces on pDNA integrity

Given the potential for shear force-mediated pDNA degradation during nebulization in a jet nebulizer, optimal transfection efficiency of an aerosolized lipid:pDNA complex would be expected to occur when all of the pDNA is complexed. The integrity of the pDNA during aerosolization using a Puritan Bennett Raindrop nebulizer was examined as a function of the molar ratio of cationic lipid:pDNA. In Fig. 2, agarose gel electrophoresis of samples removed from the nebulizer reservoir at various time points throughout the aerosolization process showed that uncomplexed pDNA was degraded during aerosolization. Thus, for example, free pDNA in complexes prepared at a 0.25:1 ratio became progressively more degraded with time, as can be seen in the samples run in the absence of detergent (lanes 1–8 for each lipid:pDNA ratio). Degradation also occurred with time at higher lipid:pDNA ratios, but was less obvious because the complexed pDNA did not leave the sample well. The integrity of the pDNA in the complexes at higher ratios was visualized by dissociating the complex with detergent prior to electrophoresis (lanes 9–16). Under these conditions, it could be seen that some pDNA degradation occurred even at a 1.25:1 ratio. It should be noted that the bright band within the degraded pDNA smear was determined to be rhodamine-PE, most likely bound to SDS. This was obvious upon visualization of the gels, as this band became stronger as the lipid:pDNA ratio was increased and had a red fluorescence, while the DNA fluoresced green. The extent of pDNA degradation at a given time of nebulization was seen to decrease progressively as the ratio of cationic lipid:pDNA was increased, *i.e.*, as more of the pDNA became complexed with lipid.

The extent and rate of pDNA degradation observed were found to be dependent on the nebulizer. Using a different nebulizer, namely the Pari LC Jet Plus, more rapid degradation of free pDNA was observed, but no degradation of complexed pDNA was seen (data not shown). The increased rate of free pDNA degradation was most likely due to the higher consumption rate (the volume of material leaving the nebulizer per unit time) of the Pari nebulizer (~0.55 ml/min) compared to that of the Puritan Bennett Raindrop (~0.175 ml/min), which for the material remaining in the reservoir translated into more cycles through the nebulizer per minute.

Transfection efficiency of aerosolized cationic lipid:pDNA complexes in vitro

The ability of aerosolized cationic lipid:pDNA complexes to transfect cells *in vitro* was examined as a function of the mo-

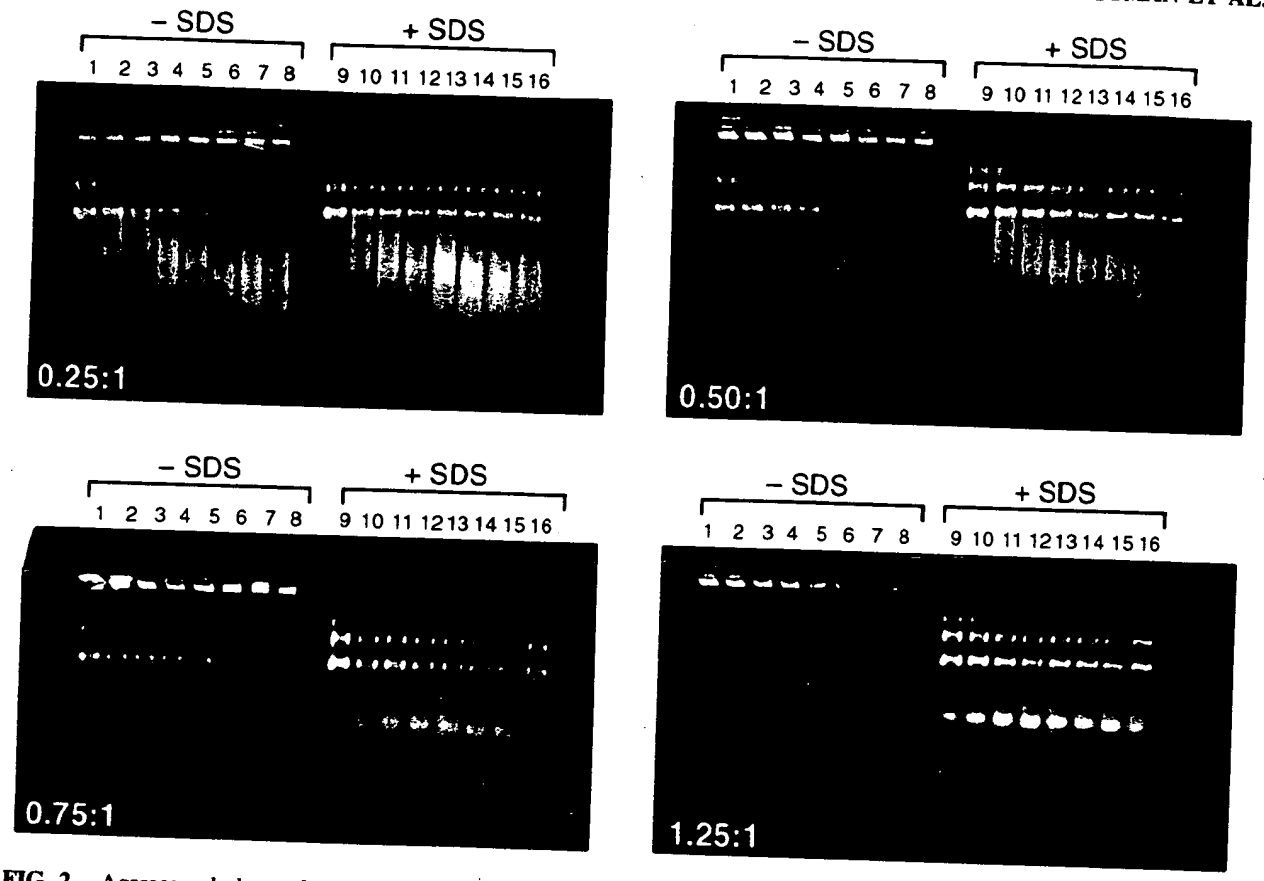

FIG. 2. Agarose gel electrophoresis of samples removed from the nebulizer reservoir was performed in the absence or presence of detergent to disrupt the complex. Samples were removed before aerosolization, at time points of 0, 5, 10, 15, 20, 25 and 30 min, and at the end of the nebulization (~40 min). Samples were diluted with water or 1% SDS (0.33% final concentration) and loading dye was added. Samples were run on a 0.75% agarose gel for 1 hr and then stained overnight with SYBR Green.

lar ratio of cationic lipid:pDNA. Figure 3 shows that the highest levels of CFT1 cell transfection by the aerosolized complex were obtained when the complex was prepared at a molar ratio of 0.75:1, with a steady increase in transfection efficiency as the molar ratio of lipid to DNA was increased from 0.25:1 to 0.75:1. Importantly, the activity of the aerosolized complex was at least as great as that of the starting material at the equivalent concentration, *i.e.*, aerosolization did not lead to a loss of transfection activity. In fact, in this experiment, aerosolization appeared to increase the activity of the complex. The reason for this increase is not clear, but may be related to the homogenizing action of the nebulizer and the creation of a more uniform complex. There were also differences between the specific activities of the starting complex and the material left in the nebulizer. Because the complexes removed from the nebulizer before and after aerosolization were diluted to the same lipid concentration before being serially diluted and added to the cells, this increased activity most likely reflects a change in the homogeneity of the complex. The loss of activity in the sample prepared at a 1:25:1 ratio may reflect an overestimation of the DNA concentration since the molar ratio of the components did not stay constant through aerosolization at this ratio (see Fig. 1B). In several other experiments, the activity of the complex in the nebulizer at the end of the aerosolization was approximately equal to or somewhat greater than the activity of the starting material, although when higher concentrations of DNA were employed, the material remaining in the nebulizer pot was less active than the starting material (data not shown).

Particle size of aerosol

The aerosol generated by nebulizing complexes prepared at different molar ratios of cationic lipid:pDNA was characterized using an Anderson Cascade Impactor and a fluorescent lipid to monitor the size distribution of the complex. Figure 4 demonstrates that the distribution of aerosol droplet sizes produced by the Puritan Bennett Raindrop nebulizer was in the respirable size range and that this was similar for complexes prepared over the entire range of molar ratios of cationic lipid:DNA tested. The peak aerosol droplet size became progressively smaller as the lipid:DNA ratio was increased, but the mass median aerodynamic diameter (mmad) differed by only 0.19 μm between the extremes of lipid:DNA molar ratios employed. The geometric standard deviation ranged from 3.26 to 2.78 for the complexes prepared at molar ratios of 0.25 and 1.25:1, respectively.

Although the air pressure through the Bennett Raindrop nebulizer was maintained at 50 psi, the flow of air through the nebulizer had to be restricted to 8.4 liter/min instead of the maximally obtainable 13.6 liter/min to minimize loss of sample due to splattering. The splattering of relatively viscous samples of cationic lipid:DNA complexes out of the nebulizer proved to be a significant problem with the Puritan-Bennett Raindrop nebu-

lizer. Because of this relatively low flow rate, the consumption rates of the cationic lipid:pDNA complexes employing this nebulizer were on the order of 0.175 ml/min. When cationic lipid vesicles alone were nebulized, no splattering was observed, and the nebulizer could be run at its maximal flow rate, resulting in significantly higher consumption rates of ~0.6 ml/min.

Transfection of mouse lungs by a cationic lipid:pDNA aerosol

During the course of these aerosol characterization studies, a new cationic lipid was identified that was significantly more efficacious than lipid GL-53 in intranasal instillation experiments in mice. Although structurally similar to lipid GL-53, this new lipid (lipid GL-67) was found to have optimal activity when formulated with DOPE at a molar ratio of 1:2 (see Lee *et al.*, 1996). To maximize the transfection efficiency of an aerosol delivery using GL-67, pilot experiments were performed to evaluate its aerosol characteristics. Lipid:pDNA complexes were prepared using cationic lipid GL-67 at a cationic lipid:pDNA molar ratio of 0.75:1 (optimal ratio for *in vitro* transfection; see Fig. 3) and the transfer efficiency of the complex was evaluated as described above for lipid GL-53:pDNA complexes. The GL-67:pDNA complex was found to be efficiently transferred by aerosol using the P/B Raindrop nebulizer in the presence of 25 m*M* NaCl, as was found for lipid #GL-53 (see above). Agarose gel electrophoresis of the complex prepared at the 0.75:1 molar ratio indicated that a small amount of pDNA remained uncomplexed at this ratio and was degraded during aerosolization; the majority of complexed pDNA was found to remain intact throughout the aerosolization procedure (data not shown).

Employing this formulation, groups of 4 BALB/c mice were exposed to an aerosol of from one to four reservoirs of lipid GL-67:pCF1-CAT in a nose-only exposure chamber. After exposing all the animals to one 10-ml reservoir of complex, a process that took approximately 40 min, 4 animals were removed and the remaining animals were exposed to a second reservoir. The remaining 8 mice were allowed to rest for a period of 2 hr before exposing both groups of 4 mice to a third dose and one group to fourth dose of aerosol. Figure 5 shows that the lungs of mice exposed to the cationic lipid:pCF1-CAT aerosol exhibited a dose-dependent expression of CAT activity. Mean levels of CAT expression ranged from 1.31 ± 0.56 to 17.33 ± 9.13 pg CAT/100 mg of tissue for animals exposed to from one to four reservoirs of aerosolized lipid:pDNA complexes. For comparison, intranasal instillation of 50 μl of the starting material into 3 mice resulted in a mean CAT expression of 475 ± 122 pg CAT/100 mg of lung tissue.

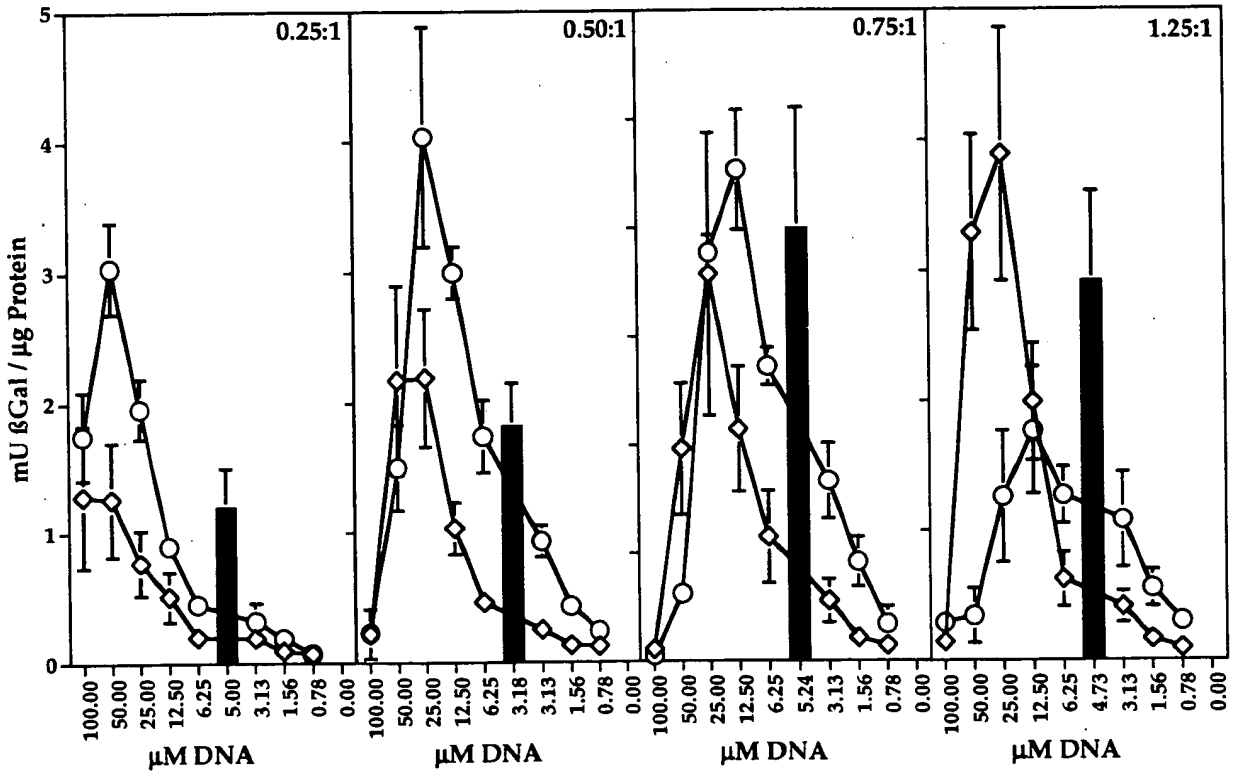

FIG. 3. *In vitro* transfection efficiency of lipid GL-53:DOPE/pCF1-β-Gal complexes prepared as a function of cationic lipid:pDNA ratio. Complexes were prepared in water and incubated for 10 min at room temperature. Following addition of NaCl to a concentration of 150 m*M*, the complexes were aerosolized onto CFT1 cells in a microtiter plate in an acrylic box. Known amounts of starting and ending material were added to unexposed cells. Symbols represent expression levels of β-Gal observed from cells exposed to the starting material (◇), ending material (○), and the bars represent the levels from cells exposed to the aerosol. Values shown depict means of three determinations; error bars reflect standard deviation.

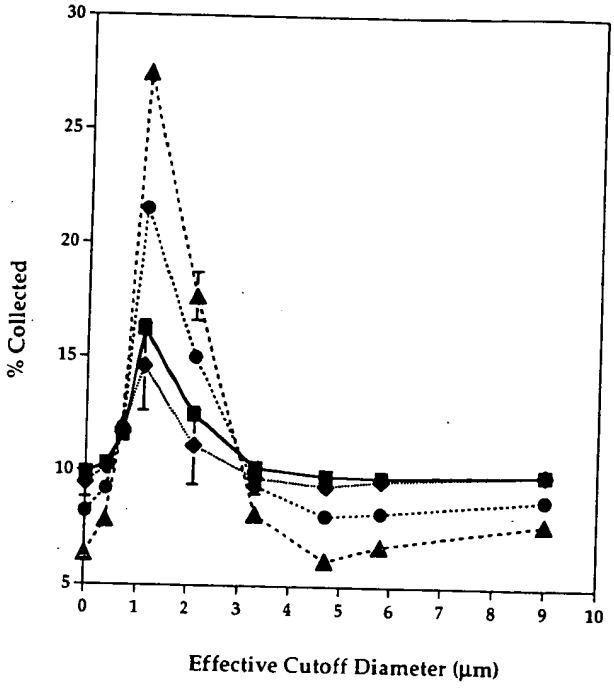

FIG. 4. Aerosol size distributions as a function of molar ratio. Lipid GL-53:DOPE/DNA complexes were prepared at the desired cationic lipid:DNA ratio. Samples were aerosolized with a Puritan Bennett Raindrop nebulizer (50 psi, 8.4 liters/min). Aerosol was generated for 4–5 min and sampled with an Anderson cascade impactor to determine the aerosol particle size. Lipid vesicles were labeled with rhodamine-PE for detection. Cationic lipid:pDNA molar ratios were 0.25 (■), 0.50 (◆), 0.75 (●), and 1.25:1 (▲). Values shown depict means of three determinations; error bars reflect standard deviation.

DISCUSSION

The ability to treat diseases effectively by gene therapy will require delivery of potent vectors to the appropriate target tissues. For diseases that affect the lung, such as CF, the most likely practical route of administration is by aerosol. Previous investigations have shown that aerosol delivery of cationic lipid:pDNA complexes to animal lungs can result in transgene expression (Stribling *et al.*, 1992; Alton *et al.*, 1993; Canonico *et al.*, Conary *et al.*, 1994; 1994; McLachlan *et al.*, 1995). However, these studies involved the use of a single lipid:pDNA formulation and have not reported optimization of the parameters required for the most efficient delivery of functional cationic lipid:pDNA complexes by an aerosol route.

To optimize the conditions required for aerosol delivery of lipid:pDNA complexes, we have examined several parameters, including the ionic strength of the suspending medium, the cationic lipid:pDNA ratio, the zeta potentials of the complexes, and the extent of pDNA binding to the cationic lipid. These parameters were optimized for: (i) maximal transfer of the complex through the aerosol while maintaining the initial cationic lipid:pDNA ratio, (ii) maximal complexation of the pDNA to protect it from shear, and (iii) maximal *in vitro* transfection activity of the aerosolized complex. Once an optimal aerosol formulation was found, it was characterized for its ability to deliver functional transgenes in an animal model, both in terms of aerosol droplet size and transfection activity.

The most efficient transfer of complexes, *i.e.*, the greatest amount of pDNA transferred while maintaining the initial lipid:pDNA molar ratio, was observed when NaCl was present in the suspending medium (Fig. 1). In nonionic media such as water or 5% trehalose (data not shown), the aerosol transfer efficiency of the pDNA was found to be reduced and the lipid:pDNA molar ratio was poorly maintained. This ionic strength effect became more obvious at higher ratios of cationic lipid:pDNA (Fig. 1). The effect of ionic strength on the zeta potential of the complex may in part account for these effects. It was observed that as the charge on the complex approached neutrality it tended to precipitate and adsorb more readily to surfaces. Based on the zeta potential data shown in Fig. 1C, increasing the ionic strength of the suspending medium has the effect of maintaining a negative surface charge on the complex at higher mole ratios of cationic lipid:pDNA, and may thereby prevent precipitation and improve the aerosol transfer characteristics of the complex. To maximize transfer of the complexes containing GL-53 or GL-67 by aerosol and to maintain the initial molar ratio of cationic lipid:pDNA in the aerosolized material, the data suggested that optimal aerosolization should occur in saline (≥25 m*M* NaCl) at cationic lipid:DNA molar ratios ≤0.75:1.

To protect pDNA from shearing during aerosolization, one would predict that it should be maximally complexed with the cationic lipid. This prediction is validated by the data shown in

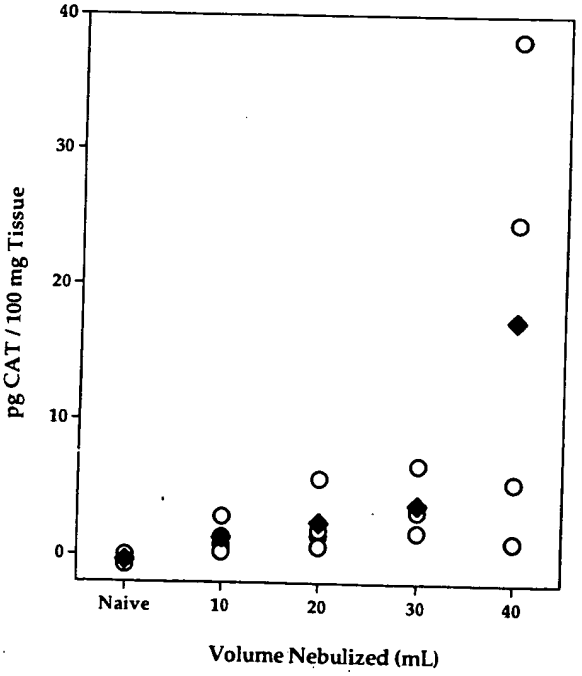

FIG. 5. BALB/c mice were exposed to between 10 and 40 ml of aerosol containing lipid GL-67:DOPE (1:2)/pCF1-CAT at a molar ratio of 0.75:1 and 2 m*M* DNA in 25 m*M* NaCl in an Intox nose-only exposure chamber. Two days after exposure, the mice were sacrificed, the lungs excised and assayed for CAT activity as described in the Materials and Methods section. Symbols indicate CAT levels of individual animals (○) or mean values (◆).

Fig. 2. That is, as the molar ratio of cationic lipid:pDNA was increased, less pDNA degradation was seen over the course of the aerosolization. However, even at the highest molar ratio tested, 1.25:1, at which all pDNA was complexed to lipid, a fraction of the pDNA eventually became degraded as a result of the nebulization process. These results therefore imply that aerosolization would be optimal at molar ratios $\geq$1.25:1. However, at these lipid:DNA ratios, the complexes were found to aggregate and precipitate during nebulization, resulting in less efficient transfer of the complex. Taken together, these DNA protection data and aerosol transfer data (Fig. 1) predict that optimal transfection by aerosol would occur in saline at a molar ratio for which the effects of pDNA transfer are balanced by the effects of pDNA protection.

This hypothesis was tested *in vitro* by aerosolizing cationic lipid:pDNA complexes onto tissue culture cells as a function of the cationic lipid:pDNA ratio. The data shown in Fig. 3 indicate that the effects of transfer and pDNA protection resulted in optimal transfection at a molar ratio of 0.75:1. Not only was a maximum amount of pDNA transferred at this ratio, but the transferred complex appeared to be optimally "potent" at this ratio. In other words, a comparison of the relative amounts of enzymatic activity generated normalized to the amount of pDNA transferred as a function of cationic lipid:pDNA ratio showed that potency was greatest for complexes aerosolized at the 0.75:1 ratio. Potencies of 0.24, 0.56, 0.76, and 0.61 mU β-Gal/1 μM pDNA (1 μM pDNA $\cong$ 33 ng pDNA/100 μl) were observed at molar ratios of 0.25, 0.50, 0.75, and 1.25:1, respectively. Thus, optimal *in vitro* transfection by an aerosol of lipid:pDNA complex was achieved in saline at a cationic lipid:pDNA ratio for which most of the pDNA was bound to lipid (Fig. 2), the complex possessed a negative zeta potential of approximately 50 mV (Fig. 1C), pDNA transfer was maximal (Fig. 1A), and the ratio was maintained throughout nebulization (Fig. 1B).

Optimal *in vivo* aerosol deposition in the respiratory tract requires aerosol droplet sizes in the 1- to 5-μm range (Bates *et al.*, 1966). Characterization of the aerosol droplet sizes generated by nebulizing the cationic lipid:pDNA complexes from saline (Fig. 4) demonstrated that the mean droplet diameters of the cationic lipid:pDNA complex preparations were in the 1- to 2-μm size range and therefore should be appropriate for transfection of the respiratory tract. This hypothesis was tested in a mouse model (Fig. 5). The resultant data demonstrated that the *in vitro* optimized aerosol formulation was capable of transfecting mouse lung in a dose-dependent fashion. Animal-to-animal variation was significant at the highest dose, with a mean expression of ~17 pg CAT/100 mg of lung tissue.

This level of expression was significantly lower than that obtained by intranasal instillation of material removed from the nebulizer reservoir before aerosolization (50 μl of complex gave ~425 pg CAT/100 mg of lung tissue), and most likely was due to differences in the doses received by the animals by the two delivery routes. The aerosol dose received by the mice is estimated to be much less than the 50 μl instilled. Deposition studies that involved extracting the lipid component of aerosolized rhodamine-PE labeled complexes from the lungs of mice with organic solvents by the method of Bligh and Dyer (1959) indicated that only approximately 2 μl of complex were deposited in a mouse lung for every 10 ml of material aerosolized (data not shown). When compared on the basis of delivered dose, aerosolization and instillation gave similar specific expression levels. Aerosolization of the complex resulted in approximately 2 pg of CAT/100 mg per μl delivered whereas instillation produced approximately 8 pg of CAT/100 mg per μl delivered.

It is important to realize that the optimized aerosol formation determined from these experiments is significantly different from that found to be optimal for instillation (Lee *et al.*, 1996). Optimal lung expression following instillation of GL-67:pDNA complexes was found to require a cationic lipid:pDNA ratio of ~0.25 and the total absence of excipients. In contrast, the optimal ratio of cationic lipid GL-67:pDNA found for aerosol delivery was 0.75, and a NaCl concentration of at least 25 mM was required. These modifications of the instillation formulation were necessitated by the need for efficient plasmid transfer and protection from degradation during nebulization. The optimized aerosol formulation is ~20 to 40-fold *less* active by instillation from the formulation that had been optimized for delivery by intranasal instillation. That is, intranasal instillation of 50 μl of the aerosol formulation (1.5 mM lipid GL-67:2 mM DNA in 25 mM NaCl) resulted in CAT expression levels of 425 pg of CAT/100 mg of tissue compared to approximately 10 ng of CAT/100 mg of tissue for 50 μl of a formulation optimized for intranasal instillation (0.5 mM GL-67:2 mM DNA in water). However, the formulations optimized for intranasal instillation were either much less active than the optimized aerosol formulation or completely inactive when delivered *via* an aerosol.

Although it is clear that the present aerosol formulation is capable of transfecting lung tissue by an aerosol route, it is also clear that there is a need to exceed the current expression levels. In principle, expression levels can be increased by increasing the deposition of the complex, *i.e.*, the "dose," or by increasing the potency of the complex. Major limitations of the present optimized aerosol formulation that must be overcome to obtain greater levels of transfection by aerosolization of cationic lipid:pDNA complexes are: (i) the suspension instability of complexes prepared at higher concentrations under conditions in which all of the pDNA is complexed with lipid for protection against nebulizer-induced degradation, and (ii) the requirement for an ionic excipient, *e.g.*, NaCl, in the formulation, which depresses transfection activity. Present studies are focused on developing new formulations of cationic lipid:pDNA complexes with the potential of increasing aerosol-mediated transfection. This research will help determine the practical utility of aerosol delivery of cationic lipid:pDNA vectors for the gene therapy of respiratory indications.

ACKNOWLEDGMENTS

The authors wish to thank Nick Wan, Dave McNeilly, and MariBeth Cherry for pDNA production and Ed Lee and Matt Lane for cationic lipid synthesis.

REFERENCES

AIDA, Y., and PABST, M.J. (1990). Removal of endotoxin from protein solutions by phase separation using Triton X-114. J. Immunol. Meth. **132,** 191–195.

ALTON, E.W.F.W., MIDDLETON, P.G., CAPLEN, N.J., SMITH, S.N., STEEL, D.M., MUNKONGE, F.M., JEFFERY, P.K., GEDDES, D.M., HART, S.L., WILLIAMSON, R., FASOLD, K.I., MILLER, A.D., DICKINSON, P., STEVENSON, B.J., McLACHLAN, G., DORIN, J.R., and PORTEOUS, D.J. (1993). Non-invasive liposome-mediated gene delivery can correct the ion transport defect in cystic fibrosis mutant mice. Nature Genet. **5,** 135–142.

BATES, D.V., FISH, B.R., HATCH, T.F., MERCER, T.T., and MORROW, P.E. (1966). Deposition and retention models for internal dosimetry of the human respiratory tract. Health Physics **12,** 173–207.

BLIGH, E.G., and DYER, W.J. (1959). A rapid method of total lipid extraction and purification. Can. J. Biochem. Physiol. **37,** 911–937.

CANONICO, A.E., CONARY, J.T., MEYRICK, B.O., and BRIGHAM, K.L. (1994). Aerosol and intravenous transfection of human α1-antitrypsin gene to lungs of rabbits. Am. J. Respir. Cell Moll. Biol. **10,** 24–29.

CONARY, J.T., PARKER, R.E., CHRISTMAN, B.W., FAULKS, R.D., KING, G.A., MEYRICK, B.O., and BRIGHAM, K.L. (1994). Protection of rabbit lungs from endotoxin injury by in vivo hyperexpression of the prostaglandin G/H synthase gene. J. Clin. Invest. **93,** 1834–1840.

FASBENDER, A.J., ZABNER, J., and WELSH, M.J. (1995). Optimization of cationic lipid-mediated gene transfer to airway epithelia. Am. J. Physiol. **269,** L45–L51.

FELGNER, P.L., GADEK, T.R., HOLM, M., ROMAN, R., CHAN, H.W., WENZ, M., NORTHROP, J.P., RINGOLD, G.M., and DANIELSON, M. (1987). Lipofectin: A highly efficient, lipid-mediated DNA-transfection procedure. Proc. Natl. Acad. Sci. USA **84,** 7413–7417.

FELGNER, J.H., KUMAR, R., SRIDHAR, C.N., WHEELER, C.J., TSAI, Y.J., BORDER, R., RAMSEY, P., MARTIN, M., and FELGNER, P.L. (1994). Enhanced gene delivery and mechanism studies with a novel series of cationic lipid formulations. J. Biol. Chem. **269,** 2550–2561.

LEE, E.R., MARSHALL, J., SIEGEL, C.S., JIANG, C., YEW, N.S., NICHOLS, M.R., NIETUPSKI, J.B., ZIEGLER, R.J., LANE, M.B., WANG, K.X., WAN, N.C., SCHEULE, R.K., HARRIS, D.J., SMITH, A.E., and CHENG, S.H. (1996). Detailed analysis of structures and formulations of cationic lipids for efficient gene transfer to the lung. Hum. Gene Ther. **7,** 1701–1717.

LIU, Y., LIGGITT, D., ZHONG, W., GUANHUAN, T., GAENSLER, K., and DEBS, R. (1995). Cationic liposome-mediated intravenous gene delivery. J. Biol. Chem. **270,** 24864–24870.

LOGAN, J.J., BEBOK, Z., WALKER, L.C., PENG, S., FELGNER, P.L., SIEGAL, G.P., FRIZZELL, R.A., DONG, J., HOWARD, M., MATALON, S., LINDSEY, J.R., DuVALL, M., and SORSCHER, E.J. (1995). Cationic lipids for reporter gene and CFTR transfer to rat pulmonary epithelium. Gene Ther. **2,** 38–49.

McLACHLAN, G., DAVIDSON, D.J., STEVENSON, B.J., DICKINSON, P., DAVIDSON-SMITH, H., DORIN, J.R., and PORTEOUS, D.J. (1995). Evaluation in vitro and in vivo of cationic liposome-expression construct complexes for cystic fibrosis gene therapy. Gene Ther. **2,** 614–622.

SCHWARZ, L.A., JOHNSON, J.L., BLACK, M., CHENG, S.H., HOGAN, M.E., and WALDREP, J.C. (1996). Delivery of DNA-cationic liposome complexes by small-particle aerosol. Hum. Gene Ther. **7,** 731–741.

SOLODIN, I., BROWN, C.S., BRUNO, M.S., CHOW, C-Y., JANG, E-H., DEBS, R.J., and HEATH, T.D. (1995). A novel series of amphiphilic imidazolium compounds for in vitro and in vivo gene delivery. Biochemistry **35,** 13537–13544.

STRIBLING, R., BRUNETTE, E., LIGGITT, D., GAENSLER, K., and DEBS, R. (1992). Aerosol gene delivery in vivo. Proc. Natl. Acad. Sci. USA **89,** 11277–11281.

YANKASKAS, J.R., HAIZLIP, J.E., CONRAD, M., KOVAL, D., SARKADI, B., SCHLEGEL, R., and BOUCHER, R.C. (1993). Papilloma virus immortalized tracheal epithelial cells retain a well-differentiated phenotype. Am. J. Physiol. **264** (Cell Physiol. **33**), C1219–C1230.

YOSHIMURA, K., ROSENFELD, M.A., NAKAMURA, H., SCHERER, E.M., PAVIRANI, A., LECOCQ, J-P., and CRYSTAL, R.G. (1992). Expression of the human cystic fibrosis transmembrane conductance regulator gene in the mouse lung after in vivo intratracheal plasmid-mediated gene transfer. Nucleic Acids Res. **20,** 3233–3240.

Address reprint requests to:
Dr. Simon Eastman
Genzyme Corporation
One Mountain Road
Framingham, MA 01701-9322

Received for publication September 20, 1996; accepted after revision November 26, 1996.

STIC-ILL RB155.8.H85

From: Schnizer, Richard
Sent: Tuesday, July 17, 2001 6:31 AM
To: STIC-ILL
Subject: 09/330,903

Please send me copies of:

TI Simulated lung ***transfection*** by nebulization of liposome cDNA complexes using a cascade impactor seeded with 2-CFSME0-cells.
AU Schreier H; Gagne L; Conary J T; Laurian G
SO JOURNAL OF AEROSOL MEDICINE, (1998 Spring) 11 (1) 1-13.

TI Delivery of DNA-cationic liposome complexes by small-particle ***aerosol*** .
AU Schwarz L A; Johnson J L; Black M; Cheng S H; Hogan M E; Waldrep J C
SO HUMAN GENE THERAPY, (1996 Apr 10) 7 (6) 731-41.

TI Optimization of formulations and conditions for the ***aerosol*** delivery of functional cationic lipid:DNA complexes.
AU Eastman S J; Tousignant J D; Lukason M J; Murray H; Siegel C S; Constantino P; Harris D J; Cheng S H; Scheule R K
SO HUMAN GENE THERAPY, (1997 Feb 10) 8 (3) 313-22.

Thank you-

Richard Schnizer, Ph.D.
Patent Examiner
Art Unit 1632
CM1 12E17
703-306-5441

HUMAN GENE THERAPY 7:731–741 (April 10, 1996)
Mary Ann Liebert, Inc.

Delivery of DNA–Cationic Liposome Complexes by Small-Particle Aerosol

LINDSAY A. SCHWARZ,[1] JENNIFER L. JOHNSON,[1] MELANIE BLACK,[1] SENG H. CHENG,[2] MICHAEL E. HOGAN,[1] and J. CLIFFORD WALDREP[1]

ABSTRACT

Aerosol delivery of gene therapy for treatment of lung diseases allows topical treatment of the airways with DNA concentrations not obtainable by systemic administration. We have investigated delivery of cationic liposomes complexed to plasmid DNA in a small particle aerosol. Plasmid cDNA–DMRIE/DOPE complexes were nebulized using either an Aerotech II or Puritan-Bennett 1600 (PB1600) nebulizer. Reservoir sampling showed that DNA–DMRIE/DOPE complexes were damaged to a significant degree during nebulization, such that activity of transfected gene was diminished. Of the nebulizers analyzed, DNA–DMRIE/DOPE complexes were more stable in the PB1600. The loss of effective transfection by DNA–DMRIE/DOPE, as detected by decreased reporter gene activity in A549 lung cells, was consistent with denaturation of the DMRIE/DOPE. In contrast, nebulized DNA–DOSPA/DOPE complexes retained complete ability to transfect. Adjustments to flow rate and reservoir volume of the PB1600 allowed a longer period of delivery of active DNA–DMRIE/DOPE particles. DNA–DMRIE/DOPE was radiolabeled with Technetium-99m (^{99m}Tc), nebulized, and the output captured in either an Andersen Sampler (AS) (Andersen, 1958) cascade impactor particle size analyzer or an all glass impinger. cDNA–cationic lipid complexes were detected in size ranges of 0.4–10 μm, with most particles found between 1–2 μm. Aerosol output was consistent from 0 to 5 min. These results show the feasibility of aerosol delivery of DNA–cationic lipids for the purposes of gene therapy to the lung.

OVERVIEW SUMMARY

DNA–cationic lipid complexes were nebulized using either of two nebulizers with differently designed jets, the Aerotech II or Puritan Bennett 1600. Damage to the DNA–DMRIE/DOPE complexes during nebulization was shown by a decrease in activity of the transfected gene. In contrast, DNA–DOSPA/DOPE was not significantly damaged by nebulization in the PB1600 nebulizer. Damage to DNA–DMRIE/DOPE complexes was consistent with the separation of the DOPE from the DNA–DMRIE occurring with the reflux of the DNA–lipid through the nebulizer jets. These results indicate that a more stable DNA–cationic lipid complex is desirable for aerosol delivery of gene therapy. Effective DNA–DMRIE/DOPE particles could be delivered for a longer period of time by decreasing the flow rate and increasing the reservoir volume. Using Technetium-99m-labeled complexes, the particle size of the nebulized DNA–DMRIE/DOPE complexes was shown to be primarily in the 1 to 2-μm range, which would target the lower airways.

INTRODUCTION

GENE TRANSFER TO THE RESPIRATORY TRACT for the correction of genetic defects such as cystic fibrosis or α-1-antitrypsin deficiency is currently being tested in clinical trials (Eissa *et al.*, 1994; Nabel *et al.*, 1994; Welsh *et al.*, 1994). Expression of genes transfected to human and animal lung tissue using cationic lipids has been demonstrated *in vivo* and the DNA–lipid was well tolerated by the host (Stribling *et al.*, 1992; Yoshimura *et al.*, 1992; Hyde *et al.*, 1993; San *et al.*, 1993; Canonico *et al.*, 1994; Nabel *et al.*, 1994; Logan *et al.*, 1994). Although there are several ways to deliver an aqueous preparation of the DNA–cationic lipid to the lung, such as intratra-

[1]Department of Molecular Physiology and Biophysics, Baylor College of Medicine, Houston TX 77204.
[2]Genzyme Corporation, Framingham, MA 01701-9322.

cheal or intranasal instillation (Yoshimura *et al.*, 1992), genetic material in aqueous solution has been placed in a nebulizer and delivered as an aerosol (Stribling *et al.*, 1992; Canonico *et al.*, 1994; McLachlan *et al.*, 1994). Delivery of genes to the lung by aerosol is appealing because the procedure is noninvasive and genetic material can be delivered directly to the tissue of interest. DNA may also be delivered to the lung in quantities not obtainable by systemic administration, and aerosol delivery avoids delivery to organs not targeted for gene therapy.

A major obstacle to the use of DNA–cationic liposome aerosol to lungs has been low transfection efficiency. In some cases, large quantities of DNA–lipid were required to see a modest response (Stribling *et al.*, 1992; Canonico *et al.*, 1994). It is currently unclear as to whether or not this low efficiency is due to damage of the DNA–lipid complex during nebulization, poor uptake, or low expression of the transfected gene.

We have used DNA–cationic lipid complexes to develop standard methodologies suitable for delivery of DNA–cationic lipid complexes to the lung as an aerosol. We have found that considerable damage occurs to some DNA–lipid complexes using several nebulizers. To improve efficiency, DNA–cationic lipid nebulization requires clearly defined parameters with regard to reservoir volume, flow rate, and particle size. These results should help direct future DNA–liposome aerosol delivery for the purposes of gene therapy.

MATERIALS AND METHODS

cDNA

Escherichia coli bacterial pastes containing plasmid pCMVβgal were obtained from Genzyme Corp. (Framingham, MA). Plasmid DNA was extracted and purified using the Qiagen Ultrapure 100 column (Qiagen, Chatsworth, CA). DNA concentration was determined by A_{260} in the ultraviolet range (1 unit of optical density at a UV wavelength of 260 nm equals 50 μg/ml) and comparing similar concentrations of Qiagen-purified DNA with CsCl-purified DNA.

Lipids

2,3-Dioleyloxy-*N*-[2(sperminecarboxamido) ethyl]-*N,N*-dimethyl-1-propanaminium trifluoroacetate (DOSPA), dioleoyl phosphatidylethanolamine (DOPE) (DOSPA/DOPE, Lipofectamine) was purchased from GIBCO/BRL. *N*-(2-hydroxyethyl)-*N,N*-dimethyl-2,3-bis (tetradecytoxy)-1-propanaminium bromide (DMRIE)/DOPE was obtained from Vical (San Diego, CA). DMRIE/DOPE was rehydrated with 1 ml of sterile, endotoxin-free water and rocked for 30 min at room temperature prior to use.

DNA–liposome preparation

For most efficient use of materials, the DNA–lipid ratio was optimized as follows. A constant concentration of plasmid cDNA (2.5 μg) was combined with various concentrations of cationic lipid in water to generate a panel of DNA:lipid ratios. DNA–lipid mixtures were allowed to incubate for 15 min at room temperature, and the complexes resolved on a 1% agarose gel in 1× Tris-acetate (40 m*M*)-EDTA (2 m*M*) (TAE) buffer. All experiments used the first DNA:lipid concentration where the net charge appeared to be zero in that the DNA–lipid complex remained at the gel origin. This procedure was repeated for each new lot number of lipid. In addition, the same range of DNA–lipid concentrations was tested for transfection efficiency on A549 cells and found to corroborate the optimal DNA:lipid determined by gel analysis. A 1:4 DNA-to-lipid ratio for DMRIE/DOPE and a 1:3 DNA-to-lipid ratio for DOSPA/DOPE was used. For nebulization, DNA was diluted to a 80 μg/ml in 2.5 ml of water and added drop-wise to the diluted lipid DMRIE/DOPE, 320 μg/ml; DOSPA/DOPE, 240 μg/ml, each in 2.5 ml of water). The diluted DNA–lipid was incubated for 15 min at room temperature. Size of the DNA–cationic liposomal complexes was analyzed by light scatter in a Coulter Counter calibrated with defined-size latex beads. At room temperature, using DMRIE/DOPE at the 1:4 ratio, complexes were in a range of 3–5 μm.

Nebulizers and conditions

The Puritan-Bennett 1600 nebulizer was modified to produce a liposome aerosol of 1–2 μm mass median aerodynamic diameter (MMAD) by the use of only one jet (PB 1600, Carlsbad, CA) (single jet, SJ). A flow rate of 15 liters/min was used unless otherwise specified (Waldrep *et al.*, 1993b). A flow rate of 10 liters/min was employed with the AEROTECH II (ATII, Bedford, MA). Unless specified otherwise, the reservoirs contained a volume of 5 ml.

Generation of DNA–lipid small-particle aerosol

Lipid–DNA mixtures were added to the reservoir of a jet nebulizer. Compressed air was forced through the nebulizer at 50 pounds per square inch (psi) and the air flow rate from the compressor was adjusted with a flow meter (Puritan, Carlsbad, CA). The reservoir contents were sampled (100 μl) before nebulization (T = 0), after 3, 6, and 10 min of nebulization, and at virtual dryness, unless otherwise specified. Alternatively, output was captured in an all-glass impinger (AGI) (model 7542, Ace Glass, Vineland, NJ) containing 5 ml of water (Waldrep *et al.*, 1993b).

Aerosol particle-size determination

^{99m}Sodium Pertechnetate (^{99m}Tc) Studies: DNA–lipid was labeled with ^{99m}Tc as described (Vidgren *et al.*, 1995). Forty micrograms of DNA was combined with 160 μg of DMRIE/DOPE in 1 ml of sterile water and allowed to incubate for 15 min. 3M stannous chloride, (0.5 ml) was added to DNA–lipid followed by 1 ml of ^{99m}Tc, (2 mCi/ml; Syncor International Corp, Houston TX). The mixture was incubated for 30 min at room temperature. Incorporation of the ^{99m}Tc was determined by filtration in a Centri-free micropartition filter (Amicon, Beverly MA), which retains the labeled liposomes and filters the unincorporated label. Incorporation of ^{99m}Tc was routinely 99%. Volume was brought to 5 ml with water and solution nebulized in a PB1600 nebulizer and a 30-sec blast was captured in an Andersen Sampler Cascade Impactor (Andersen-Graseby, Atlanta, GA). Following nebulization, stainless steel plates were removed from the Andersen Sampler and directly counted for 1 min with a Ludlum Geiger-Mueller counter

(model 2200 portable scaler/rate meter) equipped with a gamma detector at a distance 15 cm from the source. While the unneubulized DNA-DMRIE/DOPE complexes are 3–5 μm in size, the complexes in water droplets are resized in the nebulizer jets (Waldrep et al, 1993b).

Transfection of A549 cells

Reservoir Sampling: A 100-μl aliquot of the reservoir sample was combined with 400 μl of sterile water, and mixed with an equal volume (0.5 ml) of 2× Optimem (Life Technologies, GIBCO/BRL). For transfection, A549 cells (30% confluent) were overlaid with DNA–cationic lipid complexes and incubated for 2–2.5 hr at 37°C in a humidified, 5% CO_2 incubator. Overlay was replaced with Dulbecco's minimal essential medium (DMEM; Life Technologies/GIBCO) plus 10% fetal bovine serum (FBS; Hyclone) and cells further incubated for 48 hr. Cells were either fixed and stained for β-galactosidase activity (β-Gal; 5′-3′ Inc., Boulder, CO) (Dannenberg and Suga, 1981) or lysed and assayed for total protein using the BCA microtiter assay as specified by the manufacturer (Pierce Chemical Co., Rockford IL) and for β-Gal activity using a Chlorophenored-β-D-galactopyranoside colorimetric microtiter assay as described (CPRG) (Boeringher-Mannheim, Germany) (Eustice *et al.*, 1991).

Output Sampling: Output was captured in an AGI as described (Waldrep *et al.*, 1993b). At the completion of nebulization, the water from the AGI was combined with an equal volume of 2× Optimem, and 1 ml transfected on A549 cell monolayers; cells were subsequently lysed and assayed for β-Gal activity as described above.

Characterization of nebulized particles

DNA: After nebulization, DNA was stripped from the DMRIE/DOPE by bringing the concentration of sodium dodecyl sulfate (SDS) in the sample to 0.1% and heating at 55°C for 20 min. DNA was resolved on a 1% agarose gel in TAE buffer. The DNA was denatured in the gel with base and transferred to nylon filter (Hybond, Amersham, UK). The filter was hybridized to a ^{32}P-labeled homologous probe (pCMVβgal), labeled by random priming as described (Feinberg and Vogelstein, 1983). After washing, the blot was exposed to film (XAR-5, Kodak) for autoradiography.

DMRIE-DOPE: A 160-μg/ml amount of DMRIE/DOPE in 5 ml of water was nebulized in a PB 1600 jet nebulizer as described, using the specified flow rate (Waldrep *et al.*, 1993b). Samples were removed at T = 0, 3, 6, and 10 min. 100 ul of each sample was combined with 4 ug of DNA, incubated at room temperature for 15 min and transfected into A549 cells as described above. Alternatively, 100 μl was dried under a stream of N_2 gas. Samples were resuspended in 40 μl of methanol-acetonitrile mobile phase and 20 μl injected into a Waters HPLC (NovaPak Silica) (Grit *et al.*, 1991). DOPE (10 μg) (Avanti Polar Lipids, Birmingham, AL) was similarly dissolved and served as the HPLC standard for the DOPE component of DMRIE/DOPE. DMRIE alone was unavailable. The lipid was detected using a SEDEX 55 mass evaporator (SEDERE, Alfortville, Cedex, France). A final reservoir sample was dried under N_2, resuspended in tertiary butanol (EM Science), frozen, and lyophilized. DMRIE/DOPE was reconstituted in 500 μl of water, 4 μg of DNA added, and incubated for 15 min at room temperature. An equal volume of 2× Optimem was added and A549 transfected.

RESULTS

Nebulizers deliver DNA–liposome complexes with different efficiencies

Two jet nebulizers with different designs, the PB 1600 and AT II, were chosen for testing. Plasmid DNA (200 μg) (pCMVβgal) and DMRIE/DOPE (800 μg) were diluted in 5 ml of water to give a DNA:lipid ratio by weight of 1 μg of DNA to 4 μg of lipid. The suspension was added to the nebulizer reservoir and nebulized. Figure 1 compares the activity of transfectable material remaining in the reservoir of the ATII and the PB1600 at various times during nebulization. Activity of the DNA–lipid complexes sampled from the ATII was decreased to 30% of starting activity within 3 min. Further decreases in activity with time were not seen; activity remained in the 25–30% range. In contrast, 85% of the starting activity remained in the reservoir of the PB1600 at 3 min and by 6 min, 50% of starting activity was still evident. Loss of activity was linear with time, which would suggest a loss of activity relative to the amount of cycling through the jets (DNA–lipid complexes were stable upon standing). Because the least damage was done using the PB 1600, the remaining studies focused on the use of this nebulizer.

Transfectability of DNA–DMRIE/DOPE decreases due to cationic lipid complex denaturation

To determine the nature of loss of transfection efficiency, samples harvested from the reservoir during nebulization were treated with 0.1% SDS to dissociate the DNA from the lipid so that DNA structure could be examined. The retention of the non-SDS-treated DNA–DMRIE/DOPE samples at the gel origin show that the cationic moiety in the lipid remained complexed to the DNA. SDS-treated samples resolved on an agarose gel showed that the DNA eluted from lipid had structures similar to that of freshly diluted DNA run concomitantly (Fig. 2, lane 1); three bands can be seen in the control as well as nebulized samples with the highest molecular-weight band representing linear, the middle band representing circular nicked, and the lowest molecular-weight band representing the supercoiled plasmid DNA. Because the supercoiled structure is the most fragile of the three plasmid structures, the fact that there was no loss in supercoiled DNA, indicates that the DNA was quite stable in the presence of cationic lipid, even during nebulization. In contrast, naked DNA was rapidly degraded by nebulization (3 min or less; data not shown).

To examine the effect of nebulization on the cationic lipid alone, DMRIE/DOPE (160 μg/ml) without DNA was diluted in 5 ml of water, nebulized, and combined with DNA after nebulization. Transfection efficiency virtually paralleled that seen when DNA–DMRIE/DOPE was nebulized as a complex, suggesting that the DMRIE/DOPE was altered by the nebulization process (Fig. 3A). In attempts to determine the nature of the alteration to the lipid complex, the samples were analyzed by HPLC, using a mass evaporation detector, which would also

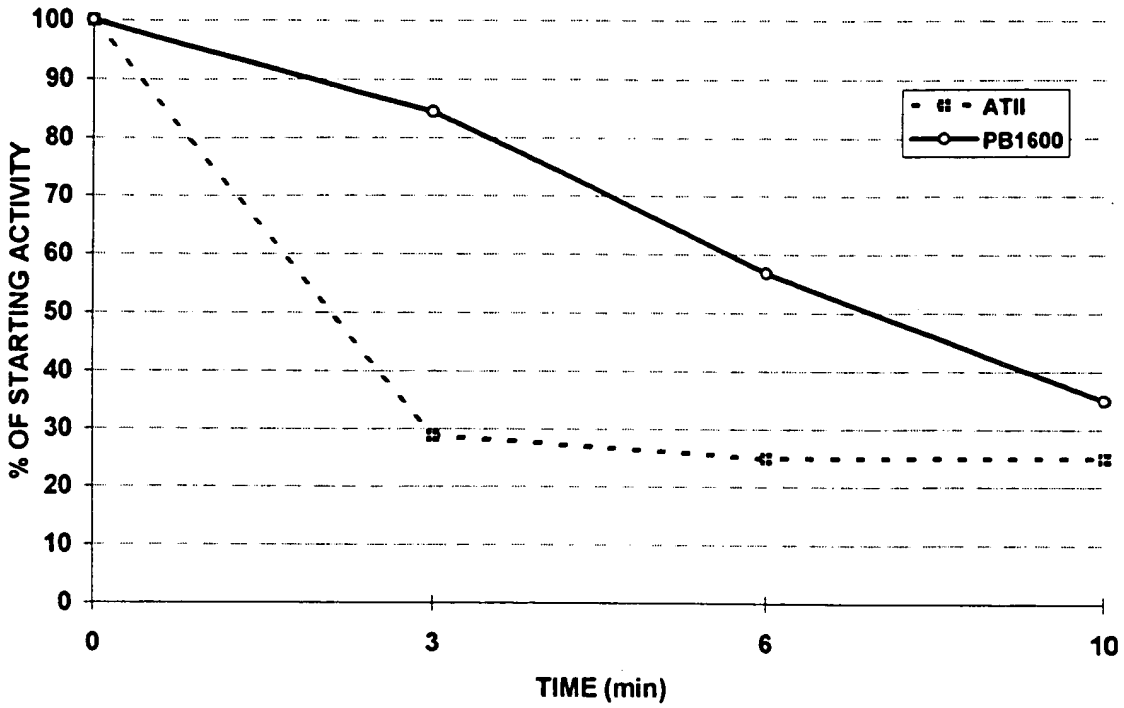

FIG. 1. Transfection efficiency of DNA–DMRIE/DOPE complexes during nebulization. A total of 200 μg of pCMVβgal and 800 μg of DMRIE/DOPE were combined in 5 ml of distilled water and incubated for 45 min. Suspension was nebulized according to manufacturer's specifications: Aerotech II, 10 liters/min; PB1600 SJ, 15 liters/min. A sample of 100 μl was harvested from the reservoir at T = 0, 3, 6, and 10 min. Fifty microliters of this sample was combined with 450 μl of water, mixed with 2× OPTIMEM, and A549 cells were transfected. At 48 hr, cell lysates were harvested and assayed for β-Gal activity. Results are presented as percent of starting activity (T = 0) ([activity at T = *n*/activity of T = 0] × 100) and are representative of three experiments.

detect oxidized lipid forms (Grit *et al.*, 1991). The peak of DMRIE and peak of DOPE showed that retention times were consistent between un-nebulized and nebulized samples. New or oxidized by-products were not seen (Table 1). The areas under the peaks for the two components showed that the lipids concentrated by about 40% during nebulization, representing a loss of water vapor in an excess of DNA–lipid. Although a trend toward a greater loss of DOPE over DMRIE was seen in several experiments, the difference was not numerically significant.

In the absence of oxidative damage, it was possible that the DNA–lipid complexes underwent a change such that the DOPE separated from the DNA–DMRIE. In fact, Felgner *et al.* (1994) have shown that transfection by DNA–DMRIE does not occur in the absence of DOPE. In attempts to determine the relationship of DNA–DMRIE/DOPE during nebulization, DMRIE/DOPE was nebulized in the absence of DNA as described above and aliquots were harvested at various times. The reservoir samples were split; one aliquot was retained as a nebulized, untreated control. The other aliquot was dried under a stream of N_2 and liposomes were relyophilized to reform the DMRIE/DOPE complex as described in Materials and Methods. DNA was added to the reformed liposomes as well as to the nebulized, untreated control and the samples were transfected into A549 cells. As can be seen in Fig. 3A, when the liposomes were reformed by resolubilization and lyophilization before adding DNA, reporter activity in transfected A549 cells was restored. In fact, increased activity was seen with the reconsti-

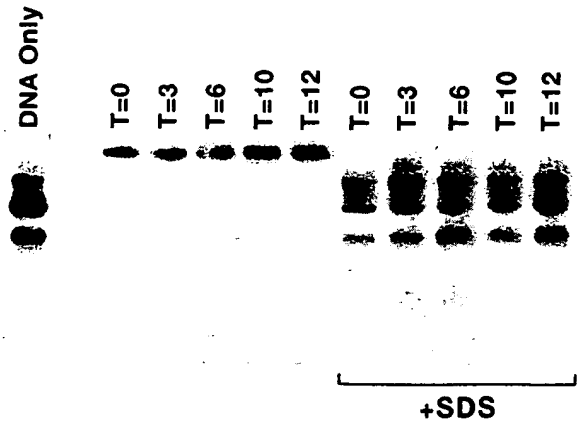

FIG. 2. DMRIE/DOPE stabilizes DNA during nebulization. Two hundred micrograms of pCMVβgal and 800 μg of DMRIE/DOPE were combined in 5 ml of distilled water and incubated for 45 min. Suspension was nebulized in a PB 1600-SJ nebulizer according to the manufacturer's specifications. Aliquots were removed at the times specified and half of the aliquot was treated with 0.1% (final concentration) SDS at 55°C for 10 min to elute the lipid. SDS-treated and untreated DNA samples were resolved by electrophoresis in a 1% agarose gel. DNA in the gel was denatured and blotted onto a nylon filter and hybridized to a homologous 32P-labeled pCMVβgal probe. After washing, the blot was subjected to autoradiography. SDS-treated, un-nebulized plasmid DNA serves as a control. The results are representative of two experiments.

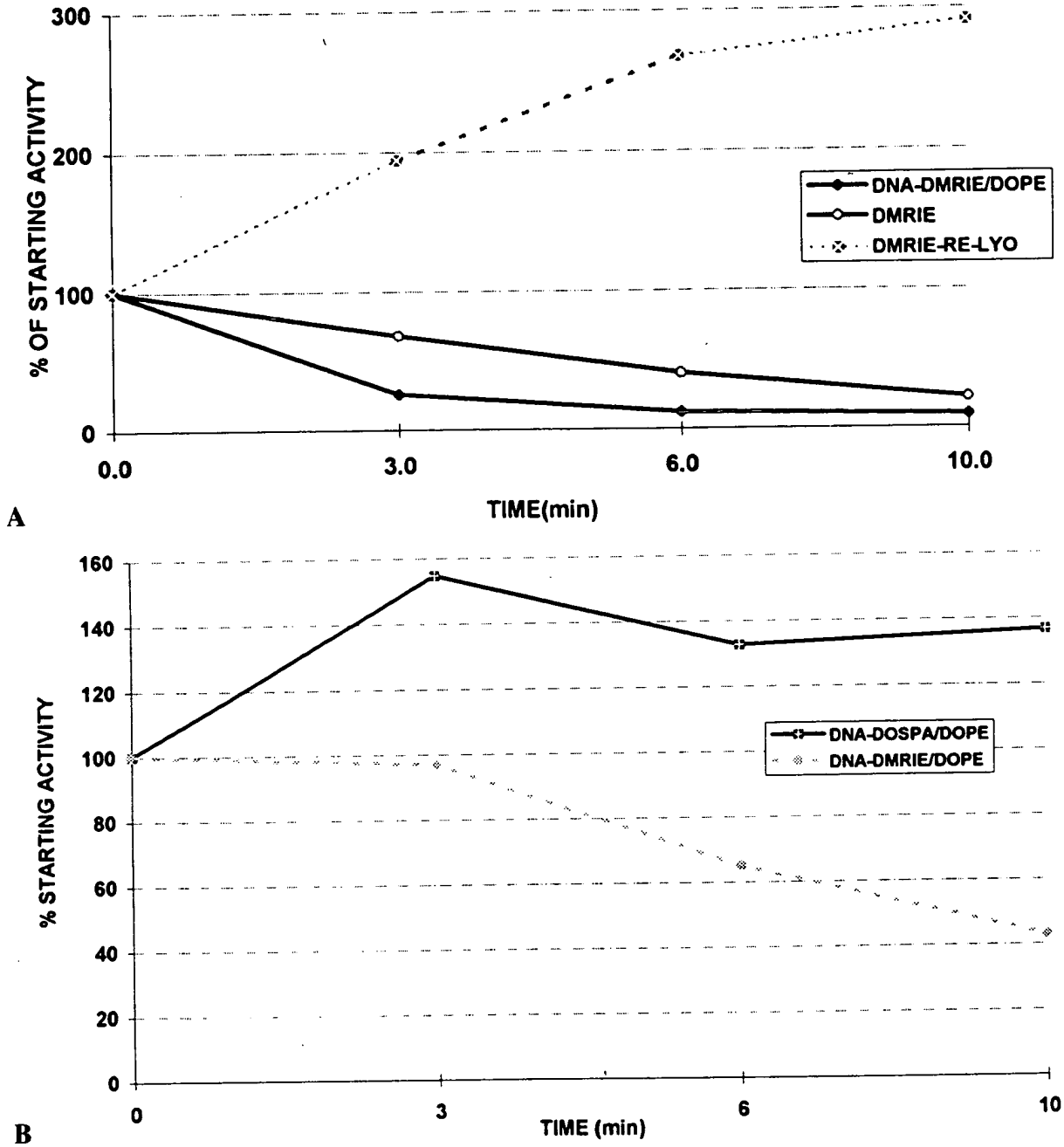

FIG. 3. Structure of cationic lipid–DNA complexes during nebulization. A. DNA–DMRIE/DOPE or DMRIE/DOPE alone was nebulized in the PB1600 jet nebulizer. Reservoir samples were harvested at T = 0, 3, 6, and 10 min. DNA–DMRIE/DOPE samples were mixed with 2× transfection medium and transfected into A549 cells. One aliquot of nebulized DMRIE/DOPE was combined immediately with 4 μg of DNA and transfected into A549 cells. Another aliquot of the nebulized DMRIE/DOPE samples was dried under N_2, redissolved in tertiary butanol, frozen, lyophilized, and dissolved in sterile, LPS-free water. DNA was added, and the complex was incubated at room temperature for 15 min. B. A 5-ml sample of DNA–DOSPA/DOPE was nebulized in a PB1600. Aliquots were remove at T = 0, 3, 6, and 10 min. All nebulizer samples were combined with 2× Optimem and A549 cells were transfected. Cell lysates were harvested and assayed for β-Gal activity. Results are presented as a percentage of starting activity, meaning the T = 0 time point ([activity at T = *n*/activity of T = 0] × 100). Data shown are representative of three experiments.

tuted material. The enhanced activity might have been due to the concentration of the lipids during nebulization, as was seen by HPLC analysis. Lyophilization of freshly reconstituted DMRIE/DOPE (T = 0 time point, Fig. 3A) did not demonstrate enhanced transfection, ruling out that relyophilization of DMRIE/DOPE increased activity. The type of denaturation is consistent with DOPE becoming dissociated from the DNA–DMRIE during nebulization.

To determine whether other cationic lipid combinations are similarly denatured during nebulization, DNA–DOSPA/DOPE

TABLE 1. HPLC ANALYSIS OF NEBULIZED CATIONIC LIPID[a]

Neb. time (min)	*DMRIE (Ret. time)*	*DOPE (Ret. time)*	*% DMRIE*	*% DOPE*	*Total area*
0	1.132	1.892	0.8	15.9	1.5×10^7
3	1.132	1.900	0.8	20.1	1.9×10^7
6	1.128	1.898	0.8	19.7	1.9×10^7
10	1.133	1.905	1.1	22.6	2.2×10^7
15	1.137	1.898	1.2	17.2	1.7×10^7
Total			4.6	95.4	9.3×10^7

[a]DOPE STD retention times: 1.957. Data are representative of three experiments.

was nebulized under similar conditions. As seen in Fig. 3B, the activity of DNA–DOSPA/DOPE held up considerably longer than did the DMRIE/DOPE nebulized concomitantly. Thus, DMRIE/DOPE appeared more sensitive to denaturation during nebulization than did DOSPA/DOPE.

Nebulization variables that preserve the cationic lipid complex

If cycling through the jets, indeed, caused a generalized denaturation of DNA–DMRIE/DOPE, decreasing the frequency of cycling particles through the jets might preserve the complexes. Two ways of decreasing the reflux frequency are to increase the reservoir volume and decrease the flow rate. When reservoir volume was increased from 5 to 10 ml while maintaining the DNA–DMRIE/DOPE concentration, transfection activity of the DNA–DMRIE was essentially 100% of the starting material through the first 3 min and decreased to 50% activity by 20 min (Fig. 4). In contrast, when the reservoir contained only 5 ml, activity was only 25% of the starting activity at 10 min. Moreover, decreasing the volume to 1 ml caused rapid, total degradation of the DNA–lipid, even when fresh 1-ml aliquots were added at 3-min intervals (L.A.S., J.L.J., unpublished observation). These results suggest that the quality of the DNA–DMRIE/DOPE complexes was greatly affected by volume, possibly due to a change in reflux frequency at the earlier time points.

Transfection of nebulized DNA–lipid complexes obtained from the PB1600 nebulizer with the flow rate at either 15 liters/min, 10 liters/min, or 8 liters/min was also evaluated. While reducing the compressed air flow rate from 15 to 10 liters/min did not change the transfection efficiency of the reservoir contents (data not shown), decreasing the flow rate to 8 liters/min markedly increased the length of time active transfection complexes could be recovered from the reservoir (Fig. 5A).

Lowering the flow rate also lowers the output. It might be that, because of the decrease in output at 8 liters/min, by 3 min, less material may have circulated through the jets than when

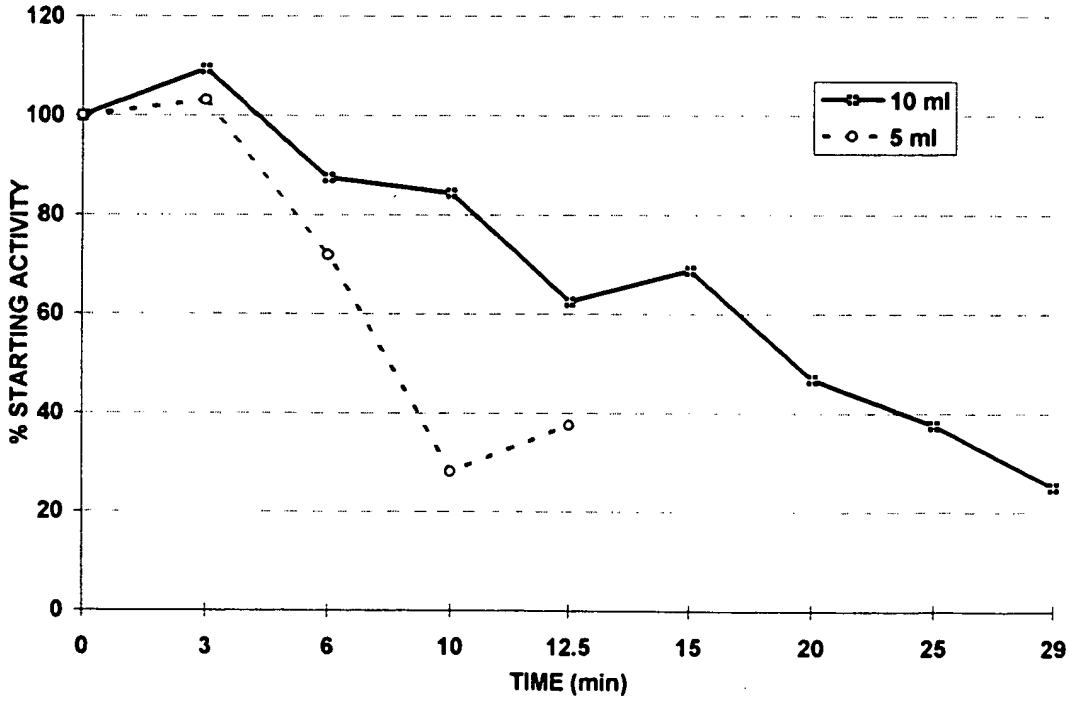

FIG. 4. Effect of reservoir volume on DNA–DMRIE/DOPE aerosol delivery in PB1600 SJ. A total of 200 μg of pCMVβgal and 800 μg of DMRIE/DOPE were combined in 5 ml of distilled water or, total of 400 μg and 1.6 mg of DMRIE/DOPE in 10 ml of water were incubated for 45 min. Suspension was nebulized at 50 psi, 15 liters/min. A sample of 100 μl was harvested from the reservoir at T = 0, 3, 6, 10, 15, 20, 25, and 30 min. Fifty microliters of this sample was diluted with 450 μl of water and combined with 2× OPTIMEM; A549 cells were transfected. At 48 hr, cell lysates were harvested and assayed for β-Gal activity. Results are presented as percent of starting activity, meaning the T = 0 time point ([activity at T = *n*/activity of T = 0] × 100). Data shown are representative of three experiments.

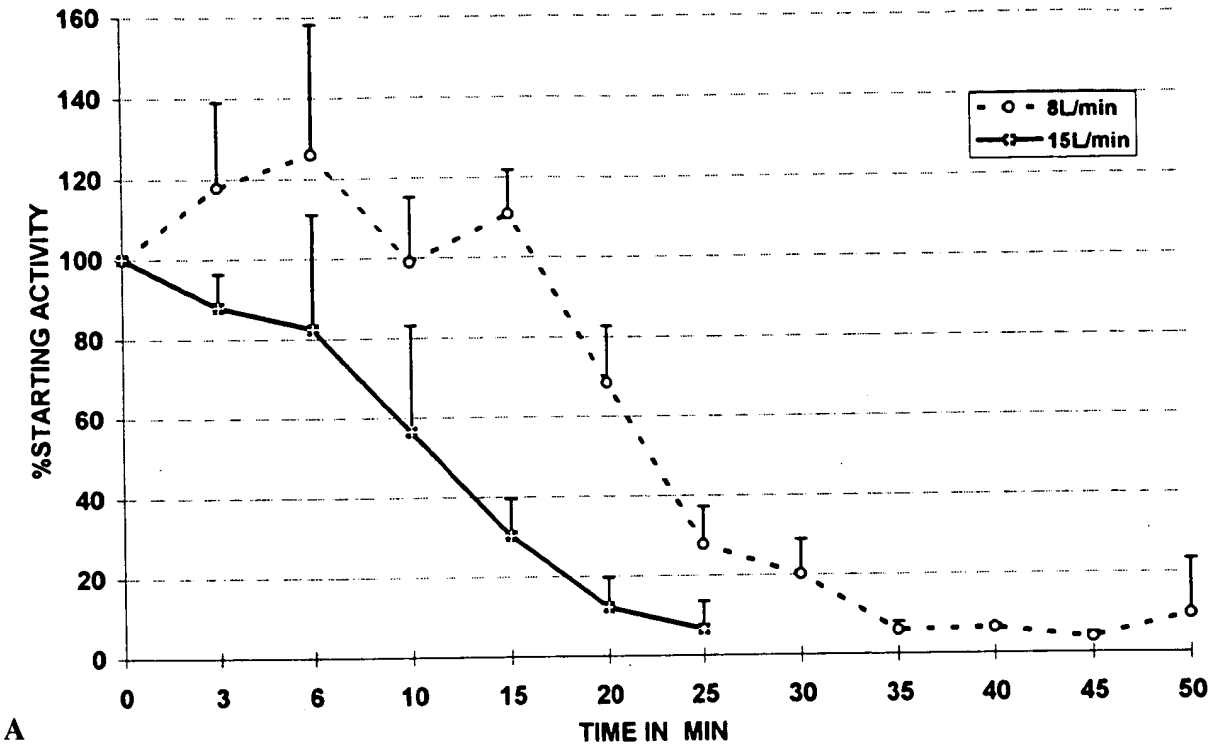

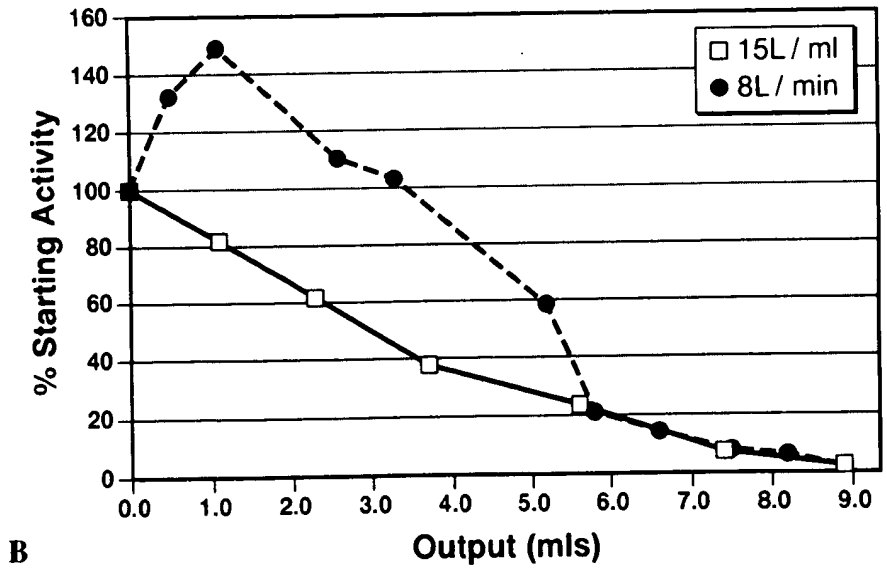

FIG. 5. Effect of flow rate on DNA–DMRIE/DOPE aerosol delivered in PB 1600 SJ. A total of 400 μg of pCMVβgal and 1.6 mg of DMRIE/DOPE were combined in 10 ml of distilled water and incubated for 45 min. A nebulizer with suspension was weighed prior to nebulization and suspensions were nebulized at 50 psi, 15 liters/min or 8 liters/min. A sample of 100 μl was harvested from the reservoir at T = 0, 3, 6, 10, 15, 20, 25, and 30 min and the nebulizer was weighed at each time point to determine weight loss as output. A total of 100 μl of this sample was combined with 400 μl of water, combined with 2× OPTI-MEM, and A549 cells were transfected. At 48 hr, cell lysates were harvested and assayed for β-Gal activity. Results are presented as percent of starting activity, meaning the T = 0 time point ([activity at T = *n*/activity of T = 0] × 100). Data shown are a compilation of three experiments. A. β-Gal activity *versus* time of nebulization, B. Output *versus* activity.

the nebulizer is run at the flow rate of 15 liters/min. Thus, transfection efficiency might only appear greater at 8 liter/min. When a direct comparison of the β-Gal activity and output in 8 liters/min and 15 liters/min samples was made using a reservoir volume of 10 ml, the β-Gal activity was greater when flow rate was reduced to 8 liters/min (Fig. 5B). For the first 10 min, activity recovered from both nebulizers is relatively similar; particles contained greater than 80–90% β-Gal activity. Between 10 and 20 min, a difference in β-Gal activity was seen between the two flow rates. For example, when 2.0 ml of out-

put was nebulized at either flow rate, the β-Gal activity was greater in the nebulizer run at 8 liters/min (100% *vs.* 60%).

To compare the effects of cycling through the jets at 15 liters/min or 8 liters/min, a small cellophane bag was fitted to the nebulizer lid to capture reflux material, while allowing the intake straw to remain in the suspension through a small slit in the bag. Reflux material was sampled after each cycle through the jets. Using a 10-ml reservoir volume and a 15 liters/min flow rate, 30% of the β-Gal activity was lost with one pass through the jet. With five passes, activity was decreased to 50% of the starting activity. In contrast, using a flow rate of 8 liters/min, DNA–DMRIE/DOPE maintained its ability to transfect (100% activity through five passes). Thus, lowering the flow rate to 8 liters/min appeared to decrease the damage to the DNA–DMRIE/DOPE in the jets without decreasing the total output.

Particle size of nebulized DNA–cationic liposome droplets

pCMVβgal-DMRIE/DOPE were combined to give a DNA:lipid ratio of 1 μg of DNA to 4 μg, respectively, and the complex was labeled with ^{99m}Tc. Four milliliters of labeled complexes were added to the reservoir of the PB1600 and nebulized through an Anderson Sampler; particle size was determined. As seen in Fig. 6, although a range of droplet sizes is seen, water droplets containing DNA–DMRIE/DOPE complexes were found mainly in two sizes—16% of the particles were greater than 10 μm, whereas 58% were in a range of 2–0.5 μm with an MMAD of approximately 2 μm. Moreover, when samples from 0–30 sec were compared to 5–5.5 min, the output was essentially the same, as determined by the Andersen Sampler as well as capture in all-glass impingers (AGI) (data not shown). The particles in a size range of 10 μm and greater would be swallowed but the particle size range of 1–2 μm is optimal for the delivery of droplets to the medium and small airways (Andersen, 1958; Waldrep *et al.*, 1993b; Vidgren *et al.*, 1995). Particles entrained into the aqueous diluent of the AGI transfected A549 cells, suggesting that the aerosol particles contain active DNA–DMRIE/DOPE complexes (data not shown, Schwarz *et al.*, 1993).

DISCUSSION

Cationic liposomal DNA transfer into the lung has been explored by others with mixed results (Stribling *et al.*, 1992; San *et al.*, 1993; Canonico *et al.*, 1994). In a report by Stribling *et al.*, (1992), the use of 12 mg of DNA–DOTMA/DOPE was necessary to see transfection of mouse airways. To deliver a similarly proportional dose of DNA–cationic lipid in humans would be prohibitive.

In another animal study, the human α1-antitrypsin gene in complex with DOTMA/DOPE was nebulized to rabbits *via* a face mask (Canonico *et al.*, 1994) and gene expression was determined. Using a dose of 0.5 mg of DNA in complexes with DOTMA/DOPE, the human α_1-antitrypsin gene protein and

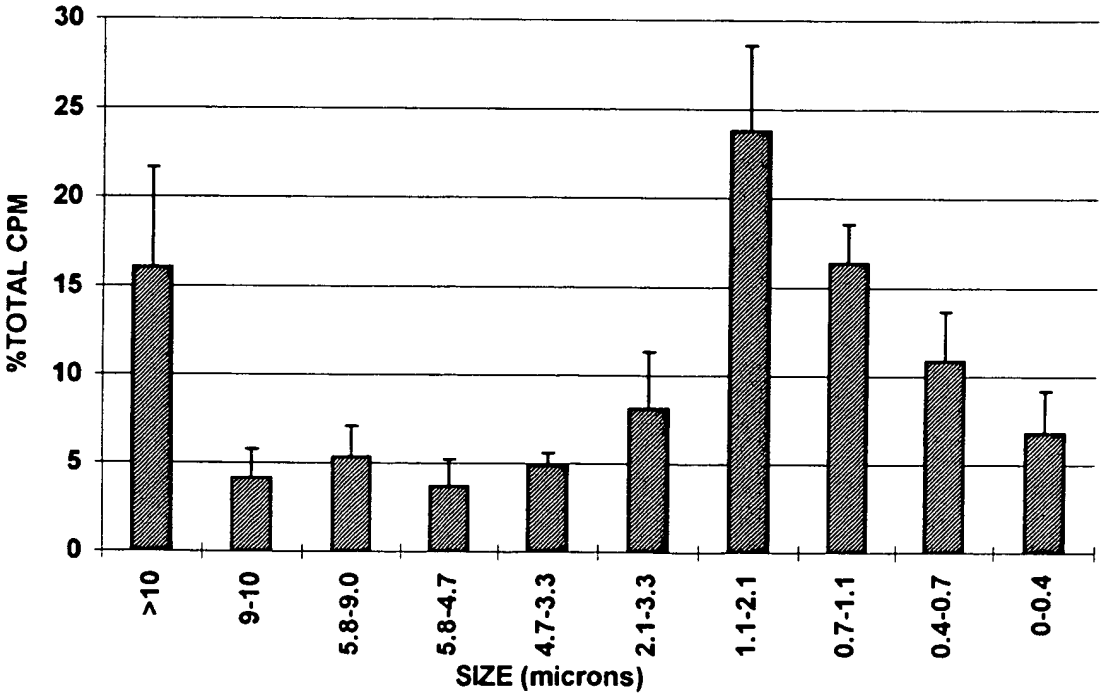

FIG. 6. ^{99m}-Tc studies. pCMVβgal DNA (40 μg) was combined with DMRIE/DOPE (160 μg) in 1 ml of water and incubated at room temperature for 1 hr. DNA–DMRIE/DOPE was labeled with ^{99m}Tc as described in Material and Methods. The labeled mixture was placed in the PB1600 jet nebulizer, which was attached to an Andersen Sampler. Labeled material was nebulized for 30 sec and particles were captured in the AS. The stainless steel plates were counted and particle size was determined. Data are presented as percent of the total cpm. The figure represents the mean and standard deviation of four experiments.

mRNA were detectable for at least 7 days when delivered by aerosol, as determined by Western blot and RNA blot analysis, respectively. Immunohistochemistry showed that gene expression after aerosol administration tended to be localized on the surface of the airways. These studies emphasize the benefit of using aerosol for gene therapy to the lung.

McLachlan *et al.* (1994) treated mouse lungs by aerosol using DNA (266 μg/treatment) in combination with cationic lipid (DOTMA/DOPE). These investigators found that a series of five aerosol treatments in 5 days was necessary to observe gene expression. By histological staining, expression of the β-Gal gene was primarily observed in the airways for up to 42 days. DNA–cationic lipid quality was not assessed in any of these previous studies.

Before the widespread use of aerosol for the purpose of gene therapy, it will be important to define fully the parameters that govern efficient delivery of DNA–lipid to the lung. We have performed a systematic analysis to investigate the most efficient way to prepare DNA–cationic lipid aerosol for delivery to the lung. Initially, we tested nebulizers of different design; we present the data of two representative nebulizers. The ATII denatured the DNA–DMRIE/DOPE and was, thus, unsuitable for nebulization of cationic lipid and DNA. We found that the DNA–DMRIE/DOPE was also rapidly degraded in a nebulizer similar to that used in the Stribling study, the Marquest Respirgard. Several differences in the two studies should be noted. Our study was performed *in vitro* using DMRIE/DOPE as the lipid, and nebulization was performed at the manufacturer's recommended flow rate of 6 liters/min. The nebulization procedure described by Stribling's group employed a flow rate of 4 liters/min. The slight decrease in flow rate and lipid composition may have allowed the modest delivery of DNA–cationic lipid to mouse lungs. The integrity of the nebulized material in the Stribling study was not determined.

It is likely that the system employed by Canonico *et al.* (1994) was more efficient (0.5 mg of DNA), in part, because of the animal model; rabbits have larger airways and, by using rabbits, a face mask could be utilized. They used a Malinkrodt nebulizer and DOTMA/DOPE, a combination that we did not test. No analysis as to the quality of the nebulized material was made.

Regarding nebulizer performance, our data suggest that repeated cycling of the DNA–DMRIE/DOPE through the jets caused a generalized denaturation of the DNA–DMRIE/DOPE. Although not definitive, the data were consistent with a dissociation of the DOPE from the complex. The most probable explanation for why the ATII nebulizer more rapidly destroyed the DNA–lipid complexes might be the more efficient output by this nebulizer at 10 liters/min, and, thus, a greater frequency of DNA–lipid cycling through the jets (Waldrep *et al.*, 1993a).

Material harvested from the Puritan-Bennett 1600 nebulizer produced a consistent pattern of transfection. When the reservoir volume was increased to 10 ml or greater and the flow rate was decreased to 8 liters/min, functional integrity of DNA–DMRIE/DOPE was maintained in the reservoir for a longer period of time. Each of these modifications may effect nebulization by reducing the frequency at which the DNA–cationic lipid complex cycles through the jets (flow rate). Moreover, when five successive cycles of nebulization through the jets at a flow rate of either 8 or 15 liters/min was analyzed; a greater number of active DNA–DMRIE/DOPE complexes remained after the five cycles at the flow rate of 8 liters/min. These results suggest that the flow rate of 8 liter/min may also decrease the physical stress occurring within the jet.

Although the exact nature of the damage that occurs to the DMRIE/DOPE is currently unknown, it is possible that one or more of the following may play a role—surface tension of the particles or transition temperature of the lipids. Neither precoating the nebulizer with cationic lipid nor preparing the DNA–lipid to provide an excess DMRIE/DOPE or DOPE improved the activity of the nebulized DNA–lipid complexes, suggesting that surface tension may not be the one critical feature in lipid denaturation.

The transition temperature has been shown to affect nebulizer output; the lower the transition temperature of the lipid, the more stable the aerosol (Waldrep *et al.*, 1993b). Transition temperature may be important in our study because the reservoir and output temperatures drop 10°C during laboratory nebulization due to evaporation of water. The transition temperature of the lipid is determined by chain length and presence as well as by the number of double bonds. For example, the transition temperature increases with chain length and degree of saturation (for review on lipids and transition temperature, see Gennis, 1989). Cooling a lipid below its transition temperature affects the fluidity of the lipid, causing the lipid to undergo an order–disorder transition; the lipid becomes a more rigid crystalline structure. The actual transition temperature for DMRIE has been reported to be 37°C (Felgner *et al.*, 1994), well above the operating temperature of the nebulizer. The temperature of DOPE is −16°C (Avanti Polar Lipids, personal communication). In contrast to DMRIE, the transition temperature for DOPSA, would be expected to be around 18°C, on the basis of chain length and degree of unsaturation. Although the phase transition of the combined lipids is not known, it is possible that lipids that are closer in transition temperature may be more stable, as was seen for DOPSA and DOPE.

It is also well established that a more stable lipid combination is formed when the lipids are similar in degree of unsaturation and chain length (see Gennis, 1989). Both the DOSPA and DOPE components of this lipid combination contain oleic side chains (C-18) as well as a similar number of *cis* double bonds. DMRIE contains a chain length of 14 carbons and is saturated. On the basis of these facts, one would predict that the DOTMA/DOPE combination used by Stribling *et al.* (1993) and Canonico *et al.* (1994) may have been more stable, as DOTMA and DOPE both contain 18 carbon atoms and a single *cis* double bond. Possibilities regarding the effects of chain length and saturation will be addressed in future investigations.

As noted by Felgner *et al.* (1994), transfection efficiency decreases with increasing chain length. In contrast, saturation appeared less important. For example, the 18-carbon, unsaturated cationic lipid (DSRIE, 1,2-disteryloxypropyl-3-dimethyl-hydroxyethyl ammonium bromide) had less activity than the 14-carbon, saturated DMRIE. Indeed, in the absence of nebulization, the more stable lipid combination (DOSPA/DOPE) was less efficient at transfection per microgram of DNA than the less stable lipid DMRIE/DOPE. Thus, our data using DOSPA/DOPE shows the importance of designing lipid complexes, which have a more stable association, but the chemical design must also balance characteristics that will allow efficient cellular uptake.

Curiously, when nebulized DMRIE/DOPE was redissolved

and relyophilized before adding DNA, the transfection was restored and enhanced above the T = 0 time point. Because the lipid was nebulized in the absence of DNA for this experiment, a concentration of the DMRIE/DOPE complexes in the nebulizer might have resulted in a lipid excess over the original DNA:lipid ratio. As mentioned previously, we analyzed the effect of excess cationic lipid on transfection efficiency of nebulized DNA–lipid combinations, but found no improvement. Another interpretation of the data may be that if one lipid component was concentrating more rapidly, a more efficient ratio of DMRIE/DOPE might have been formed during relyophilization. Because the lipids components themselves were not available, this hypothesis was not tested.

The particle size of the output was analyzed by using ^{99m}Tc-labeled DNA–DMRIE/DOPE. The particles appeared to be in one of two size ranges: greater than 10 μm or 1–2 μm. Although the larger particles would most likely be swallowed, the 1- to 2-μm range is suitable for delivery to the lower airways (Waldrep *et al.*, 1993b; Vidgren *et al.*, 1995).

Established methods for measuring the quantity of drug in aerosols include capture of output in either an Andersen Sampler or by capture in an all-glass impinger (AGI). Drug harvested from the stages of the Andersen Sampler or the diluent in the AGI is typically measured by analytical techniques such as HPLC (Waldrep *et al.*, 1993b). Measuring the effective output of nebulized DNA–cationic lipid presented technical problems. Whereas either DNA or lipid could be directly measured by a variety of techniques, the actual quantitation of DNA or DMRIE/DOPE would not indicate whether or not the nebulized DNA-DMRIE/DOPE would transfect effectively. As shown in Fig. 2, high-quality DNA was collected and visible on a gel 25 min after nebulization, and yet this material did not transfect effectively.

In attempts to gain perspective on a concentration range in the output, we utilized the ^{99m}Tc data used to analyze the output yield. We determined that 9% of all available reservoir cpm were delivered in 6 min, or 14.4 μg of the total DNA. If we assume the material delivered was on average of an efficiency of 87.5% (as determined by bioassay), we could have delivered as much as 12.6 μg of effective DNA in this timed period.

There is plenty of room for improving the efficiency of gene delivery by the aerosol route. Technical problems that contributed to poor efficiency in this study included the loss of DNA–lipid on surfaces such as reservoir and corrugated output tubing. Attempts to wash the deposited DNA–DMRIE/DOPE from various surfaces (glass, polypropylene, polystyrene, stainless steel) were unsuccessful. A valuable contribution to the field would be a nebulizer that did not rely on cycling material through the jets and lengths of tubing, much like the action of a metered-dose inhaler.

These experiments demonstrate the pitfalls as well as the feasibility of delivering genes using cationic lipids to the lung. Optimizing conditions for each nebulizer and lipid combination are recommended, because flow rate and volume appeared to be critical in the delivery of transfection-competent DNA–lipid. Ultimately, the development of standardized conditions may allow patients to have treatment during an office visit as is currently done for some asthmatics. If gene therapy for patients begins early after the onset of symptoms, a considerable decrease in morbidity and mortality is anticipated.

ACKNOWLEDGMENTS

This work was supported by a contract from Genzyme Corp. to the Clayton Foundation for Research (Houston, TX) and funding from the Clayton Foundation. The authors wish to acknowledge Dr. Vernon Knight for a critical reading of this manuscript and for helpful comments.

REFERENCES

ANDERSEN, A.A. (1958). New sampler for the collection, sizing and enumeration of viable airborne particles. J. Bacteriol. **76,** 471–484.

CANONICO, A.E., CONARY, J.T., MEYRICK, B.O., and BRIGHAM, K.L. (1994). Aerosol and intravenous transfection of human α-1-antitrypsin gene to lungs of rabbits. Am. J. Respir. Cell Mol. Biol. **10,** 24–29.

DANNENBERG, A.M., and SUGA, M. (1981). Histochemical stains for macrophages in cell smears and tissue sections: β-Galactosidase, acid phosphatase, nonspecific esterase, succinic dehydrogenase and cytochrome oxidase. In *Methods for Studying Mononuclear Phagocytes.* D.O. Adams, M.J. Edelson, and H.S. Koren, eds. (Academic Press, New York) pp. 375–395.

EISSA, N.T., CHU, C.S., DANEL, C., and CRYSTAL, R.G. (1994). Evaluation of the respiratory epithelium of normals and individuals with cystic fibrosis for the pressure of adenovirus E1a sequences relevant to the use of E1a(-) adenovirus vectors for gene therapy for the respiratory manifestations of cystic fibrosis. Hum. Gene Ther. **5,** 1105–1114.

EUSTICE, D.C., FELDMAN, P.A., COLBERG-POLEY, A.M., BUCKERY, R. M., and NEUBAURER, R.H. (1991). A sensitive method for the detection of beta-galactosidase in transfected mammalian cells. Biotechniques **11,** 739–743.

FEINBERG, A., and VOGELSTEIN, B. (1983). A technique for radiolabeling DNA restriction endonuclease fragments to high specific activity. Anal. Biochem. **132,** 6–13.

FELGNER, J.H., KUMAR, R., SRIDHAR, C.N., WHEELER, C.J., TSAI, Y.J., BORDER, R., RAMSEY, P., MARTIN, M., and FELGNER, P.L. (1994). Enhanced gene delivery and mechanism studies with novel series of cationic lipid formulations. J. Biol. Chem. **269,** 2550–2561.

GENNIS, R.B. (1989). *Biomembranes: Molecular Structure and Function.* (Springer-Verlag Advanced Texts in Chemistry. C.R. Cantor, ed. (Springer Verlag, New York).

GRIT, M., CROMMELIN, D.J.A., and LANG, J. (1991). Determination of phosphatidylcholine, phosphatidylglycerol and their lysoforms from liposome dispersions by high-performance liquid chromatography using high sensitivity refractive index detection. J. Chromatogr. **585,** 239–246.

HYDE, S.C., GILL, D.R., HIGGINS, C.F., TREZISE, A.E.O., MACVINISH, L.J., CUTHBERT, A.W., RATCLIFF, R., EVANS, M.J., and COLLEDGE, W.H. (1993). Correction of the ion transport defect in cystic fibrosis transgenic mice by gene therapy. Nature **362,** 250–255.

LOGAN, J.J., BEBOK, Z., WALKER, L.C., PENG, S., FELGNER, P.L., CHENG, S.H., SIEGAL, G.P., BRIZZEL, R.A., DONG, J.-y, HOWARD, M., MATALON, S., DUVAL, M., and SORCHER, E.J. (1994). Cationic lipids for CFTR gene transfer. Abstract #178. Pediatric Pulmonology (Suppl.) **10,** 228.

McLACHLAN, G., DAVIDSON, D., STEVENSON, B.J., DORIN, J.R., and PORTEOUS, D.J. (1994). Optimization of aerosolized gene delivery to respiratory epithelium. Abstract #180. Pediatric Pulmonology (Suppl.) **10:**229.

NABEL, E.C., YANG, Z., MULLER, D., CHANG, E.A., GAO, X.,

HUANG, L., CHO, K.J., and NABEL, G.J. (1994). Safety and toxicity of catheter gene delivery to the pulmonary vasculature in a patient with metastatic melanoma. Hum. Gene Ther. **5**, 1089–1094.

SAN, H., YANG, Z.-y., POMPILI, V.J., JAFFE, M.L., PLAUTZ, G.E., XU, L., FELGNER, J.H., WHEELER, C.J., FELGNER, P.L., GAO, X., HUANG, L., GORDON, D., NABEL, G.J., and NABEL, E.G. (1993). Safety and short-term toxicity of a novel cationic lipid formulation for human gene therapy. Hum. Gene Ther. **4**, 781–788.

SCHWARZ, L.A., WALDREP, J.C., and KNIGHT, J.V. (1993). Delivery of DNA-liposome complexes by small particle aerosol. J. Cell. Biochem. (Suppl.) **17E**, SZ325.

STRIBLING, R., BRUNETTE, E., LIGGITT, D., GAENSLER, K., and DEBS, R. (1992). Aerosol gene delivery in vivo. Proc. Natl. Acad. Sci. USA **89**, 11277–11281.

VIDGREN, M., WALDREP, J.C., ARPPE, J., BLACK, M., RODARTE, J.A., COLE, W., and KNIGHT, V. (1995). A study of 99m technetium-labeled beclomethasone dipropionate dilauroylphosphatidylcholine liposome aerosol in normal volunteers. Int. J. Pharm **115**, 209–216.

WALDREP, J.C., KEHYANI, K., BLACK, M., and KNIGHT, V. (1993a). Operating characteristics of 18 different continuous-flow jet nebulizers with beclomethasone dipropionate liposome aerosol. Int J. Pharm **97**, 205–212.

WALDREP, J.C., SCHERER, P.W., KEYHANI, K., and KNIGHT, V. (1993b). Cyclosporin A liposome aerosol: Particle size and calculated respiratory deposition. Int. J. Pharm. **97**, 205–212.

WELSH, M.J., SMITH, A.E., ZABNER, J., RICH, D.P., GRAHAM, S.M., GREGORY, R.J., PLATT, B.M., and MOSCICKI, R.A. (1994). Cystic fibrosis gene therapy using an adenovirus vector: In vivo safety and efficacy in nasal epithelium. Hum Gene Ther. **5**, 209–219.

YOSHIMURA, K., ROSENFELD, M.A., NAKAMURA, H., SCHERER, E.M., PAVIRANI, A., LECOCQ, J.-P., and CRYSTAL, R.G. (1992). Expression of the human cystic fibrosis transmembrane conductance regulator gene in the mouse lung after in vivo intratracheal plasmid-mediated gene transfer. Nucleic Acids Res. **20**, 3233–3240.

Address reprint requests to:
Dr. Lindsay A. Schwarz
Department of Pharmacological and Pharmaceutical Sciences
University of Houston
Houston, TX 77204

Received for publication September 7, 1995; accepted after revision December 20, 1995.

STIC-ILL

NO

From: Schnizer, Richard
Sent: Tuesday, July 17, 2001 6:31 AM
To: STIC-ILL
Subject: 09/330,903

3555564

Please send me copies of:

TI Simulated lung ***transfection*** by nebulization of liposome cDNA complexes using a cascade impactor seeded with 2-CFSME0-cells.
AU Schreier H; Gagne L; Conary J T; Laurian G
SO JOURNAL OF AEROSOL MEDICINE, (1998 Spring) 11 (1) 1-13.

3769264

TI Delivery of DNA-cationic liposome complexes by small-particle ***aerosol*** .
AU Schwarz L A; Johnson J L; Black M; Cheng S H; Hogan M E; Waldrep J C
SO HUMAN GENE THERAPY, (1996 Apr 10) 7 (6) 731-41.

TI Optimization of formulations and conditions for the ***aerosol*** delivery of functional cationic lipid:DNA complexes.
AU Eastman S J; Tousignant J D; Lukason M J; Murray H; Siegel C S; Constantino P; Harris D J; Cheng S H; Scheule R K
SO HUMAN GENE THERAPY, (1997 Feb 10) 8 (3) 313-22.

Thank you-

Richard Schnizer, Ph.D.
Patent Examiner
Art Unit 1632
CM1 12E17
703-306-5441

10177217

JOURNAL OF AEROSOL MEDICINE
Volume 11, Number 1, 1998
Mary Ann Liebert, Inc.
Pp. 1–13

Simulated Lung Transfection by Nebulization of Liposome cDNA Complexes Using a Cascade Impactor Seeded with 2-CFSME$_o$-Cells

HANS SCHREIER, LUCIE GAGNÉ, JON T. CONARY, and GUILLAUME LAURIAN

Advanced Therapies, Inc., Novato, California

ABSTRACT

The aim of this study was to devise a simulation aerosol system for quasirealistic gene transfection that could eventually be used to study the characteristics of aerosol delivery, stability, delivery efficiency, and expression efficacy of gene products. It consisted of (1) a PARI aerosol generator and PARI LL jet; (2) an Andersen cascade impactor with a calibrated vacuum pump, fitted with a glass "throat," nebulizer in which stages were seeded with pulmonary cells of interest (e.g., 2-CFSME$_o$-); and (3) a hot room set to 37°C and ≈70% relative humidity. Cell viability remained at 95% to 99%. A prostaglandin G/H synthase (PGH)- and a human α_1-antitrypsin (AAT)-expressing plasmid, respectively, driven by a cytomegalovirus promoter (pCMV$_4$-PGH, pCMV$_4$-AAT) and a heat-insensitive placental alkaline phosphatase (PAP)-expressing plasmid driven by a Rous sarcoma virus promoter (pRSV-PAP) were employed; cationic liposomes consisted of N-[1-(2,3-dioleyloxy)propyl]-N,N,N-trimethylammonium chloride/dioleoylphosphatidylethanolamine (DOTMA/DOPE) or 3β-[N-(N',N'-dimethylaminoethane)-carbamoyl]-cholesterol/DOPE (DC-Chol/DOPE). The fluorescent dye Toto-1 was used to visualize aerosol distribution and to monitor cellular uptake. Alternatively, pCMV$_4$-PGH deposited onto impactor stages covered with nitrocellulose membranes was hybridized with random primer-^{32}P-radiolabeled pCMV$_4$-PGH and autoradiographed. The mass median aerodynamic diameter (MMAD) of the plasmid, liposomes, and liposome-plasmid complexes and their effect on the mass output were monitored. A majority of gene product was delivered to stages 1 through 5, corresponding to an area ranging from the pharynx to the terminal bronchi, excluding the alveolar space. A corresponding, although very low, transfection of cells with pRSV-PAP was found, with the majority of transfected cells on stages 4 and 5. The MMAD was significantly affected by the presence of the

DNA constructs alone or by DNA constructs complexed with cationic liposomes; the control phosphate buffered saline (PBS) MMAD of 2.3 μm increased to 3.5 μm for DC-Chol liposomes and 4.5 μm for the DC-Chol/PGH complex; DOTMA-based liposomes and liposome DNA complexes precipitated during aerosolization. Mass output was reduced for cationic liposomes from 0.61 g/min (PBS control) to 0.35 g/min. Large plasmid (pRSV-PAP, 10.1 kb) was more rapidly degraded by aerosolization than smaller plasmid (pCMV$_4$-AAT, 6.2 kb), although complexation with cationic liposomes provided some protection in both cases.

Key words: gene therapy, plasmids, cystic fibrosis, pulmonary diseases, cationic liposomes, aerosol, lung simulation, cascade impactor

INTRODUCTION

GENE THERAPY is emerging as a clinically viable therapeutic regimen for genetic, neoplastic, and infectious diseases.[1] A prominent example is cystic fibrosis (CF), a genetic disease resulting from a mutation of the cystic fibrosis transmembrane conductance regulator (CFTR) gene. Partial correction has been accomplished using complementary DNA (cDNA) inserted into adenoviral[2] or liposome plasmid vectors[3,4] delivered to the nasal and pulmonary epithelium. CFTR gene expression in the nasal cavity of CF patients using 3β-[N(N',N'-dimethylaminoethane)-carbamoyl]-cholesterol/dioleoylphosphatidylethanolamine (DC-Chol/DOPE) liposomes complexed with plasmid CFTR has been reported recently.[5] Progress in CF gene therapy using cationic liposomes as carriers has been critically reviewed by Schreier and Sawyer.[6]

Although adenoviral vectors are delivery vehicles per se, plasmid cDNA has been most efficiently delivered to date in vitro and in vivo by complexation with cationic liposomes.[7–9] In vivo transfection of mouse lungs using cationic liposomes complexed with a reporter plasmid coding for chloramphenicol acetyl transferase has been shown by intravenous injection and intratracheal instillation[10] as well as by aerosol delivery.[11]

Despite a wealth of in vivo data and the fact that human studies employing cationic liposome plasmid complexes are ongoing, there is a fundamental lack of understanding regarding their performance under nebulization conditions. Methodology that facilitates monitoring of the pulmonary delivery process in a quasirealistic fashion would be desirable. As an outgrowth of our studies on the design and characterization of liposome aerosol formulations,[12–16] we have devised an in vitro system that mimics pulmonary transfection with aerosolized liposome DNA complexes under standardized conditions. This system employs calibrated aerosol delivery to a cascade impactor, which serves as an artificial "lung," and is linked to the aerosol device via a glass "throat." Here, we describe the technical aspects of the system, including (1) characteristics of delivery (droplet size, mass output, stability, cell viability), (2) pulmonary distribution of liposome DNA complexes using random primer ^{32}P-hybridization and Toto-1 (Molecular Probes, Eugene, OR) fluorescent labeled plasmid (a cytomegalovirus promoter-prostaglandin G/H synthase [pCMV$_4$-PGH]), and (3) expression of a model plasmid (promoter Rous sarcoma virus-placental alkaline phosphatase [pRSV-PAP]). Although quantitation of these processes has not been attempted here, the system could clearly be adapted to yield quantitative information on the efficiency of delivery and efficacy of expression. Studies towards this end are now underway.

MATERIALS AND METHODS

Simulated lung (cascade impactor)

The simulated lung setup is shown in Figure 1. An Andersen Mark II cascade impactor (Andersen, Atlanta, GA) was used, as we had gained extensive experience in analyzing liposome formulations with this system before.[12,16] The cascade impactor consists of eight stages, with the orifice diameter of each stage corresponding to "stages" of the human lung from the pharynx to the alveoli. The inlet was fitted with a glass bulb (7 cm ϕ) which represents the throat of the system. Inspiration air flow was generated by a calibrated vacuum pump set at 1 actual cubic foot per minute, corresponding to 28.3 L/min, which is representative of the flow of air during tidal breathing in humans.

Prior to experimentation, all parts were equilibrated in a hot room set to 37°C and at a relative humidity of 65% to 75%. This level of humidity mimics the partial pressure of water vapor in the tracheobronchial tree. Immediately before the system was assembled in the hot room, the stainless steel plates covering each stage were partially covered with ultraviolet (UV) sterilized 1-cm^2 microscope cover slips onto which 2-CFSME$_o$- cells (see below) had been seeded. An example of stainless steel plates mounted with microscope cover slips upon which cells are seeded is shown in Figure 2.

After completion of the experiment and disassembly of the impactor, the cells were returned to 35-mm culture dishes, replenished with 1 mL of media (DMEM/F12), and incubated for 30 minutes at 37°C in 5% CO_2, 95% relative humidity. When cells were incubated for longer than 24 hours, the medium was replaced every 24 hours.

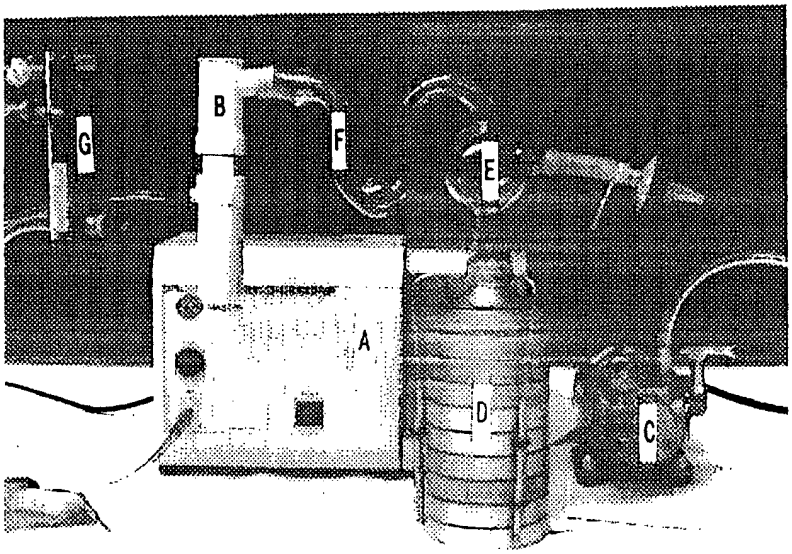

FIG. 1. Simulated lung (cascade impactor). (A) PARImaster compressor, (B) PARI LL Jet aerosol generator, (C) calibrated vacuum pump (28 L/min inflow), (D) Andersen Mark II cascade impactor, (E) glass throat, (F) *U*-tube connector (to retain large droplets), (G) flow meter.

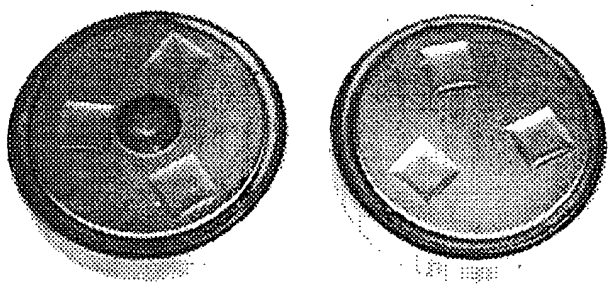

FIG. 2. Stainless steel plates of the Andersen cascade impactor seeded with 2-CFSME$_o$- cells on 1-cm^2 microscope coverslips.

Aerosolization

A PARImaster compressor (PARI Respiratory Equipment, Inc., Richmond, VA) fitted with a PARI LL Jet nebulizer was used. For deposition and delivery studies, the system was operated uninterrupted for a total duration of 2 to 5 minutes. In order to assess the aerosol performance characteristics of the nebulizer in the presence of plasmid (pCMV$_4$-PGH), cationic liposomes, and liposome DNA complexes (see below), the plasmid or liposome dispersions were prepared in a 160 mmol (≈300 mosm) of 5,6-carboxyfluorescein (Eastman Kodak, Rochester, NY) solution. The fluorescent mixture was aerosolized (10 actuations for 3 seconds each, with 5-second intervals), and the amount deposited on the glass throat, impactor stages, and the bottom filter was quantitated spectrophotometrically at a wavelength of 480 nm. Mass median aerodynamic diameter (MMAD) was determined from a plot of size (μm) as determined by the compactor stage orifice versus cumulative percentage of undersized mass. Mass output was determined gravimetrically by repeated weighing of the amount remaining in the nebulizer following a 1-minute aerosol generation.

Cells and cell viability

2-CFSME$_o$- cells, a transformed human bronchial epithelial cell line carrying the F508 deletion of the CFTR gene,[17] were routinely maintained in DMEM/F12 media (Gibco, Grand Island, NY). Cells were seeded on 1-cm^2 microscope coverslips for transfer to the impactor stages (see above) and used at 85% to 90% confluency. The cells were the generous gift of Dr. R. Frizzell (University of Alabama, Birmingham, AL). The viability of the 2-CFSME$_o$- cells in the cascade impactor was monitored by aerosolizing 4% trypan blue solution onto the cells for 10 × 3 seconds with 5-second intervals and by counting viable versus nonviable cells in five fields of each plate on each stage.

SIMULATED LUNG TRANSFECTION BY NEBULIZATION

Preparation of cationic liposomes and liposome DNA complexes

Two types of cationic lipids were employed: N-[1-(2,3-dioleyloxy)propyl]-N,N,N-trimethylammonium chloride (DOTMA)[7] and 3β-[N-(N',N'-dimethyl aminoethane)-carbamoyl]-cholesterol (DC-Chol)[9] both mixed 1:1 (wt/wt) with DOPE (Avanti Polar Lipids, Alabaster, AL). The DOTMA and DC-Chol were generous gifts from Syntex Research (Palo Alto, CA) and Dr. Leaf Huang, (University of Pittsburgh, Pittsburgh, PA), respectively.

DOTMA/DOPE liposomes were prepared by dissolving equal amounts of each component (5.5:4.5 DOTMA/DOPE molar ratio) in $CHCl_3$, removing the organic phase by rotoevaporation, and resuspending the lipid film in sterile double-distilled water under gentle swirling. The crude dispersion was agitated on a wrist-action shaker for 1 hour at room temperature. Liposomes were reduced in diameter to less than 200 nm by high-pressure homogenization with an Emulsiflex-20,000-B3 (Avestin, Ottawa, Canada) using approximately 15 cycles at 16,000 psi of N_2 pressure. Liposome size was determined with a Nicomp Model 370 laser particle sizer (Particle Sizing Systems, St. Barbara, CA). The final lipid concentration was determined colorimetrically as described elsewhere.[18] Liposomes were prepared at a stock concentration of 10 mg/mL (15 μmol/mL) total lipid; working concentrations were 1 mg/mL or less. Liposomes were stored in glass vials at 4°C under nitrogen.

DC-Chol/DOPE liposomes were produced by mixing equal amounts of each component (6:4 DC-Chol/DOPE molar ratio) in $CHCl_3$, followed by rotoevaporation and dispersion in water as above. The flask was briefly sonicated to ensure removal of all lipid from the vessel wall, and hydration was continued in the refrigerator overnight before the preparation was homogenized as above.

The liposome size was measured by laser particle sizing (Nicomp Model 370; Particle Sizing Systems) and showed diameters in the range of 200 to 300 nm for both DC-Chol/DOPE and DOTMA/DOPE liposomes.

Cationic liposome DNA complexes were prepared by combining liposomes and plasmid solutions dropwise under gentle swirling, following dilution of both components with water. Typically, final concentrations were 540 μg lipid mixed with 180 μg of plasmid in a minimum volume of 2.2 mL of water (necessary volume for a 2-minute continuous aerosolization in the PARI LL Jet).

To determine the retention of the physical characteristics of the cationic liposomes alone as well as of liposome DNA complexes during aerosolization, the aerosol mist escaping from the nebulizer (without the cascade impactor connected) was collected in ice-cold 50-mL centrifuge tubes for laser particle sizing as described for liposomes above.

Plasmids

An ovine PGH-containing plasmid and a human α_1-antitrypsin (AAT)-containing plasmid, driven by a cytomegalovirus (CMV) promoter, $pCMV_4$-PGH at 7.5 kb and $pCMV_4$-AAT at 6.2 kb, respectively, were constructed.[19] Plasmids were replicated in *Escherichia coli* strain NM522 and purified using Quiagen Gigapreps (Qiagen, Chatsworth, CA) according to the manufacturer's protocol. Purity of plasmids and integrity of the cDNA inserts were determined by electrophoresis using 1% agarose gels. Gels were stained with 0.5 mg per 100 mL of ethidium bromide and photographed with a DS 34 Polaroid Direct Screen Instant Camera (Polaroid Corp., Cambridge, MA). The plasmid coding for heat-in-

sensitive PAP (10.1 kb, driven by pRSV) was the generous gift of Dr. Lloyd Culp (Case Western Reserve University, Cleveland, OH). It was replicated and purified as above. This plasmid (pRSV-PAP) was used to generate visual images reflecting PAP expression efficacy of cells on the cascade impactor stages.

To determine plasmid integrity during nebulization, aerosol was collected as described above, and 1% agarose gel electrophoresis of the collected material as well as of samples removed from the nebulizer jet was performed and compared with that from an untreated control and with DNA standards. A positive control was generated by sonicating aliquots for 1 minute in a concentric bath sonicator (Laboratory Supplies, Hicksville, NY).

Fluorescent labeling of pCMV$_4$-PGH

Plasmid was labeled with the dimeric cyanine nucleic acid stain Toto-1 in 40 mmol of Tris acetate, pH 8.0, containing 2 mmol of EDTA. DNA (1 mg/mL) was added to a one-tenth dilution of the dye at a ratio of 1:3 vol/vol, precipitated with Na acetate and ethanol, collected by centrifugation, washed with 70% ethanol, and resuspended in Tris acetate buffer at a concentration of 0.5 mg/mL. Integrity of the labeled plasmid was determined by electrophoresis in 1% agarose gel. The pattern of plasmid delivery to the individual stages of the impactor was visualized by depositing the aerosol on saran wrap coating the stainless steel stages; the wrap was transferred to a UV plate reader, and the fluorescent pattern emitted was photographed with a DS 34 Polaroid Direct Screen Instant Camera (Polaroid Corp., Cambridge, MA). To determine the extent of cellular delivery, coverslips were removed from the stages following aerosol exposure, briefly washed with phosphate buffered saline (PBS), and examined microscopically with a Nikon Diaphot Phase Contrast-2 ELWD 0.3 fluorescence microscope (Nippon, Tokyo, Japan).

Hybridization of pCMV$_4$-PGH

To determine further the efficiency of delivery of the delivered gene product, plasmid deposited on the impactor stages was transferred onto nitrocellulose membranes, denatured, and neutralized using standard conditions. Denatured DNA was fixed to the membranes by UV cross-linking prior to hybridization. Hybridization was performed with random primer-^{32}P-radiolabeled pCMV$_4$-PGH at 45°C. Membranes were washed stringently and autoradiographed.

PAP staining

To determine the transfection efficacy, heat-insensitive PAP, the expression product of pRSV-PAP, was analyzed. The presence of PAP is indicated by purple-black coloration of the cells, which was photographed for documentation as above (4× and 10× magnification). Following each aerosolization cycle, the cascade impactor was disassembled as rapidly as possible, and the cells were returned to the incubator. Cells were incubated for 48 hours with one change of medium at 24 hours and then analyzed for PAP expression. The coverslips were washed three times at 4°C with PBS prior to fixation with formaldehyde/glutaraldehyde 2%/0.2% in PBS at 4°C for 5 minutes. Cells were washed again three times with PBS at room temperature. Then, 1 mL of PBS was added and the cells were incubated at 65°C in a water bath for 30 minutes to degrade endogenous alkaline phosphatase; PAP was detected by staining for 30 minutes at 37°C with a staining solution consisting of 1 mL of 40 mg/mL X-phosphate (5-bromo-4-chloro-3-indolyl phosphate) in

dimethylformamide, 1 mL of 40 mg/mL p-nitro blue tetrazolium in 50% dimethylformamide, and 38 mL of 0.1-mol Tris HCl, pH 10.0. Cells were washed in PBS prior to microscopic inspection for purple-black staining.

RESULTS

Cell viability

2-CFSME$_0$- cells showed no distress due to the deposition in the cascade impactor and the aerosolization procedure; viability as determined by trypan blue exclusion was 95% to 99% on all stages.

Aerosol performance characteristics

The PARImaster and PARI LL Jet generated an aerosol MMAD of 2.3 μm (69.3% < 5.8 μm) and a mass output of 0.614 ± 0.010 g/min under standard conditions (PBS). As listed in Table 1, performance characteristics were greatly influenced by the presence of cationic liposomes and liposome DNA complexes, respectively, with MMAD increasing to 3.5 μm and 4.5 μm for DC-Chol/DOPE liposomes and DC-Chol/DOPE liposome DNA complexes, respectively. The mass output of DC-Chol/DOPE liposomes decreased to 0.347 ± 0.008 g/min. DOTMA/DOPE liposomes and their complexes with DNA precipitated.

Plasmid stability

Plasmid stability was a factor of both plasmid size and complexation with cationic lipid. As can be seen in Figure 3A, the relatively large pRSV-PAP (10.1 kb) was readily destroyed while circulating through the nebulizer orifice, although the smaller pCMV$_4$-AAT (6.3 kb) appeared to remain intact during the entire 5-minute aerosolization time (Fig. 3C). The various bands seen indicate that the plasmid existed in at least three forms (three bands on agarose gel), which were most likely a dimeric, open circular, and supercoiled form. No additional bands were formed during the aerosolization. pRSV-PAP was signifi-

TABLE 1. PERFORMANCE CHARACTERISTICS OF THE PARI LL JET AEROSOLIZER IN THE PRESENCE OF CATIONIC LIPOSOMES AND CATIONIC LIPOSOME DNA COMPLEXES

Type of lipsome/ lipsome-DNA complex	*Mass median aerodynamic diameter*		*Mass Output*
	(μm)	*% < 5.8 μm*	*(g/min)(n = 5)*
PBS (control)	2.3	69.3	0.614 ± 0.010
Plasmid (pCMV$_4$-PGH)	3.0	64.3	Not done
DC-Chol/DOPE (5 mg/mL)	3.5	65.3	0.347 ± 0.008
DC-Chol/DOPE/plasmid	4.5	62.3	Not done
DOTMA/DOPE (5 mg/mL)	[a]	[a]	Not applicable
DOTMA/DOPE/plasmid	[a]	[a]	Not applicable

[a]Precipitation.

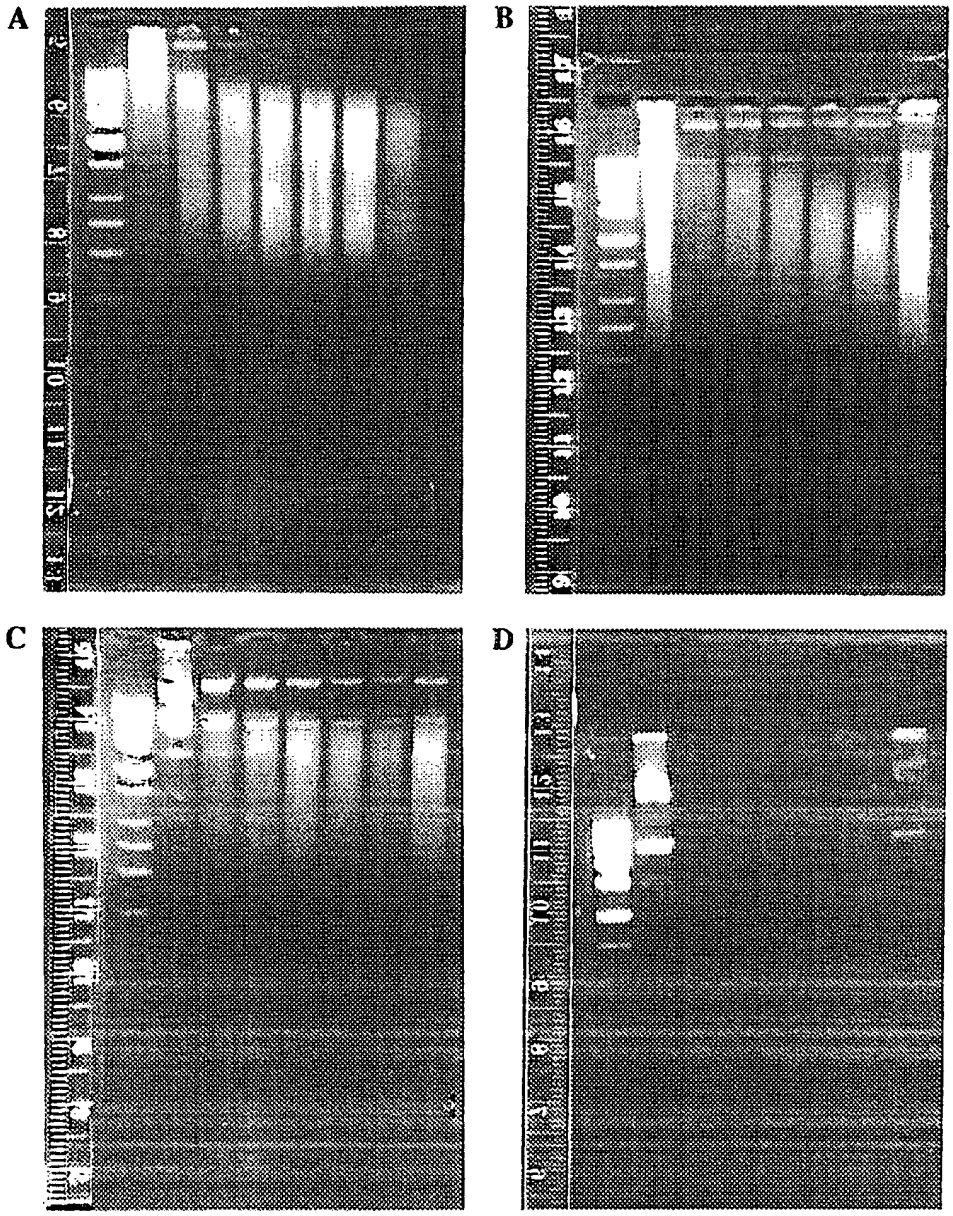

FIG. 3. Stability of plasmid during aerosolization with a PARI LL Jet. (A) pRSV-PAP (10.1 kb) alone. Lanes: (1) DNA standard; (2) plasmid control; (3–7) aerosolized for 1, 2, 3, 4, and 5 minutes; (8) plasmid remaining in nebulizer reservoir. (B) pRSV-PAP-DC-Chol/DOPE (3:1 w/w) complex. Lanes as for (A). (C) $pCMV_4$-AAT (6.2 kb) alone. Lanes as for (A). (D) $pCMV_4$-AAT-DC-Chol/DOPE (3:1 wt/wt) complex. Lanes as for (A). Agarose gels (1%) were stained with 0.5 mg per 100 mL of ethidium bromide.

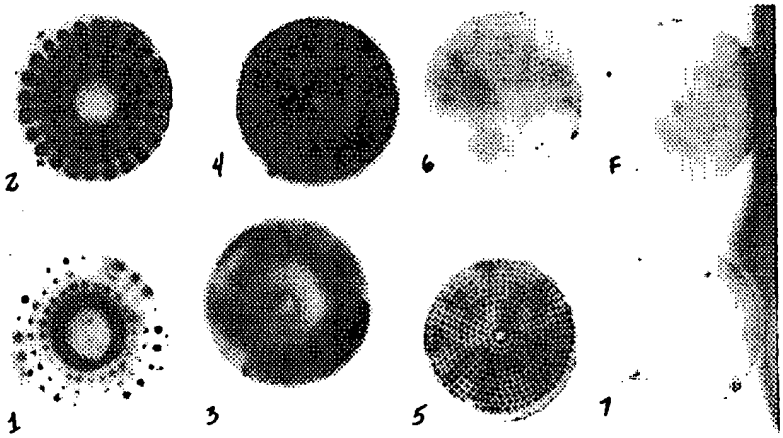

FIG. 4. Delivery pattern and efficiency of delivery as shown by plasmid hybridization. To determine the relative efficiency of delivery on each stage, $pCMV_4$-PGH plasmid was deposited onto nitrocellulose membranes on the impactor stages, denatured, and neutralized using standard conditions. Hybridization was performed with random primer-^{32}P-radiolabeled $pCMV_4$-PGH at 45°C, and membranes were autoradiographed (see Materials and Methods section).

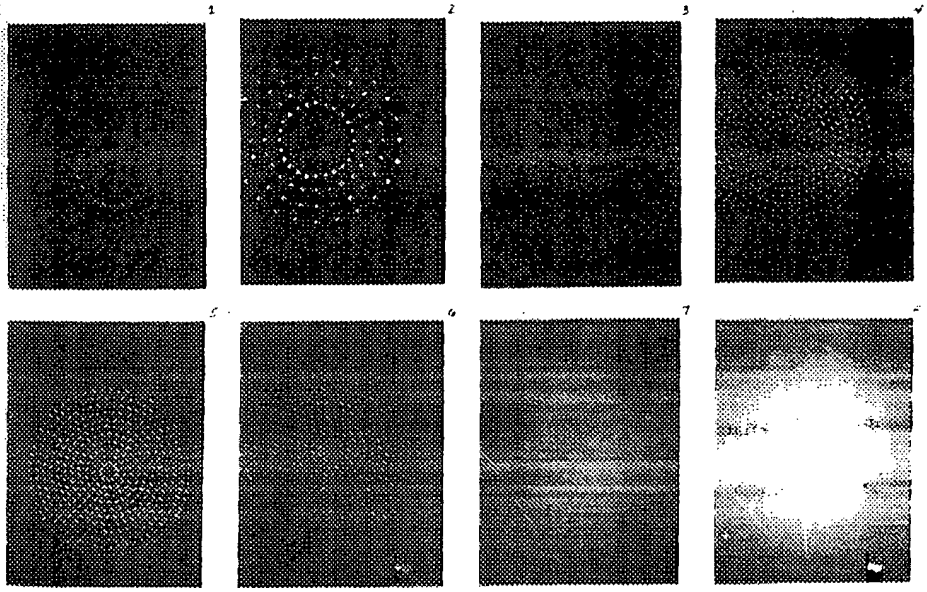

FIG. 5. Relative efficiency of plasmid delivery on each stage as shown by fluorescence photography. $pCMV_4$-PGH was labeled with Toto-1 and complexed with DC-Chol/DOPE liposomes (see Materials and Methods section). Impactor stages 1 through 7 and bottom plate containing a filter disc (F) were covered with saran wrap; the fluorescent pattern was photographed following transfer of the wraps to a UV plate reader.

cantly protected when complexed with DC-Chol/DOPE liposomes as seen in Figure 3B. Although this is also true for $pCMV_4$-AAT as indicated by lane 8 of Figure 3D (i.e., the residual aerosol remaining in the reservoir after a 5-minute aerosolization), there was no aerosol collected from the mouth of the PARI LL Jet, indicating that the material had likely precipitated in the reservoir and was not circulating through the nebulizer.

Relative efficiency of plasmid delivery

Plasmid was efficiently delivered to all stages of the impactor, except stages 6 and 7 (i.e., corresponding to the alveolar space). This was shown by both hybridization experiments (Fig. 4) as well as by deposition of plasmid-intercalated fluorescent dye (Toto-1) onto saran wrap coating the impactor stages (Fig. 5). Deposition was in a regular pattern which was determined by the arrangement of the impactor stage orifices. The distinct radioactive "ring" around the inlets of stages 0 and 1 indicates that substantial tracheal and pharyngeal deposition would occur under the aerosol conditions employed here.

Intracellular delivery of pRSV-PAP to and expression in 2-CFSME$_o$- cells

When Toto-1–labeled $pCMV_4$-PAP complexed with DC-Chol/DOPE liposomes was aerosolized onto 2-CFSME$_o$- cells, intracellular fluorescence was abundant (not shown).

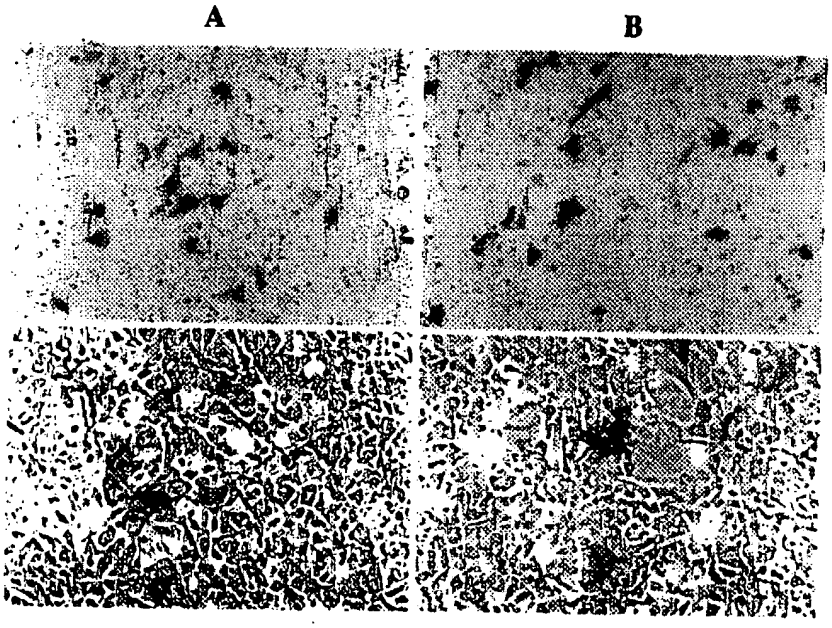

FIG. 6. Transfection of pRSV-PAP in 2-CFSME$_o$- cells upon aerosolization of the plasmid complexed with DC-Chol/DOPE liposomes and staining (see Materials and Methods section). Examples from stage #2 (A) and stage #4 (B) are shown. A significant number of cells expressed the transgene. Transfection was found on stages 0 through 5 (pharynx to terminal bronchi) but not on the stages representing the alveolar space. (A) This example shows several cells expressing PAP aligned in a circular fashion, probably reflecting the circular contact area with an aerosol droplet. Magnification are 4× (top panels) and 10× (bottom panels).

Autofluorescence was clearly differentiated from bright images generated by the labeled plasmid product.

The abundant presence of intracellularly delivered plasmid did not translate into corresponding levels of exuberant transfection, however. As shown in Figure 6, transfection can be seen in a fair number of cells and appears to be located in areas where aerosol droplets were deposited onto the cell layer (see example on the left-hand side of Fig. 6). Although transfection efficiency within these distinct areas was estimated to be in the range of 10% to 15%, overall, the fraction of transfected cells was minute (1%–2%), and this was found independent of the lipid mixture (DC-Chol/DOPE or DOTMA/DOPE) employed.

DISCUSSION

A cascade impactor fitted with a glass throat and seeded with cells has been utilized to mimic pulmonary delivery and cellular uptake of a plasmid gene product complexed with cationic liposomes. The aim of this study was to design an in vitro system that would eventually allow assessment and comparison of the performance characteristics of various gene drug products under controlled, reproducible, and quasirealistic test conditions. A vital component was the availability of a hot room set to 37°C and a maximum relative humidity of approximately 75%. Under these conditions, the cells remained viable for the duration of the experiment (total time elapsed until cells were returned to the culture medium was approximately 20 minutes). It should be noted that the viability was assessed under actual experimental conditions, that is, the vital stain was aerosolized onto the cells rather than added as solution following completion of the experiment.

The relative efficiency of delivery to the stages of the artificial lung as well as that of intracellular delivery to target cells was assessed with a plasmid-intercalated fluorescent dye (Toto-1). The use of noncovalently bound dyes as a measure for nuclear uptake of plasmid has encountered skepticism, as dissociation of label from the DNA carrier complex and concomitant false-positive labeling of endogenous DNA by nuclear migration and genomic intercalation of diffusible dye is likely to occur. It should be noted that the dye was used here solely as a reporter for intracellular delivery. No quantitation or nuclear delivery of the plasmid product is claimed on the basis of these data.

The hybridization experiment (see Fig. 4) confirms the "pulmonary" distribution of plasmid seen with the fluorescent marker (see Fig. 5). It should be noted that the appearance of inhomogeneous deposition of aerosol onto some of the stainless steel plates is an artifact of the manipulation associated with transfer and handling of the membranes.

Although the extent of expression, especially the estimated 10% to 15% of cells expressing within the perimeter of deposition of aerosol droplets, is within the range of expression that has been seen with these and comparable systems in vitro, the question as to what the reason is for the glaring discrepancy between cellular uptake and nuclear expression (see Fig. 6) remains unanswered. To date, it is unclear whether the rate-limiting step is cellular uptake, endosomal release, intracellular trafficking, nuclear uptake, intranuclear transcription and translation, or a combination thereof. This issue is discussed in more detail by Schreier and Sawyer.[6]

An obvious limitation of the simulation system is the fact that the calibration of the stages reflecting specific layers in the lung is controlled by the inspiratory flow generated by a calibrated vacuum pump. Hence, changes in inspiration (e.g., due to obstruction), can-

not be evaluated with this system. Also, the unidirectional flow does not take into account events occurring during exhalation. Furthermore, the irregular deposition (as dictated by the arrangement of the stage orifices, see Figs. 4 and 5) onto a limited amount of fluid layer on the cell surface may not reflect a less hindered lateral diffusion of the aerosol droplet upon inhalation in the lung; therefore, this may contribute to an underestimation of transfection efficacy. Planned modifications of the simulation system include (1) comparison of normal bronchial cells with mutant cells such as the 2-CFSME$_o$- cells used here; (2) seeding with relevant cell types at the corresponding stages (e.g., epithelial, type II, alveolar macrophages); (3) addition of surfactant (bronchoalveolar lavage fluid) and mucus coating; (4) testing of different nebulizers and aerosol configurations; (5) testing of different liposome formulations, lipid concentrations, and lipid:plasmid ratios; (6) toxicity testing, including effects of endotoxin and quantification of cytokine release; and (7) development of quantitative methods. Also, to fully validate the simulation system, a head-to-head comparison with an analogous in vivo study would be desirable.

We submit that the simulation system presented here may aid in the effort to elucidate the fate of gene products upon delivery to the lung and thus may help us to understand and rationally perfect gene delivery systems.

ACKNOWLEDGMENTS

This study was supported by a Cystic Fibrosis Foundation research grant #Z984 (H.S.). Generous material gifts were received from the Syntex Corporation, Palo Alto, CA (DOTMA); Dr. L. Huang, University of Pittsburgh, PA (DC-Chol); Dr. R. Frizzell, University of Alabama at Birmingham, AL (2-CFSME$_o$- cells); and Dr. L. Culp, Case Western Reserve University, Cleveland, OH (pRSV-PAP). Dr. B. Trapnell, Genetic Therapy, Inc., Gaithersburg, MD, contributed to the idea of constructing the cascade impactor seeded with cells. Early studies of this project were conducted at Vanderbilt University School of Medicine, Nashville, TN: we thank Dr. K.L. Brigham for support of this project. G.L. was an exchange student from the Université Champagne-Ardennes, Faculté de Pharmacie, Reims, France.

REFERENCES

1. Schreier, H. 1994. The new frontier: Gene and oligonucleotide therapy. *Pharm. Acta Helv.* 68:145–159.
2. Rosenfeld, M.A., K. Yoshimura, B.C. Trapnell, K. Yoneyama, E.R. Rosenthal, W. Dalemans, M. Fukayama, J. Bargon, L.E. Stier, L. Stratford-Perricaudet, M. Perricaudet, W.B. Guggino, A. Pavirani, J.P. Lecocq, and R.G. Crystal. 1992. In vivo transfer of the human cystic fibrosis transmembrane conductance regulator gene to the airway epithelium. *Cell* 68:143–155.
3. Hyde, S.C., D.R. Gill, C.F. Higgins, A.E.O. Trezise, L.J. MacVinish, A.W. Cuthbert, R. Ratcliff, M.J. Evans and W.H. Colledge. 1993. Correction of the ion transport defect in cystic fibrosis transgenic mice by gene therapy. *Nature* 362:250–255.
4. Alton, E.W.F., P.G. Middleton, N.J. Caplen, S.N. Smith, D.M. Steel, F.M. Munkonge, P.K. Jeffery, D.M. Geddes, S.L. Hart, R. Williamson, K.I. Fasold, A.D. Miller, P. Dickinson, B.J. Stevenson, G. McLachlan, J.R. Dorin, and D.J. Porteous. 1993. Non-invasive liposome-mediated gene delivery can correct the ion transport defect in cystic fibrosis mutant mice. *Nature Genetics* 5:135–142.

5. Caplen, N.J., E.W.F. Alton, P.G. Middleton, J.R. Dorin, B.J. Stevenson, X. Gao, S.R. Durham, P.K. Jeffery, M.E. Hodson, C.H. Coutelle, L. Huang, D.J. Porteous, R. Williamson, and D.M. Geddes. 1995. Liposome-mediated CFTR gene transfer to the nasal epithelium of patients with cystic fibrosis. *Nat. Med.* 1:39–46.

6. Schreier, H. and S.M. Sawyer. 1996. Liposomal DNA vectors for cystic fibrosis gene therapy. Current applications, limitations, and future directions. *Advanced Drug Delivery Review* 19:73–87.

7. Felgner, P.L., T.R. Gadek, M. Holm, R. Roman, H.W. Chan, M. Wenz, J.P. Northrop, G.M. Ringold, and M. Danielsen. 1987. Lipofection: A highly efficient, lipid-mediated DNA-transfection procedure. *Proc. Natl. Acad. Sci. U.S.A.* 84:7413–7417.

8. Felgner, J.H., R. Kumar, C.N. Sridhar, C.J. Wheeler, Y.J. Tsai, R. Border, P. Ramsey, M. Martin, and P.L. Felgner. 1994. Enhanced gene delivery and mechanism studies with a novel series of cationic liposome formulations. *J. Biol. Chem.* 269:2550–2561.

9. Gao, X. and L. Huang. 1991. A novel cationic liposome reagent for efficient transfection of mammalian cells. *Biochem. Biophys. Res. Comm.* 179:280–285.

10. Brigham, K.L., B.O. Meyrick, B. Christman, M. Magnuson, G. King, and L.C. Berry, Jr. 1989. In vivo transfection of murine lungs with a functioning prokaryotic gene using a liposome vehicle. *Am. J. Med. Sci.* 298:278–281.

11. Stribling, R., E. Brunette, D. Liggitt, K. Gaensler, and R. Debs. 1992. Aerosol gene delivery in vivo. *Proc. Natl. Acad. Sci. U.S.A.* 89:11277–11281.

12. Niven, R.W. and H. Schreier. 1990. Nebulization of liposomes. I. Effects of lipid composition. *Pharm. Res.* 7:1127–1133.

13. Niven, R.W., M. Speer, and H. Schreier. 1991. Nebulization of liposomes. II. The effects of size and modeling of solute release profiles. *Pharm. Res.* 8:217–221.

14. Niven, R.W., M.T. Carvajal, and H. Schreier. 1992. Nebulization of liposomes. III. The effects of operating conditions and local environment. *Pharm. Res.* 9:515–520.

15. Schreier, H., R.J. Gonzalez-Rothi, and A.A. Stecenko. 1993. Pulmonary delivery of liposomes. *J. Controlled Release* 24:209–223.

16. Schreier, H., W.C. Mobley, N. Concessio, R.W. Niven, and A. Hickey. Formulation and *in vitro* performance of liposome powder aerosols. *S.T.P. Pharma Sciences* 4:38–44.

17. Cozens, A.L., M.J. Yezzi, L. Chin, W.E. Finkbeiner, J.A. Wagner, and D.C. Gruenert. 1992. Characterization of immortal cystic fibrosis tracheobronchial epithelial cells. *Proc. Natl. Acad. Sci. U.S.A.* 89:5171–5175.

18. Mobley, W.C. and H. Schreier. 1994. Phase transition temperature reduction and glass formation in dehydroprotected lyophilized liposomes. *J. Controlled Release* 31:73–87.

19. Conary, J.T., R.E. Parker, B.W. Christman, R.D. Faulks, G.A. Ling, B.D. Meyrick, and K.L. Brigham. 1994. Protection of rabbit lungs from endotoxin injury by in vivo hyperexpression of the prostaglandin G/H synthase gene. *J. Clin. Invest.* 93:1834–1840.

Reviewed by: J. Clifford Waldrep, Ph.D.
Charles Densmore, M.D.

Address reprint requests to:
Dr. H. Schreier
Advanced Therapies, Inc.
371 Bel Marin Keys, #210
Novato, California 94949